MONOAMINE TRANSPORTER SUBSTRATES AND INHIBITORS

By

Ernesto Solis, Jr.

Dissertation

Submitted to the Faculty of the

Graduate School of Vanderbilt University

in partial fulfillment of the requirements

for the degree of

DOCTOR OF PHILOSOPHY

in

Neuroscience

December, 2012

Nashville, Tennessee

Approved:

Kevin P. Currie

Maureen K. Hahn

Sandra J. Rosenthal

Randy D. Blakely

Louis J. DeFelice

DEDICATION

Para mi mamá, Josefina Sosa Mosqueda.

I dedicate my dissertation to my mother, whose love for us, her children, surpasses everything I will ever know.

ACKNOWLEDGEMENTS

"Defeat is not the worst of failures. Not to have tried is the true failure."

~George E. Woodberry

It has been a wild journey, replete with challenges, full of twists and unexpected turns. My graduate years were at times a struggle due to some unforeseen circumstances, but despite many obstacles I faced, I persevered and never once did I doubt myself, never once was I compelled to give up along the way, never once did I consider not fighting to achieve my primary academic goal. For this I am proud, for this I stand tall. Achieving the Ph.D. in Neuroscience is something I sought after with enthusiasm and resolve. I am proud of pursuing my passion.

Being able to work in Neuroscience (the study of the brain, which encompasses every last single thing we do, from thinking and moving to singing and loving) is truly amazing. You learn and study what makes you be able to learn and study. A neuroscientist is a contemporary renaissance man, a philosopher, an inventor, an artist, a scholar, inquisitive by nature, and one who never ceases to seek knowledge about the nature of being a human being. I am happy and humbled to be a part of this group.

There are an inordinate number of people I must thank who contributed to my academic path and helped me get this far.

First of all, I want to thank three people who I will be eternally grateful towards. I truly mean it when I say that I would literally not have made it to this point without them. What these people have in common is that they believed in me when nobody else did,

they encouraged me when I needed it most, they judged me not just based on academic performance, but for what they saw in me as a person. They are people who I am fortunate to have run into in my life because, by having experienced their kindness and their genuine caring for others, they inspire me to be a better person. These people are Knowles A. Overholser, Elaine Sanders-Bush, and Louis J. DeFelice.

Dr. Overholser gave the opportunity to continue my undergraduate education at Vanderbilt University and supported my move from the School of Engineering to the School of Arts and Science to pursue Neuroscience as my major.

It was a pleasure the first time I met Elaine in early undergrad at a prospective biomedical science graduate student get-together at a professor's home. I was a young, naive kid and all I knew at the time is that I loved Neuroscience (from an introductory course I had taken) and that I wanted to study the brain. I couldn't stop talking about this and this information was passed along to Elaine since she came to find me (the young man who she heard was interested in Neuroscience). Elaine's enthusiasm was contagious and I shared her passion for Neuroscience research. She encouraged me to pursue research and gave me advice and guidance through the years that ensued. What always stood out about Elaine is that she always wanted the best for me and listened closely to me to then provide advice on what to do; but above all, she wanted for me to pursue what makes me happy (she even supported my transient thought of considering veterinarian school while already involved in research). I will forever cherish her genuine caring.

Lou is the kind of mentor that you can only imagine of having. I am incredibly fortunate to have worked with not only one of the brightest minds I have ever been around, but also one of the greatest people I have ever known. Lou's zest for research,

enthusiasm for science, passion for life, and relentless energy are qualities that cannot be measured, but that have a huge positive impact on everyone who has the privilege to be around him. I am just one of the countless number of people he has affected in a positive manner. Lou possesses just about every quality a great mentor has including a great ability to teach and train, good listening skills, patience, a positive attitude, accessibility, willingness to always help, high expectations, and a great mind for conducting scientific research. As a student the most important attributes that were imparted on me during my time with Lou are his humility and his empathy and caring for students because, above all, I believe in life it is important to try to make connections and to help each other in a positive manner. I will do my best to carry on Lou's legacy and I hope to be able to affect others in positive manner just like Lou affected me. I am happy and proud to have had Lou as my scientific mentor in graduate school.

I am thankful for the support and servitude provided by my thesis committee members Randy D. Blakely, Maureen K. Hahn, Sandra J. Rosenthal, and my committee chair Kevin P. Currie. They were a great group and always provided insightful comments about my research. I especially thank Kevin for being so thorough and helpful about the expectations after my committee meetings.

I'd like to thank the colleagues who I had the pleasure to work with during my stance in the DeFelice lab: Joel W. Schwartz, Sergei Y. Noskov, Ian D. Tomlinson, Keith Henry, Hideki Iwamoto, Jose Miguel Eltit, Edgar Leal-Pinto, Keith Brooks, Krasnodara N. Cameron, Stefania Averaimo, Rachel Deitz, and Frances White.

I am grateful for the folks at Virginia Commonwealth University Department of Physiology and Biophysics who gave me a home and treated me as one of their own. In

particular, I am especially thankful for the VCU Physiology and Biophysics Department Chair Diomedes Logothetis, and the administrative staff, Christina I. Meliagros, Elizabeth A. Moore, and Matthew B. Lessick.

I must also thank the Neuroscience Program administrative staff at Vanderbilt University. These are wonderful people that truly helped me throughout my graduate years and include Mary Early-Zald, Mary Michael-Woolman, Shirin Pulous, and Rosalind C. Johnson.

I am lucky to have many friends who have been there for me through the years and who shared support during my graduate school years including Iris B. Leu, Claudia Martinez, David T. Masdon, David M. Manny, Michael O. Priolo, Rudy F. Martinez, Angeline Cione, Igor Zdravkovic, Oscar Rodriguez, Brandon M. Pukoszek, Alex Pukoszek, David Rodriguez, David E. Williams, and Daniel Ruiz. It really feels all of these friends were placed in my path to make my walk more pleasant and comforting.

I am blessed and thankful to have met Candice Nicole Hatcher, a beautiful woman who has shown me that true love can still be found here.

I must mention the most important part of my life, my loving and always goofy family, which includes my beloved sisters Monica Valeria Zavala, Karla Angelica Solis, and Alejandra Reyes (each of whom will always be my favorite), my brother-in-law Leobardo Reyes, my nephew Levi Gabriel, and my nieces Genesis Alexandra and Leah Francesca Reyes. My family makes my life whole and gives me strength. I am grateful every single day for being blessed to have their love and support.

To my father, wherever you are watching from I hope that you are proud of me. I will always carry you with me and will never forget your words. I know how deeply you loved me.

Finally, I dedicate the culmination of my million years of schoolwork to the number one person who made me who I am today. My mother, Josefina Sosa, who through her actions taught me all I ever needed to know in life, which is to love despite anything. Her love for her children is greater than anything I could ever imagine. There are not enough words to express how much I love my mother.

TABLE OF CONTENTS

Page

LIST OF TABLES

Page

LIST OF FIGURES

Page

LIST OF ABBREVIATIONS

CNS = central nervous system

PNS = peripheral nervous system

ENS = enteric nervous system

SN = substantia nigra

VTA = ventral tegmental area

5HT = serotonin, 5-hydroxytryptamine

SERT = serotonin transporter

hSERT = human serotonin transporter

OCD = obsessive compulsive disorder

PTSD = post traumatic stress disorder

DA = dopamine, 3,4-dihydroxyphenethylamine

DOPA = dihydroxyphenylalanine

DAT = dopamine transporter

hDAT = human dopamine transporter

ADHD = attention-deficit/hyperactivity disorder

NE = norepinephrine

Epi = epinephrine

NET = norepinephrine transporter

hNET = human norepinephrine transporter

NT = neurotransmitter

SLC = solute carrier

ATP = adenosine triphosphate

ADP = adenosine diphosphate

ABC = ATP-binding cassette (transporter)

ATPases = a class of enzymes that catalyze ATP into ADP and a free phosphate ion

SLC1 = solute carrier 1

SLC6 = solute carrier 6

NSS = neurotransmitter sodium symporter

SLC6A4 = SLC family 6 neurotransmitter transporter, serotonin, member 4 gene

SLC6A3 = SLC family 6 neurotransmitter transporter, dopamine, member 3 gene

VMAT = vesicular monoamine transporter

VMAT2 = vesicular monoamine transporter 2

GABA = γ–aminobutyric acid

VNTR = variable number tandem repeat

SNP = single nucleotide polymorphism

5HTTLPR = serotonin transporter-linked polymorphic region

MAO = monoamine oxidase

MAOI = monoamine oxidase inhibitor

TCA = tricyclic antidepressant

SSRI = selective serotonin reuptake inhibitor

NRI = selective norepinephrine reuptake inhibitor

FLX = fluoxetine, Prozac

COC = cocaine

β-CIT = β-carbomethoxy-3β-(4-iodophenyl)tropane, cocaine analog

TM = transmembrane

TMD = transmembrane domain

METH = methamphetamine, N-methyl-1-phenylpropan-2-amine

MDMA = 3,4-methylenedioxy-N-methylamphetamine

MPH = methylphenidate, Ritalin

DiI = 1,1'-dioctadecyl-3,3,3',3'-tetramethylindocarbocyanine perchlorate

AFU = arbitrary fluorescent units

AMPH = (racemic) amphetamine, α-methylphenethylamine

S(+)AMPH = dextrorotary-amphetamine, S(+)amphetamine

R(–)AMPH = levorotary-amphetamine, R(–)amphetamine

METH = (racemic) methamphetamine, N-methyl-1-phenylpropan-2-amine

S(+)METH = dextrorotary-methamphetamine, S(+)methamphetamine

R(–)METH = levorotary-methamphetamine, R(–)methamphetamine

pCA = *para*-chloroamphetamine

MDMA = (racemic) methylenedioxy-methamphetamine, ecstasy

S(+)MDMA = dextrorotary-MDMA, S(+)methylenedioxy-methamphetamine

R(–)MDMA = levorotary-MDMA, R(–)methylenedioxy-methamphetamine

MPP^+ = 1-methyl-4-phenylpyridinium

APP^+ = 4-(4-(dimethylamino)phenyl)-1-methylpyridinium

ASP^+ = 4-(4-(dimethylamino)styryl)-N-methylpyridinium

LeuT = leucine transporter

$LeuT_{Aa}$ = leucine transporter from *Aquifex aeolicus*

kDa = kilodalton

Å = angstrom

PKC = protein kinase C

CaMKII = Ca^{2+}/calmodulin-dependent protein kinase II

HTS = high-throughput screening

2D = two-dimensional

3D = three-dimensional

Na^{+} = sodium

Cl^{-} = chloride

K^{+} = potassium

H^{+} = proton

DES = desipramine

IMI = imipramine

TEVC = two-electrode voltage-clamp

HEK293 = human embryonic kidney (parental) cells

hSERT-HEK cells = HEK293 cells stably expressing hSERT

hNET-HEK cells = HEK293 cells stably expressing hNET

G418 = Geneticin

DMEM = Dulbecco's modified Eagle medium

FBS = fetal bovine serum

NaCl = sodium chloride

KCl = potassium chloride

ChCl = choline chloride

HEPES (4-(2-hydroxyethyl)-1-piperazine-ethanesulfonic acid

KRH = Krebs-Ringer HEPES (buffer)

RT = room temperature

DIC = differential interference contrast

NA = numerical aperture

PMT = photomultiplier tube

LSM = laser scanning microscope

ROI = region of interest

AFU = arbitrary fluorescent units

k_m = affinity constant of a substrate for an enzyme

V_{max} = maximal transport velocity

V_{min} = miminal transport velocity

n = Hill coefficient

IC_{50} = half maximal inhibitory concentration

k_i = binding affinity of an inhibitor

[S] = substrate concentration

SEM = standard error of the mean

SYTO-17 = cell-permeant red fluorescent nucleic acid stain

MitoTracker = red-fluorescent dye that stains mitochondria in live cells

V_{hold} = holding potential

V_{com} = command (or holding) potential

E1 = voltage sensing microelectrode

E2 = current injecting microelectrode

[^{3}H]-5HT = tritiated serotonin

[^{3}H]-DA = tritiated dopamine

Compound 332 = N,N-dimethyl-4-(pyridin-4-yl)aniline

Compound 321 = 4-(4-(dimethylamino)phenyl)-1-ethylpyridinium

Compound 326 = 4-(4-(dimethylamino)-2-methylphenyl)-1-methylpyridinium

Compound 330 = 4-(4-(dimethylamino)-3-fluorophenyl)-1-methylpyridinium

Compound 377 = N,N-dimethyl-4-(pyridin-3-yl)aniline

Compound 378 = 3-(4-(dimethylamino)phenyl)-1-methylpyridinium

Compound 322 = 4-(4-(dimethylamino)phenyl)-1-propylpyridinium

Compound 416 = 1-benzyl-4-(4-(dimethylamino)phenyl)pyridinium

WT = wild-type

G-scr = G-score

vdW = van der Waals energy

Lipo = lipophilic energy

Hbond = H-bond energy

Clmb = coulombic energy

Tyr = tyrosine

Ala = alanine

Asp = aspartic acid

Leu = leucine

Phe = phenylalanine

Ser = serine

Ile = isoleucine

Val = valine

Gly = glycine

TICT = twist-intramolecular-charge-transfer-state-forming (compounds)

DNA = deoxyribonucleic acid

RNA = ribonucleic acid

I(V) = current voltage (relationship or plot)

HVA = homovanillic acid

DOPAC = dihydroxyphenylacetic acid

2C-T-7 = 2-[2,5-dimethoxy-4-(propylthio)phenyl]ethanamine, hallucinogenic drug

DPT = dipropyltryptamine, drug with mixed hallucinogenic and stimulant actions

Peak = peak current

ILC = induced leak current or persistent leak current

DNE = does not exist

SAR = structure-activity relationship

ABSTRACT

A myriad of human behaviors, such as mood, awareness and motivation, are modulated by the monoamine neurotransmitters serotonin, norepinephrine and dopamine, respectively. Consequently, dysfunction of these monoaminergic systems underlies numerous medical conditions. In particular, disturbances in the serotonergic system are implicated in depression, bipolar disorder, and autism, whereas the dopaminergic system is implicated in Parkinson's disease and addiction. During neurotransmission high concentrations of monoamine neurotransmitters are released from presynaptic neurons into the synaptic cleft where they diffuse to bind and activate pre- and postsynaptic receptors. The primary way to terminate neurotransmission involves monoamine transporters, which shuttle monoamines back into presynaptic neurons where they replenish synaptic vesicle contents. The monoamine transporters are molecular targets for antidepressants and psychostimulants that function to increase monoamine levels in the brain. For example, serotonin transporter (SERT) reuptake is inhibited by Prozac to increase serotonin levels and treat various mood disorders. Similarly, dopamine transporter reuptake is altered with drugs, such as cocaine or amphetamine, which results in enhanced dopaminergic signaling and is thought to underlie reward and addictive behaviors. Transport through the monoamine transporters is not thoroughly understood, and the traditional model with fixed substrate-ion stoichiometry has been challenged in recent years with the discovery of ionic currents mediated by monoamine transporters. In an effort to better understand the activity of monoamine transporters, a variety of substrates and inhibitors are utilized. In particular, in my work I characterize fluorescent

compounds that are based on a known monoamine transporter substrate and describe their utility as reporters to study serotonin transporter activity in real-time. In addition, I describe a novel effect induced by amphetamine and related compounds at both DAT and SERT whereby even after external removal of these compounds, a persistent current remains. These studies provide information about various substrates that exert an array of distinct effects on SERT and DAT, which may enable further studies to elucidate the nature of transporter biophysics.

1. *APP^+ is a Fluorescent Substrate for the Serotonin Transporter*

One limitation to transporter research is the inability to monitor substrate uptake in real-time. Traditional methods such as radiolabeled uptake assays, though highly specific, yield poor temporal resolution. Electrophysiology on the other hand provides excellent time resolution, but currents are mediated mostly by ionic fluxes and therefore do not yield direct information about substrate transport. To investigate this issue, we collaborated with Dr. Ian D. Tomlinson and the laboratory of Dr. Sandra Rosenthal to develop compounds based on a known monoamine transporter substrate. We identified and characterized a fluorescent compound called APP^+ that is suitable to monitor SERT transport in real-time. We employed a range of techniques to elucidate thoroughly the specificity of this compound for SERT expressed in *Xenopus laevis* oocytes and mammalian cells. Finally, we used APP^+ to study binding and transport through SERT. This work will help to uncover fundamental information about hSERT, and to improve our ability to study these transporters.

2. ***Amphetamine Induces a Persistent Leak Current in the Dopamine Transporter***

Amphetamine (AMPH) and related compounds increase dopamine (DA) levels in the brain and cause profound behavioral effects. One target for these drugs is the dopamine transporter (DAT) that normally regulates synaptic DA levels. DAT agonists, such as DA and AMPH, induce DAT-mediated currents driven by sodium. By measuring DAT currents on voltage-clamped *Xenopus laevis* oocytes, we discovered a DAT leak current induced by external exposure to the S(+)amphetamine (S(+)AMPH) enantiomer that persists long after its removal. We determined that the AMPH-induced leak current in DAT depends on sodium and is blocked by cocaine. In addition, intracellular application of S(+)AMPH can induce the leak current effectively, which suggests an internal secondary binding site in DAT. Understanding this novel effect of AMPH on DAT has implications in the understanding of human behavior because AMPH-induced persistent currents likely impact dopaminergic signaling, DA release mechanisms, and AMPH abuse.

3. A Comparison of Leak and Persistent Leak Currents Induced by Methamphetamine and 3,4-Methylenedioxymethamphetamine in the Human Dopamine and Serotonin Transporters

After establishing the S(+)amphetamine-induced persistent leak current at DAT, we expanded this work to test if other DAT-mediated releaser agents related to AMPH would also induce the persistent leak current. In particular, we focused on 3,4-methylenedioxy-methamphetamine (MDMA) and methamphetamine (METH) because it is known that although MDMA and METH are structurally related they exert distinct

behavioral effects in people. However, since MDMA has preference for the serotonin transporter and METH acts more potently at DAT, we made a comparison of the effects of METH and MDMA on both SERT and DAT. Lastly, we uncovered that the AMPH derivative *para*-chloroamphetamine (pCA) confers a substantial persistent leak current at the human serotonin transporter. These findings could open new avenues towards the study of the effect drugs of abuse have on behavior.

CHAPTER I

MONOAMINE NEUROTRANSMITTER TRANSPORTERS

Overview of Monoamine Neurotransmitters

Biogenic amine transmitters are found throughout the central nervous system (CNS), the peripheral nervous system (PNS), and the enteric nervous system (ENS) where they play a role in a variety of functions. The five well-known biogenic amines are histamine, serotonin (5-hydroxytryptamine, 5HT), and the three catecholamines (DA, norepinephrine (NE), and epinephrine (Epi)) having a catechol group in their chemical structure. Histamine is synthesized in neurons found in the hypothalamus and is known to mediate arousal and attention via central projections. In addition, it plays a role in vestibular system reactivity, immune response, and possibly even in brain blood flow. Compared to the other catecholamine transmitters, epinephrine (also called adrenaline) is found in the brain at low levels and in a smaller number of neurons. Although the distribution of Epi neurons and their projections in the brain have been described, the function of this system is unknown (Purves 2008).

A significant emphasis has been placed on the remaining three biogenic monoamine neurotransmitters (NE, DA, and 5HT) because they are important in regulating numerous critical human behaviors. Consequently, disturbances in these monoaminergic systems are associated with a plethora of medical conditions, and pharmaceutical approaches are aimed at altering levels of these three monoamine neurotransmitters.

DA is synthesized in neurons found in the substantia nigra (SN) and ventral tegmental area (VTA) in the midbrain, as well as in the hypothalamus. The precursor for DA (dihydroxyphenylalanine, DOPA) is synthesized from the hydroxylation of the amino acid tyrosine by the enzyme tyrosine hydroxylase (TH). DOPA is converted to DA by the decarboxylation by DOPA decarboxylase. Dopaminergic neurons release DA to many areas of the brain and give rise to several important dopaminergic pathways. For instance, neurons from the SN project to the striatum through the nigrostriatal pathway that plays a role in the regulation of motor coordination and is deficient in diseases such as Parkinson's disease (Purves 2008). In another example, the VTA gives rise to the mesolimbic and mesocortical dopaminergic pathways that are both thought to be involved in schizophrenia. The mesolimbic pathways projects from the VTA to the nucleus accumbens that is part of the limbic system, and the mesocortical pathway projects from the VTA to several regions in the frontal cortex. Crucial behaviors that are regulated by DA include cognition, attention, working memory, motivation, and voluntary movement. Medical conditions that are associated with the dopaminergic system in the CNS include attention deficit/hyperactivity disorder (ADHD), addiction, Parkinson's disease, and schizophrenia, and in the PNS fibromyalgia.

The primary noradrenergic nucleus where NE is synthesized is the locus coeruleus, which is located in the dorsal pons. Although noradrenergic neurons make projections to most areas in the brain, there are two main noradrenergic ascending projections: the dorsal noradrenergic bundle, which projects to the hippocampus, cerebellum, forebrain, and the ventral noradrenergic bundle, which projects to the hypothalamus, midbrain, and extended amygdala (Weinshenker and Schroeder 2007). NE is synthesized from the

hydroxylation of DA by dopamine-β hydroxylase. Noradrenergic neurons innervate many regions in the body including the spinal cord, cerebellum, amygdala, thalamus, hypothalamus, and cortex among others. NE plays a major role in the PNS to regulate many crucial autonomic nervous system functions, such as heart rate, respiration, digestion, sexual arousal, the fight-or-flight response, and other visceral functions. In addition, in the CNS the noradrenergic system regulates behaviors such as cognition, attention, and learning and memory. Some diseases associated with the noradrenergic system include (for CNS) post-traumatic stress disorder (PTSD), Alzheimer's disease, and depression and (for PNS) orthostatic intolerance, hypertension, and cardiomyopathy.

The ENS is considered a subdivision of the autonomic nervous system though it can function independently to directly control the gastrointestinal system in vertebrates. Most of the 5HT in the body (about 90%) is found in the ENS in enterochromaffin cells that line the gut mucosa, where it regulates gastrointestinal movements. Furthermore, platelets take up and store 5HT secreted from enterochromaffin cells, and use the monoamine to regulate homeostasis and blood clotting. The remaining 5HT is found in the CNS and is synthesized in several clusters of neurons along the brainstem called Raphe nuclei. Serotonergic neurons from Raphe nuclei project to many regions throughout the CNS and PNS including the forebrain, thalamus, and reticular formation. 5HT is synthesized from the amino acid tryptophan in two steps. Tryptophan is converted to 5-hydroxytryptophan by tryptophan-5-hydroxylase, and then, decarboxylation of 5-hydroxytryptophan by aromatic L-amino acid decarboxylase yields 5HT. Many behaviors including aggression, appetite, sleep, and libido are regulated by 5HT. Moreover, medical conditions associated with dysfunction in the serotonergic system include (for CNS) obsessive-compulsive

disorder (OCD), major depression, bipolar disorder, autism spectrum disorders, anxiety, and eating disorders, such as anorexia and bulimia, (for PNS) pulmonary hypertension, and (for ENS) irritable bowel syndrome.

Overview of Transport Proteins

There are a large number of membrane-bound proteins that serve the function to transport all kinds of molecules across membranes and have been grouped into many classes that include ion channels, ATP-binding cassette (ABC) transporters, water channels (aquaporins), ion pumps (ATPases), and the solute carriers (Hediger, Romero et al. 2004; Fredriksson, Nordstrom et al. 2008). With at least 384 genes in humans, the solute carriers (SLCs) make up the second largest family of membrane proteins (following G protein-coupled receptors) and the largest transporting protein group (Hoglund, Nordstrom et al. 2011). There are at least 46 distinct SLC families in the human genome that encode for passive transporters, ion transporters, and exchangers that carry many molecules across membranes, including inorganic ions, amino acids, neurotransmitters, sugars, purines, fatty acids, and drugs (Fredriksson, Nordstrom et al. 2008; Hoglund, Nordstrom et al. 2011). The two major neurotransmitter transporter gene families are solute carrier 1 (SLC1) – classically termed Na^+/K^+-dependent – and solute carrier 6 (SLC6) – classically referred to as Na^+/Cl^-dependent. More recently, these transporter gene families are grouped as the neurotransmitter sodium symporter (NSS) family (Nyola, Karpowich et al. 2010). Whereas members of the SLC1 family transport dicarboxylate amino acids, such as glutamate and aspartate, members of the SLC6 family transport a variety of substrates including amino acids, such as γ–aminobutyric acid (GABA), glycine, proline, and taurine, osmolytes (betaine, creatine), and the biogenic amines 5HT, DA, and norepinephrine (Singh 2008). An underlying property of SLC1 and SLC6 family members is that they use an ionic gradient to energize the transport of

substrate across plasma membranes (Fredriksson, Nordstrom et al. 2008; He, Vasiliou et al. 2009).

Overview of the Monoamine Neurotransmitter Transporters at the CNS Synapse

The neurotransmitters NE, DA, and 5HT are released via vesicular fusion by their respective neurons into the synaptic cleft in response to depolarization of the presynaptic terminal. After neurotransmitter diffuses and activates the postsynaptic neuron, transmitter is taken back into the presynaptic neuron through transporters located at perisynaptic areas (Hoffman, Hansson et al. 1998; Tao-Cheng and Zhou 1999). The monoamine transmitter is then re-packaged into synaptic vesicles via vesicular monoamine transporters (VMATs). In particular, the vesicular monoamine transporter 2 (VMAT2), which is primarily found in the CNS, is responsible for transmitter reuptake into synaptic vesicles of dopaminergic, serotonergic and noradrenergic neurons (Wimalasena 2011).

An illustration of a serotonergic synapse (Figure 1) is shown to illustrate a specific monoamine neurotransmitter system. In response to depolarization, serotonergic nerve terminals release 5HT into the synaptic cleft, which activates postsynaptic 5HT receptors, and SERT, located at the presynaptic membrane, transports the extracellular 5HT from the cleft into the presynaptic terminal where 5HT can be re-packaged into synaptic vesicles. Similarly, in the dopaminergic synapse, the primary means to terminate the DA signal at the synapse occurs through DAT, the corresponding presynaptic plasma membrane protein at this synapse that takes up released DA back into the presynaptic terminal where the neurotransmitter is recycled and re-packaged into synaptic vesicles.

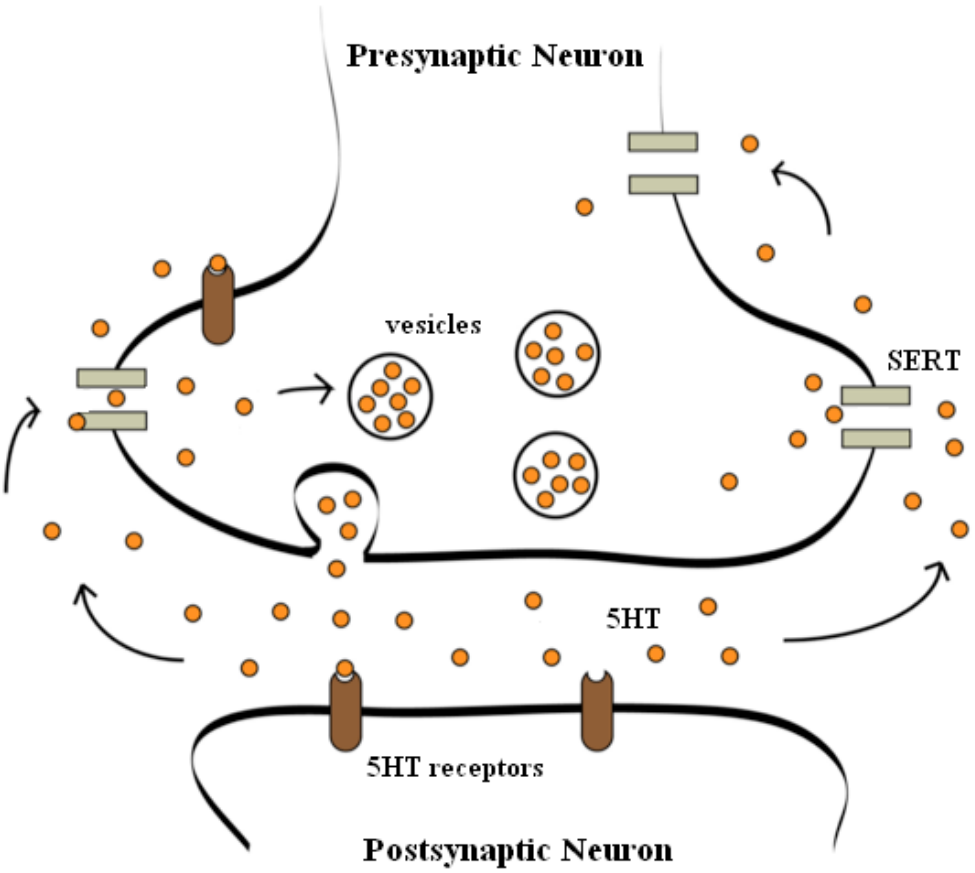

Figure 1. Serotonergic Synapse. After an action potential depolarizes the presynaptic neuron, Ca^{2+} channels at the presynaptic terminal let in Ca^{2+}, which binds to vesicular proteins triggering exocytosis of synaptic vesicles and releasing neurotransmitter 5HT into the synaptic cleft. 5HT binds to postsynaptic 5HT receptors to transmit the signal, and 5HT that diffuses from the cleft is taken up through SERT that is located in perisynaptic areas at the presynaptic terminal (Tao-Cheng and Zhou 1999), thereby terminating neurotransmission.

The Role of Serotonin in Disease

5HT is a neurotransmitter that plays a role in the regulation of many behaviors, such as mood, sleep, appetite, temperature, sexual behavior, and aggression (Schloss and Williams 1998; Stahl 1998). Defects of the serotonergic system in disease were postulated by early studies showing that plasma levels of 5HT's precursor, tryptophan, were reduced in patients with depression (Coppen, Shaw et al. 1967). Subsequent studies have implicated disturbances in the serotonergic system in many more diseases, including bipolar disorder, autism, and a spectrum of psychiatric disorders, such as anorexia nervosa, bulimia, and obsessive-compulsive disorder (OCD) (Feighner 1994; Vaswani, Linda et al. 2003; Vaswani and Kalra 2004).

The Role of the Human Serotonin Transporter in Disease

Evidence for specific roles of human SERT (hSERT) in disease comes from many genetic studies. In humans, the gene that encodes for SERT, solute carrier family 6 neurotransmitter transporter, 5HT, member 4 (*SLC6A4*), is located on chromosome 17 at 17q11.1-q12, and is organized into 14 exons (Sghendo and Mifsud 2012). Mutations associated with the hSERT gene have been shown to affect SERT function and specific polymorphisms that alter hSERT expression and activity are correlated with autism, rigid/compulsive traits related to OCD, and major depression (Murphy, Lerner et al. 2004; Prasad, Zhu et al. 2005; Sutcliffe, Delahanty et al. 2005; Prasad, Steiner et al. 2009). For instance, the promoter region of the SLC6A4 contains a polymorphism with 'short' and 'long' repeats (termed the serotonin transporter-linked polymorphic region or 5HTTLPR), and the short variation has been associated with decreased hSERT expression, anxiety-related personality traits, an increased risk of major depression, and poorer response to antidepressants in people with major depression (Lesch, Bengel et al. 1996; Sghendo and Mifsud 2012). Additionally, a gain-of-function phenotype associated with hSERT, Ile425Val, that causes constitutive activation of transport activity (Kilic, Murphy et al. 2003), has been traced to subjects exhibiting complex psychiatric phenotypes, including OCD and Asperger's Syndrome (Ozaki, Goldman et al. 2003). Ile425Val illustrates how abnormal hSERT activity can affect serotonergic signaling. In this case, it is thought that reuptake activity by the hSERT variant is abnormally increased, leading to lower 5HT concentrations at the synaptic cleft and diminishing serotonergic signaling (Kilic, Murphy et al. 2003).

Serotonin Transporters as Therapeutic Targets

The discovery in the early 1950s that the antitubercular drug, iproniazid, a monoamine oxidase inhibitor (MAOI) that blocks the effect of monoamine oxidase (MAO) to break down and inactivate monoamine neurotransmitters, had mood-elevating effects, led to the monoamine hypothesis of depression. Iproniazid increased levels of 5HT and other monoamines by inhibiting its degradation by the enzyme monoamine oxidase. Since MAOIs produced many adverse side-effects, efforts focused on the development of several classes of drugs targeting monoamine transporters, such as tricyclic antidepressants (TCAs) and selective serotonin reuptake inhibitors (SSRIs) that inhibit reuptake of 5HT into presynaptic terminals, and prolong the neurotransmitter's action at the synapse (White, Walline et al. 2005). In addition to increasing 5HT levels, TCAs exert effects as a norepinephrine reuptake inhibitor, an anticholinergic-antimuscarinic agent, an alpha1-adrenergic antagonist, an antihistamine, and even a sodium channel inhibitor, which can potentially cause lethal cardiac arrhythmias and seizures (Stahl 1998). Thus, the adverse side effects of TCAs led to focus on the development of SSRIs that targeted only SERT. Fluoxetine (FLX, Prozac) was the first drug of this kind approved as a therapeutic agent by the regulatory authorities in the USA (Sghendo and Mifsud 2012). Further SSRIs have been synthesized to lessen the adverse side effect profile of FLX, such as citalopram, escitalopram, fluvoxamine, and sertraline. These SSRIs have fewer activating side effects, such as insomnia, anxiety, and tremors, and fewer gastrointestinal side effects, such as nausea, diarrhea, anorexia, and vomiting; therefore, they are preferred over use of FLX (Sghendo and Mifsud 2012). Presently, SSRIs are the most widely prescribed drugs for the treatment of depression, OCD, and

bipolar disorder, as well as other diseases such as anxiety, anorexia, and panic disorders (Stahl 1998). In addition, the recreational drug 3,4-methylenedioxy-methamphetamine (MDMA, ecstasy) has been effectively used in the treatment of anxiety disorders; in particular, MDMA has been shown to improve post-traumatic stress disorder (PTSD) patients (Johansen and Krebs 2009; Mithoefer, Wagner et al. 2011). MDMA targets the monoamine neurotransmitter transporters, but possesses greater potency for hSERT. It is thought that MDMA increases monoamine transmitter levels in the brain by reversing the direction of transport of hSERT, hDAT, and hNET, and inducing the release of the corresponding endogenous monoamine transporter substrates (5HT, DA, and NE, respectively) (Schloss and Williams 1998).

The Role of Dopamine in Disease

Disturbances in the dopaminergic system have been implicated in numerous brain illnesses, including Huntington's chorea, Parkinson's disease, schizophrenia, attention-deficit/hyperactivity-disorder (ADHD), depression, and addiction (Barbeau 1970; Javitch and Snyder 1984; Gainetdinov and Caron 2003; Gainetdinov 2008). Perhaps the most striking illness associated with the dopaminergic system is Parkinson's disease, which is the second most common neurological disorder in the United States, and is characterized by impairment of motor function that is attributed to massive death of dopaminergic neurons comprising the nigrostriatal pathway (Javitch and Snyder 1984; Jellinger 1991).

ADHD is another illness associated with a deficient dopaminergic system, which has become one of the most common neurobehavioral disorders of childhood (Bedard, Schulz et al. 2010). ADHD is a highly heritable psychiatric disorder affecting anywhere from 4-10% of children and 5% of adults (Barr, Wigg et al. 1999; Krause, Dresel et al. 2000; Mazei-Robison, Couch et al. 2005; Mazei-Robinson and Blakely 2006; Bedard, Schulz et al. 2010). A more recent review of the scientific literature estimated the worldwide prevalence of ADHD in children to be 5.29% (Polanczyk, de Lima et al. 2007). Although the cause of ADHD is far from understood, overwhelming evidence points toward the dopaminergic system, and altered DA signaling appears to be central to the disease.

The Role of the Human Dopamine Transporter in Disease

The human dopamine transporter (hDAT) gene (*SLC6A3*) is located on chromosome 5 at 5p15.3 and contains 15 exons and 14 introns (Kawarai, Kawakami et al. 1997). Genetic studies have implicated variations to this gene in specific illnesses. In particular, polymorphisms in a variable number tandem repeat (VNTR) in the 3' untranslated region of hDAT has been linked to the ADHD phenotype (Bedard, Schulz et al. 2010), and an hDAT variation, lacking the hDAT 10-repeat allele, confers differences in how ADHD children respond to methylphenidate hydrochloride (MPH, Ritalin) treatment (Froehlich, Epstein et al. 2011). In addition, the human DAT coding variant Ala559Val identified in children diagnosed with ADHD displays anomalous AMPH-mediated DA efflux and responds differently to ADHD medications than wild-type hDAT (Mazei-Robison, Bowton et al. 2008). Moreover, a loss-of-function mutation in DAT that impairs DA reuptake is thought to cause autosomal recessive infantile parkinsonism-dystonia (Kurian, Zhen et al. 2009). More recently, single nucleotide polymorphisms (SNPs) in the DAT gene have been associated with positive symptoms of schizophrenic patients (Zheng, Shen et al. 2012). In total, at least 63 DAT variants have been described from which two SNPs, one in intron 8 and one in intron 13, were found to be moderately associated with bipolar disorder (Greenwood, Schork et al. 2006).

Dopamine Transporters as Therapeutic Targets

Management of DA levels in the brain is essential for proper function, and DA reuptake is critical to maintain DA homeostasis. In the human nervous system, DAT is largely responsible for performing this function. The human DAT (hDAT) is found presynaptically at dopaminergic synapses, on the cell body, and in neuronal dendrites. Along with DA release mechanisms and DA degradation, hDAT controls the concentration profile of extracellular DA (Spielewoy, Gonon et al. 2000); therefore, hDAT contributes to the normal function of the nervous system and to mental disorders (Hahn and Blakely 2002). Consequently, hDAT is a major molecular target for therapeutic agents, such as methylphenidate hydrochloride (MPH, Ritalin) and AMPH (Adderall). Both compounds, which are often prescribed to treat ADHD, act directly on hDAT to increase extracellular DA levels, but they do so via different actions on hDAT. Whereas MPH is a DAT reuptake inhibitor, AMPH is a DAT substrate thought to stimulate DA release through non-vesicular reverse DA transport through DAT (Wall, Gu et al. 1995; Wu and Gu 1999).

Drugs of abuse, such as methamphetamine (METH) and cocaine (COC), increase DA levels via similar mechanism as the aforementioned therapeutic agents. For example, similarly to MPH, drugs like COC inhibit DA transport by DAT, and thus increase extracellular DA. METH and related compounds, such as AMPH and Adderall, are transported by DAT to subsequently cause DA release by reversing DAT transport. Interestingly, because an abnormal increase in DA may be at the core of psychiatric disorders and drug abuse (Henry and Blakely 2008), these compounds can produce adverse reactions, such as psychosis, and the strong DA release underlies their strong

abuse potential. Regardless, they present the best treatment available for certain mental illnesses (Fleckenstein, Volz et al. 2007).

Since the psychostimulants AMPH and METH lead to the release of catecholamines (DA and NE) in the frontal lobe and limbic system (by transmitter reuptake inhibition at hDAT and hNET and transmitter efflux by hDAT and hNET), they have been used clinically to treat medical conditions that benefit from an increase in catecholaminergic neurotransmission, such as attention-deficit/hyperactivity disorder and narcolepsy (Burnette, Bailey et al. 1996; Fleckenstein, Volz et al. 2007). Due to the higher potency of the dextro-rotary AMPH isomer (S(+)AMPH) over the levo-rotary AMPH isomer (R(–)AMPH) to release DA through hDAT (Phillips, Brooke et al. 1975; Holmes and Rutledge 1976; Kuczenski, Segal et al. 1995), therapeutic agents are composed primarily of S(+)AMPH. For example, Adderall is composed of 3:1 S(+)AMPH to R(–)AMPH (Cody, Valtier et al. 2003), and Vyvanse (lisdexamphetamine) is a pro-drug composed of S(+)AMPH conjugated to L-lysine, which is metabolized entirely to S(+)AMPH (Heal, Cheetham et al. 2009; Najib 2009). Even the dextro-rotary isomer of METH is marketed as Desoxyn for the treatment of ADHD and narcolepsy (Mendelson, Uemura et al. 2006).

Clinical manifestations associated with the abuse of AMPH or its precursors or derivatives, such as phenethylamine or METH, are well documented (Potkin, Karoum et al. 1979; Romanelli and Smith 2006; Winslow, Voorhees et al. 2007). In an attempt to bypass the reward system, the non-stimulant selective NE reuptake inhibitor (NRI) atomoxetine (Strattera) has been introduced for the treatment of ADHD (Heal, Cheetham et al. 2009). Lastly, bupropion (Wellbutrin) is used to treat depression (Wu and Gu 1999;

Mazei-Robinson and Blakely 2006) through unique actions as a dual DA and NE reuptake inhibitor (Arias 2009).

Transport Mechanism of the Human Serotonin and Dopamine Transporters

Traditionally, hSERT was classified as a Na^+/Cl^--coupled co-transporter since it requires both Na^+ and Cl^- to transport substrates; more recently, hSERT and related transporters, such as the GABA and norepinephrine transporters, have been termed neurotransmitter sodium symporters, which reflects the limitation of knowledge about the ionic contribution for substrate transport (Ramamoorthy, Bauman et al. 1993). In order to transport substrate, co-transporters use the gradients of ions to concentrate their substrate against their concentration gradient. Na^+ levels are ten times higher outside than inside cells, creating a gradient that is used by hSERT to transport and concentrate 5HT against its concentration gradient (DeFelice and Blakely 1996; Rudnick 1998; Rudnick 1998). Traditionally, co-transport is described by alternating access models (see Figure 2), in which ions (Na^+ and Cl^-) and substrate (5HT) bind the transporter in its outward-facing conformation, an inward-facing conformational change is catalyzed, and the substrate and ions are transported from outside to inside. Subsequently, a counter-ion, either a proton (H^+) or a K^+, is transported from inside to outside of the plasma membrane returning the transporter to the outward-facing conformation. This model is supported by biochemical and radiolabeled uptake data (Naftalin 1984; Stein 1986; Naftalin 2005) and seems consistent with recent structural data for co-transporters (Abramson, Smirnova et al. 2003; Abramson, Smirnova et al. 2003; Yernool, Boudker et al. 2004; Yamashita, Singh et al. 2005). Similarly, it has been proposed that DAT also abides by the alternating access model, in which the transport of DA is coupled with fixed stoichiometry to the downhill movement of Na^+ ions, and that the stoichiometry for transport of substrate consists of two Na^+, and one Cl^-, coupling to a DA in the outward-facing hDAT

conformation, and either a K^+ or H^+ binds to the inward-facing conformation to return hDAT to the outward-facing conformation (McElvain and Schenk 1992; Gu, Wall et al. 1994; Sonders, Zhu et al. 1997).

Transport-associated Currents of the Serotonin and Dopamine Transporters

Early studies using biochemical approaches and radiolabeled flux led to the emergence of the "Alternating Access" model for SERT transport (illustrated in Figure 2), which proposed that the stoichiometry for each transport cycle in the mammalian SERT to be one Na^+, one Cl^-, and one 5HT co-transported into the cells, and one K^+ counter-transported (Keyes and Rudnick 1982; Rudnick and Wall 1993). As stated above, DAT was also proposed to abide by the alternating access model (AAM), but the stoichiometry for transport of substrate consists of two Na^+ and one Cl- for each DA transported (McElvain and Schenk 1992; Gu, Wall et al. 1994; Sonders, Zhu et al. 1997).

Subsequent studies have led to an emerging idea about the existence of uncoupled currents, in which transporters possess channel-like activity ("Channel in Transporter" mode shown in Figure 2) (Quick 2003; DeFelice 2004; DeFelice and Goswami 2007). In coupled currents, associated with co-transport, ions are 'coupled' to substrate and both ions and substrate are transported according to a defined stoichiometry. Since the early 1990s, uncoupled currents, in which currents associated with substrate transport are much larger than what can be accounted for by the measured stoichiometry, have been found in many neurotransmitter transporters (Mager, Min et al. 1994; Galli, DeFelice et al. 1995; Galli, Blakely et al. 1996; DeFelice and Galli 1998; DeFelice and Galli 1998; Galli, Blakely et al. 1998; Petersen and DeFelice 1999; Adams and DeFelice 2002; Ramsey and DeFelice 2002; Adams and DeFelice 2003; Li, Zhong et al. 2006).

Uncoupled currents in transporters are largely unexplained and their function is unknown, but one possibility is that these currents play a functional role in neurotransmission by depolarizing or hyperpolarizing neurons (Sonders and Amara 1996;

Ingram, Prasad et al. 2002; Quick 2002; Quick 2003; Carvelli, McDonald et al. 2004; Ryan and Mindell 2007). Even though most of the evidence for channels in SERT comes from heterologous expression systems, large 5HT-induced currents are also generated in SERT at actual serotonergic synapses (Bruns, Engert et al. 1993; Bruns 1998).

Uncoupled DAT currents have been described, but in at least one study, Cl- seems to contribute to their ionic composition (Carvelli, McDonald et al. 2004); however, in our work Na^+ is a major contributor to DAT-mediated substrate-induced currents (Rodriguez-Menchaca, Solis et al. 2012). Studies using molecular biology and fluorescence resonance energy transfer microscopy suggest SERT prefers to assemble into a multimeric complex, probably consisting of dimers or tetramers (Kilic and Rudnick 2000; Schmid, Just et al. 2001; Schmid, Scholze et al. 2001), and a recent study of transporter-associated currents in glutamate transporters proposed that channels maybe be located in the individual subunits (Larsson, Picaud et al. 1996; Leary, Stone et al. 2007). However, for the monoamine neurotransmitter transporter (*SLC6* gene) family, it is still not thoroughly established if the currents are mediated through each individual oligomer or if they function once they are assembled into multimeric complexes.

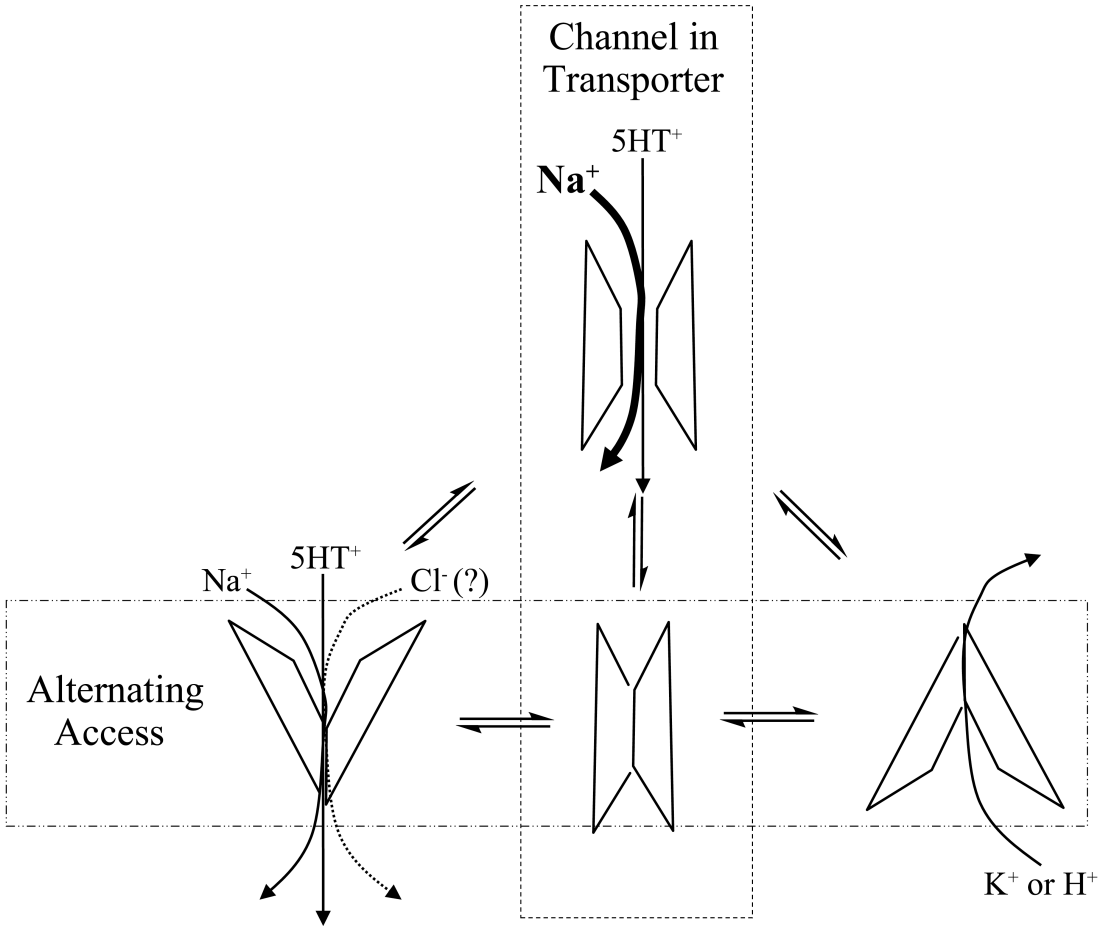

Figure 2. Substrate transport models of hSERT. The 'Alternating Access Model (AAM)' abides by a fixed stoichiometry in which 1 Na^+, 1 $5HT^+$ and 1 Cl^- are co-transported together and 1 K^+ is counter-transported returning hSERT to its outside-facing conformation. In the AAM, hSERT would be electroneutral (net charge = 0), which would yield negligible currents even if 2 Na^+ ions are co-transported (along with the 5HT and Cl^-) as has also been predicted. On the other hand, the "Channel in Transporter Model" yields uncoupled currents in which the ratio of Na^+ ions to 5HT is larger than what is accounted for by the fixed stoichiometry of the AAM. This renders hSERT electrogenic (net charge larger than what is accounted by fixed AAM stoichiometry); therefore, hSERT produces large uncoupled currents.

Serotonin and Dopamine Transporters Display a Leak Current

Since a study by Mager and colleagues in 1994, it has become well established in electrophysiological studies that monoamine transporters possess an alternate current that can be seen when inhibitors are applied to these transporters. One of the first instances was the identification of currents manifested by the rat SERT, which were termed leak currents (Mager, Min et al. 1994). For SERT many studies have employed two-electrode voltage-clamp (TEVC) in *Xenopus laevis* oocytes over-expressing SERT (clamped to potentials near physiological resting membrane potentials) to clearly show that many different inhibitors reveal the SERT leak current, which is characterized as an outward, hyperpolarizing current and is thought to be mediated primarily by Na^+. Some examples include studies using the selective serotonin reuptake inhibitors fluoxetine (FLX) (Wang, Li et al. 2006) and citalopram (both (R)- and (S)-citalopram isomers) (Storustovu, Sanchez et al. 2004), and the tricyclic antidepressants desipramine (DES) (Lin, Lester et al. 1996) and imipramine (IMI) (Barker, Moore et al. 1999).

The majority of SERT inhibitors used in research, including the ones mentioned above, have been shown to elicit long-lasting electrophysiological effects after their removal that are indicative of a distinct action on SERT compared to that of substrates (which typically induce effects that are easily washed out). For example, from our studies, we know that after exposure to FLX, there is a much weaker action of 5HT (or other substrates) at hSERT. Also, when FLX is applied alone, even removal of FLX and perfusion of standard solution does not bring the holding current back to baseline, which is different than substrates that usually wash out quickly returning to baseline. To bring this persistent FLX-induced outward current (in absence of FLX) to original baseline

levels and then to inward currents, 5HT can be applied, however, this requires perfusion for a duration that far exceeds the time it takes to induce SERT-mediated inward currents in the absence of FLX (at least 3 minutes) and the response looks dissimilar to the 5HT-induced current prior to FLX application. In agreement, the aforementioned Wang et al. study shows that exposure to FLX leads to a greatly diminished 5HT-induced hSERT-mediated current response (as measured by the peak current time constant): "the time constant for 5HT-induced current became much greater than that for the first 5HT perfusion". This study further exemplifies the long-lasting FLX effect on hSERT that distinguishes inhibitors and argues against a balance between the two currents.

Lastly, under physiologically relevant experimental concentrations, the FLX-induced outward current supersedes inward 5HT-induced currents (when 5HT and FLX are simultaneously applied – even with high 5HT concentrations). This further suggests FLX acts tightly at SERT (like a cork in a bottle) that both inhibits the endogenous transporter leak current and disables substrate-induced currents at SERT. These results are shown consistently in different studies with other SERT inhibitors, including desipramine (Lin, Lester et al. 1996), imipramine (Barker, Moore et al. 1999), and paroxetine (personal observations). In addition, the similar phenomena are seen with both isomers of citalopram (Storustovu, Sanchez et al. 2004). Storustovu et al. demonstrate that applying citalopram during an evoked 5HT-induced SERT response takes the current back to baseline (even to an outward current when using the (S)-citalopram isomer). Moreover, it is shown that treatment with citalopram (prior to 5HT application) leads to a diminished subsequent 5HT response (especially with the (S)-citalopram isomer) (Storustovu, Sanchez et al. 2004).

Analogous inhibitor-induced outward (leak) currents that occur in the absence of extracellular DA have been identified in DAT. Inhibitors for DAT, such as cocaine and cocaine analogs, induce outward currents in DAT-expressing voltage-clamped *Xenopus laevis* oocytes (Sonders, Zhu et al. 1997). The DAT-mediated outward current elicited by cocaine does wash out and return back to baseline, albeit at a slower rate than the substrate (DA)-induced inward current, and this is attributed to its action as an inhibitor – rather than a substrate – at DAT. Inhibitors with much higher affinity, such as the cocaine analog (1R)-2beta-Carbomethoxy-3beta-(4-iodophenyl)tropane (β-CIT), behave much tighter when inhibiting DAT since its evoked outward-current is difficult to wash out, not unlike the behavior seen with FLX on SERT.

Structure of the Human Serotonin and Dopamine Transporters

The *SLC6* gene family encodes for transporters having 12 transmembrane (TM) domains (TMDs) with intracellular N- and C-termini, and a large extracellular loop between TM domains 3 and 4 (topology shown in Figure 3A) that contain glycosylation sites (Chen, Reith et al. 2004). Specifically, the gene *SLC6A3* encodes for the 620-amino acid protein hDAT with a relative molecular weight of 68.4 kDa. *SLC64A* encodes for the 630-amino acid protein hSERT having a relative molecular weight of 70.22 kDa (Chen, Reith et al. 2004). A breakthrough in the elucidation of the tertiary structure of the monoamine neurotransmitter transporters came when the crystal structure a bacterial homologue, the leucine transporter from *Aquifex aeolicus* ($LeuT_{Aa}$), was obtained (Yamashita, Singh et al. 2005). The structure of $LeuT_{Aa}$, a member of the SLC gene family, was solved at 1.65 Å resolution in complex with its substrate and two Na^+ ions bound halfway across the bilayer in the unwound portions of TMD 1 and 6. There is an anti-parallel structure relating TMD 1-5 to TMD 6-10 (illustrated with grey triangles in Figure 3A). Although the overall sequence identity between the eukaryotic and prokaryotic counter parts is only 20-25%, the sequence identity in the binding pocket is thought to be up to 45-50%. Still, due to its similarities, especially at the central binding site, the crystal structure of $LeuT_{Aa}$ has been employed by many groups to produce molecular homology models of the monoamine transporters, including models for hSERT (Celik, Sinning et al. 2008; Sarker, Weissensteiner et al. 2010; Combs, Kaufmann et al. 2011; Gabrielsen, Kurczab et al. 2012) and hDAT (Indarte, Madura et al. 2008; Shan, Javitch et al. 2011). Primarily, these models are used to study interactions between the transporters and their substrates or inhibitors. An example of a homology model of SERT

showing its endogenous substrate 5HT docked within the active region of SERT (Figure 3B), and a closer view of the active region with the interactions 5HT makes within SERT (Figure 3C) illustrates how these models provide information about the interaction between substrate and transporter.

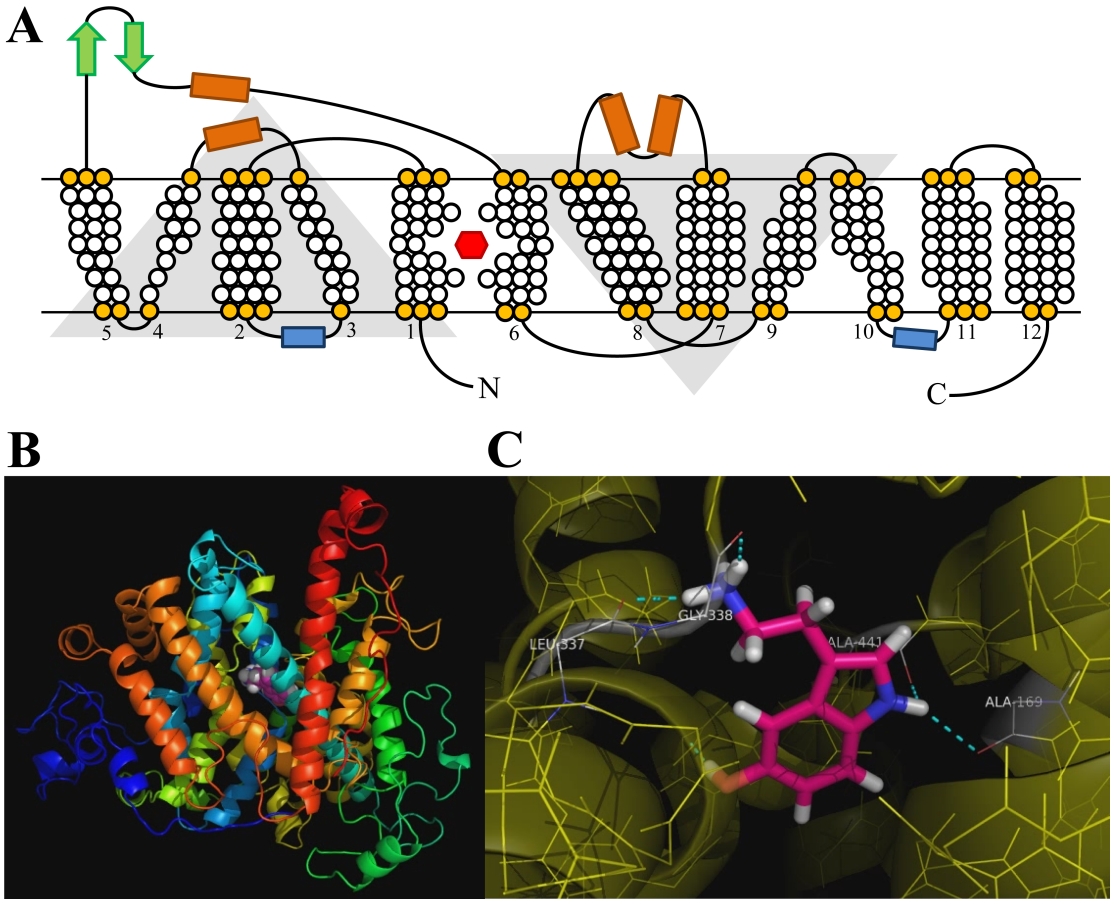

Figure 3. Topology and homology model of SERT. (A) SERT is composed of 12 transmembrane domains. Helices 1-5 are structurally similar to helices 6-10, but fold in opposing directions (represented with gray triangles) to form an anti-parallel structure. Green arrows represent β-sheets, orange rectangles represent extracellular loops, blue rectangles represent intracellular loops, and the red hexagon shows 5HT at the active region. Based on Yamashita, Singh et al. 2005. (B) Tertiary structure of hSERT based on the crystal structure of the bacteria *Aquifex aeolicus* leucine transporter. (C) The endogenous substrate 5HT (shown in pink) binds at the active region of hSERT and interacts with amino acid residues on transmembrane helices 1, 3, 6, and 8. B and C were based on the Yamashita, Singh et al. 2005 leucine transporter crystal structure and obtained from Igor Zdravkovic.

Fluorescence Substrates to Study Monoamine Transporter Activity

Previous studies in the lab took advantage of the fluorescent compound ASP^+ (4-(4-(dimethylamino)-styryl)-N-methylpyridinium) to study the human norepinephrine transporter (hNET) and the human dopamine transporter (hDAT) (Schwartz, Blakely et al. 2003; Schwartz, Novarino et al. 2005). ASP^+ was successfully utilized to study mechanistic properties of hNET fluorometrically. For example, it was discovered that ASP^+ could be used to monitor two distinct components of hNET activity, binding and uptake (Schwartz, Blakely et al. 2003). Furthermore, the ability to fluorometrically measure ASP^+ binding to hNET allowed for advanced microscopy techniques to be performed (in particular fluorescence fluctuation correlation spectroscopy), and the substrate-protein stoichiometry was determined, which provided the information that each ASP^+ molecule resided on an hNET for 526 μs before being transported (Schwartz, Novarino et al. 2005).

Although ASP^+ was well-transported by both hNET and hDAT with good k_m (~2 μM) for uptake, it yielded a very weak k_m (up to 100 μM) for transport by hSERT (Schwartz, Piston et al. 2006); therefore, development of alternative fluorescent substrates to study hSERT was warranted. ASP^+ conferred fluorescence due to resonance within its structure and the contribution of the free electrons from the dimethyl amino moiety (Figure 4). Following on this chemical property to fluoresce, compounds synthesized were based on an ASP^+ analog, 1-methyl-4-phenylpyridinium (MPP^+), which is a known monoamine transporter substrate that has reasonable affinity for monoamine transporter uptake. The addition of an electron donating dimethyl amino group to the phenyl ring of MPP^+ results in a fluorescent compound called APP^+ (Figure 4 and Figure

7A), which is also known as IDT307. This fluorescence is not evident in solution but only arises after stabilization of the two rings in a fixed conformation that is achieved after transport and immobilization by binding to intracellular proteins. The dimethyl amino group of APP^+ interacts with the rest of the structure by donating electrons to the pyrimidine ring producing resonance and yielding fluorescence within the visible range. In an effort to study mechanistic properties of SERT fluorometrically, additional fluorescent MPP^+ analogs were synthesized (Figure 7B) (Mason, Farmer et al. 2005); however, based on its brightness APP^+ proved to be the optimal fluorescent substrate to specifically study SERT activity. In fact, this compound has been marketed in a neurotransmitter uptake kit, and has applications for high-throughput screening (HTS) assays in solution using a FlexStation (Jorgensen, Nielsen et al. 2008) and for monitoring SERT regulation (Chang, Tomlinson et al. 2012). To further understand how these fluorescent compounds can be used to measure SERT activity at the cellular level, in a study described in Chapter 2, I employ fluorescence microscopy to visualize and compare APP^+ and ASP^+ in single cells expressing hSERT. Also, by use of electrophysiology I make an additional distinction between the effect these related compounds have on hSERT (Solis, Zdravkovic et al. 2012).

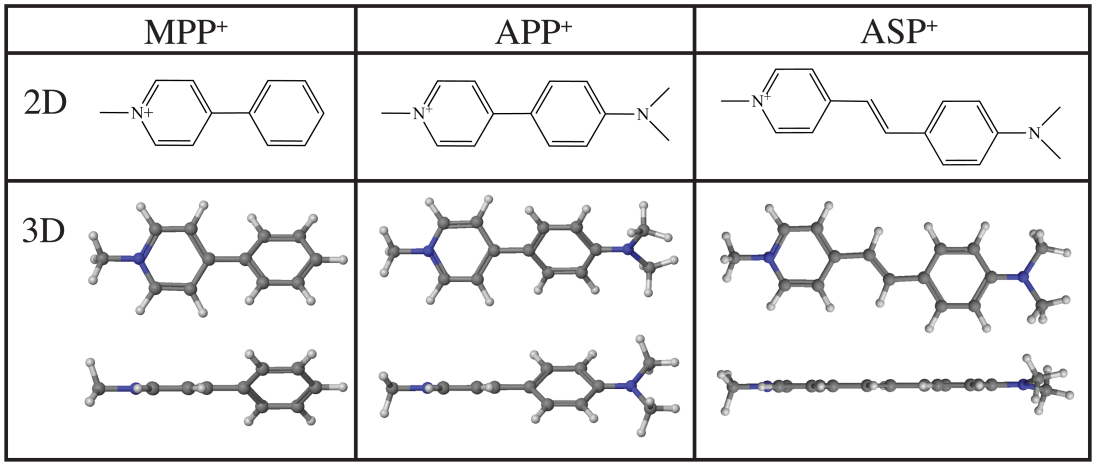

Figure 4. Structures of MPP^+ and its fluorescent analogs APP^+ and ASP^+. The addition of an electron donating dimethyl amine group to the phenyl ring of MPP^+ results in the fluorescent compound APP^+, which can be compared with ASP^+, the previously characterized fluorescent substrate for hNET (chemical structures shown in two-dimensional (2D) views, top row). Two three-dimensional (3D) views showing energy minimized MPP^+, APP^+, and ASP^+ (bottom row). Although the aromatic rings in APP^+ do not attain a co-planar conformation and favor twisted dihedral angles, ASP^+ adopts a co-planar conformation. Energy was calculated at increments of 18° rotation around the dihedral angle linking the two rings providing a torsional scan. The coordinate files created in Molden and optimized in Gaussian03, provided us with the most energetically favorable structure *in vacuo* and the most physiological relevant structure. Energy minimization performed by Igor Zdravkovic. Adapted from Solis, Zdravkovic et al. 2012.

Drugs of Abuse that Target the Monoamine Transporters

AMPH (α-methylphenethylamine) is a homologue of phenethylamine and the parent compound of a wide range of psychoactive derivatives, from the N-methylated methamphetamine (METH, N-methyl-1-phenylpropan-2-amine) to 3,4-methylenedioxy-methamphetamine (MDMA, also known as ecstasy). AMPH is widely abused and the clinical manifestations associated with the abuse of AMPH, its precursors, or its derivatives, such as phenethylamine or METH, are well documented (Potkin, Karoum et al. 1979; Romanelli and Smith 2006; Winslow, Voorhees et al. 2007). Because DAT is the primary target for AMPH, DAT is most frequently implicated in the reinforcing properties and abuse potential of AMPH (Sulzer, Maidment et al. 1993; Sulzer, Chen et al. 1995; Seidel, Singer et al. 2005). Conversely, MDMA, which is commonly used as a recreational drug and has possible neurotoxic effects (Lyles and Cadet 2003), is similar in structure to METH, and like DA it bears oxygen moieties at the *meta*- and *para*- ring-positions. MDMA can produce AMPH-like effects in various animal species (Green, Mechan et al. 2003), and in humans, it induces a sense of euphoria and diminished anxiety, leading to the therapeutic potential of MDMA for post-traumatic stress disorder (Johansen and Krebs 2009; Mithoefer, Wagner et al. 2011). Similar to AMPH and METH, the stimulant actions of MDMA are believed to involve the release of DA in the *nucleus accumbens* (Gold, Hubner et al. 1989); however, MDMA has higher potency (than METH) to induce 5HT release through hSERT (Rothman and Baumann 2006). This outcome, in which METH and MDMA elicit distinct behavioral and neurochemical responses in rodents and human despite their structural similarities, is explored in Chapter 4. In particular, we seek to find a relationship between these METH- and

MDMA-induced behavioral and neurochemical differences and the electrophysiological effect METH and MDMA elicit on their targets, hDAT and hSERT.

Mechanism of Reverse Transport of the Serotonin and Dopamine Transporters

The reward and addiction properties of AMPH, METH, and MDMA rely on their ability to increase extracellular DA and 5HT levels by mechanisms as yet only partially understood. These agents exhibit competitive inhibition on monoamine transporters, which leads to diminished uptake of their neurotransmitters, and therefore, increased levels of endogenous neurotransmitters at the synaptic cleft. An additional view for the action AMPH and related compounds have on monoamine transporter to increase monoamine neurotransmitter levels is efflux of endogenous neurotransmitters through the transporters via a mechanism called 'reverse transport' (Khoshbouei, Wang et al. 2003). Although SERT, NET, and DAT all are capable of reverse transport, DAT is the predominant monoamine transporter studied presumably due to its implications in addiction. The efflux of DA stimulated by AMPH would result in higher DA concentrations at the synaptic cleft and increased excitation of presynaptic and postsynaptic DA receptors. The principal proposed mechanisms for AMPH-induced DAT-mediated DA efflux are 1) the facilitated exchange diffusion model (Burnette, Bailey et al. 1996), 2) the channel-in-transporter DA efflux model (Kahlig, Binda et al. 2005), 3) the oligomer-based counter-transport model (Seidel, Singer et al. 2005), and 4) the vesicular depletion model (or weak-base model), in which interaction of the releasing substrate (AMPH) with the vesicular monoamine transporter disrupts vesicular storage leading to an increase in free cytoplasmic levels of transmitter (Sulzer, Maidment et al. 1993; Sulzer, Chen et al. 1995). In addition, regulation of DAT-mediated DA efflux has been reported; examples include protein kinase C (PKC)-activated DA efflux (Khoshbouei, Sen et al. 2004) and Ca^{2+}/calmodulin-dependent protein kinase II

(CaMKII) facilitating phosphorylation and leading to DAT-mediated DA efflux (Fog, Khoshbouei et al. 2006).

In contrast to the existing models, a study described in Chapter 3 explores a novel mechanism of the action of AMPH on DAT that is based on new electrophysiological data. In this model, AMPH is transported by DAT and concentrated inside the cell where the drug persists and is available to bind to the transporter at an internal site. The binding of AMPH at this internal site may maintain the transporter in a conductive state even when the external substrate is removed, leading to a persistent leak ("shelf") current; furthermore, it is proposed that external DA and other substrates can hold DAT in a constitutively-active state once internal AMPH is present. In addition, Chapter 4 describes a study that shows the persistent leak current can be elicited with additional select releasing substrates and in different monoamine transporters; in particular S(+)METH can produce a persistent leak current in hDAT, and S(+)METH and both stereoisomers of MDMA produce the same response in hSERT. There are important implications this novel mechanism would have on synaptic neurotransmission. Thus, more work still needs to be done to address the importance and implications of this novel monoamine transporter mechanism. Lastly, there might be a relationship between the ability of these releasing substrates (AMPH, METH, MDMA) and their ability to produce the persistent leak current that needs to be studied further.

CHAPTER II

4-(4-(DIMETHYLAMINO)PHENYL)-1-METHYLPYRIDINIUM (APP^+) IS A FLUORESCENT SUBSTRATE FOR THE HUMAN SEROTONIN TRANSPORTER

Parts of Chapter 2 are adapted from Solis, E., Jr., I. Zdravkovic, I. D. Tomlinson, S. Y. Noskov, S. J. Rosenthal and L. J. De Felice (2012). "4-(4-(dimethylamino)phenyl)-1-methylpyridinium (APP+) is a fluorescent substrate for the human serotonin transporter." J Biol Chem **287**(12): 8852-8863.

STUDY OVERVIEW

Background and Purpose

Monoamine transporters terminate synaptic neurotransmission and are molecular targets for antidepressants and psychostimulants. Fluorescent reporters that can monitor real-time transport are amenable for high-throughput screening. However, until now their use has mostly been successful to study the catecholamine transporters, but not the serotonin (5HT) transporter (SERT).

Experimental Approach

We use fluorescence microscopy, electrophysiology, pharmacology, and molecular modeling to compare fluorescent analogs of 1-methyl-4-phenylpyridinium (MPP^+) as reporters for the human serotonin transporter (hSERT) in single cells.

Key Results and Conclusions

The fluorescent substrate 4-(4-(dimethylamino)phenyl)-1-methylpyridinium (APP^+), also known as IDT307, exhibits superior fluorescence uptake in hSERT-expressing HEK293 cells than other MPP^+ analogs tested. APP^+ uptake is Na^+- and Cl^--dependent, displaced by 5HT, and inhibited by fluoxetine, suggesting APP^+ specifically monitors hSERT activity. ASP^+, which was previously used to study catecholamine transporters, is 10 times less potent than APP^+ at inhibiting 5HT uptake and has minimal hSERT-mediated uptake. Furthermore, in hSERT-expressing oocytes voltage-clamped to –60 mV, APP^+ induced fluoxetine-sensitive hSERT-mediated inward currents, indicating

APP^+ is a substrate, whereas ASP^+ induced hSERT-mediated outward currents, and counteracted 5HT-induced hSERT currents, indicating that ASP^+ acts as an inhibitor. Extra-precise ligand-receptor docking of APP^+ and ASP^+ in an hSERT homology model showed both ASP^+ and APP^+ docked favorably within the active region; accordingly, comparable concentrations are able to elicit their opposite electrophysiological responses.

Implications

We demonstrate that APP^+ is better suited than ASP^+ to study hSERT transport fluorometrically. APP^+ represents a new tool that will help move transporter research forward.

INTRODUCTION

The Serotonin Transporter

Serotonin (5HT, 5-hydroxytryptamine) plays a role in the regulation of many behaviors (Schloss and Williams 1998; Stahl 1998) and disturbances in the serotonergic system are implicated in a myriad of diseases (Feighner 1994; Budygin, John et al. 2002; Vaswani, Linda et al. 2003; Murphy, Lerner et al. 2004; Vaswani and Kalra 2004). Following neurotransmission SERT clears 5HT from the synaptic cleft (Richelson 1996; Amara and Sonders 1998; Hoffman, Hansson et al. 1998). Numerous antidepressants, such as fluoxetine (FLX) or citalopram, inhibit reuptake of 5HT by SERT (White, Walline et al. 2005), and drugs of abuse, such as 3,4-methylenedioxy-methamphetamine (MDMA), induce reverse 5HT transport through the transporter (Kahlig, Binda et al. 2005). SERT is a member of the solute carrier 6 gene family consisting of numerous ion-coupled co-transporters, such as the norepinephrine and dopamine transporters (Ramamoorthy, Bauman et al. 1993; Gether, Andersen et al. 2006; Hahn and Blakely 2007). These transporters use the Na^+ ionic electrochemical potential to concentrate substrates against their concentration gradient (DeFelice and Blakely 1996; Rudnick 1998; Rudnick 1998; Hahn and Blakely 2007). Traditionally, co-transport is described by the alternating access model (AAM) where ions and substrate are transported with a fixed stoichiometry (Keyes and Rudnick 1982; Rudnick and Wall 1993); however, a competing model describes a channel within the transporter capable of conducing currents mediated by substrate and ions. These substrate-induced uncoupled currents have been measured repeatedly for hSERT and have also been observed in the *Drosophila* SERT (Petersen

and DeFelice 1999; Adams and DeFelice 2002; Ramsey and DeFelice 2002; Adams and DeFelice 2003). Additionally, in the absence of substrate, a constitutive leak current exists, that for SERT, can be uncovered with inhibitors, such as FLX (Li, Zhong et al. 2006).

Assays to Measure Transporter Uptake

Traditionally, monoamine transporter activity has been assessed by radiolabeled uptake assays. However, these biochemical assays have poor temporal resolution and do not yield spatial information of the transport process. Furthermore, radiolabeled compounds are hazardous and require significant efforts in waste management. Conversely, fluorescent substrates of monoamine transporters are advantageous tools to study mechanistic properties of SERT since they provide a continuous signal that can be measured with single live-cell imaging. In addition to the temporal and spatial advantages of fluorescent substrates, their use is amenable for high-throughput screening (Haunso and Buchanan 2007; Jorgensen, Nielsen et al. 2008).

ASP^+ as a Fluorescent Substrate for hNET and hDAT

Previously, we characterized 4-(4-(dimethylamino)styryl)-N-methylpyridinium (ASP^+) as a fluorescent reporter for uptake activity for both hNET and hDAT, and utilized it to study biophysical properties of hNET. Due to the inherent ability of ASP^+ to fluoresce on the plasma membrane, we were able to take advantage of ASP^+ to study ASP^+-hNET stoichiometry and measure the residence time of ASP^+ on hNET before being transported (Schwartz, Blakely et al. 2003; Schwartz, Novarino et al. 2005).

Subsequent studies successfully utilized this compound to study the regulation of hDAT activity by several DA receptors (Bolan, Kivell et al. 2007; Zapata, Kivell et al. 2007), and further studies validated the use of ASP^+ as a useful substrate amenable for high-throughput methods, and uptake by hNET was deemed effective with high affinity (Mason, Farmer et al. 2005; Haunso and Buchanan 2007). However, while ASP^+ was transported well by both hNET and hDAT, it had marginal effectiveness as an hSERT substrate (Schwartz, Blakely et al. 2003; Mason, Farmer et al. 2005; Schwartz, Novarino et al. 2005). In fact, to see substantial hSERT-mediated uptake, incubation for long time-periods was required, and the k_m was calculated to be between 9.9 and 20 μM from measurements taken 10-60 min after ASP^+ incubation (Fowler, Seifert et al. 2006). Furthermore, ASP^+ binding to hSERT proved to be relatively weak and non-specific, yet it still exhibits the binding pattern previously observed in hNET-HEK cells, in which a rapid initial binding phase is followed by a slower uptake phase (Schwartz, Blakely et al. 2003; Schwartz, Novarino et al. 2005).

Novel Fluorescent Substrates for hSERT

To perform the biophysical studies for hSERT that were performed on hNET with ASP^+, a fluorescent substrate for hSERT would be required to fluoresce on hSERT. Specifically, information about the residence (dwell) time of a fluorescence substrate on the transporter before its transport can be determined with this property – as was performed with ASP^+ on hNET (Schwartz, Novarino et al. 2005). We designed alternative fluorescent substrates of hSERT based on the structure of 1-methyl-4-phenylpyridinium (MPP^+), a known monoamine transporter substrate that has high-affinity for transport by the catecholamine transporters (Buck and Amara 1994; Wright, Bempong et al. 1998; Bryan-Lluka, Siebert et al. 1999). The addition of an electron donating dimethyl amino group to the phenyl ring of MPP^+ results in a fluorescent compound called 4-(4-(dimethylamino)phenyl)-1-methylpyridinium (APP^+). Additional modifications to this compound have been synthesized. The fluorescent analog of MPP^+, APP^+ (also known as IDT307), has been marketed by Molecular Devices, tested as a reagent for high-throughput screening (Jorgensen, Nielsen et al. 2008; Tsuruda, Yung et al. 2010) and used to study regulation of SERT (Chang, Tomlinson et al. 2012). However, many properties for this class of fluorescent MPP^+ analogs are unknown, such as their electrophysiological profile, their interaction within the transporter, their subcellular localization, and their fluorescent characterization in single live-cell imaging. In this study, we tested several fluorescent MPP^+ analogs, selected the most efficient fluorescent substrate for hSERT, which turned out to be APP^+, and thoroughly characterized its fluorescent activity profile for hSERT in single cells.

Findings of Study

We compared the efficiency of APP^+ to target hSERT against the fluorescent compound ASP^+ that has previously been used to study hDAT and hNET (Schwartz, Blakely et al. 2003; Schwartz, Novarino et al. 2005; Schwartz, Piston et al. 2006; Bolan, Kivell et al. 2007; Haunso and Buchanan 2007; Zapata, Kivell et al. 2007). We discovered several differences between the two fluorescent compounds. In particular, ASP^+ exhibits negligible uptake through hSERT, and unlike APP^+, ASP^+ exhibits binding-associated fluorescence on the plasma membrane; however, this ASP^+ signal in hSERT-expressing cells is indistinguishable from signal in non-transfected cells. Furthermore, APP^+ is much stronger at inhibiting uptake of radiolabeled 5HT as compared to ASP^+. More strikingly, electrophysiological data indicate that ASP^+ interacts with hSERT and exhibits inhibitor-like behavior, whereas APP^+ behaves as an hSERT substrate. Lastly, ligand-receptor docking of the substrates in a homology model based on the crystallized bacterial leucine transporter (Yamashita, Singh et al. 2005) shows that both APP^+ and ASP^+ dock favorably within the active region of hSERT at different residues, which could explain their functional efficacy to induce their opposing electrophysiological effects on hSERT. These findings indicate APP^+ is a superior fluorescent substrate than ASP^+ to study hSERT.

EXPERIMENTAL PROCEDURES

Maintenance of Parental and HEK293 Cells Stably Expressing hSERT (hSERT-HEK Cells)

Cells were prepared in Dulbecco's modified Eagle medium (DMEM) supplemented with 10% fetal bovine serum (FBS), 2 mM L-glutamine, penicillin (100 units/ml), streptomycin (100 μg/mL), and G418. Trypsin-released cells were plated in MatTek glass-bottom dishes pretreated with poly-L-lysine (MatTek, Ashland MA) at 100,000-150,000 cells per dish and allowed to grow for 24-48 hr before measurements. Media for parental HEK293 cells lacks G418.

Transient Transfections

Cells were handled similarly to stable cell lines described in the manuscript. According to previously described procedures (Torres-Altoro, White et al. 2008), HEK293 cells were incubated with a mixture of Lipofectamine 2000 (Invitrogen) and cDNA plasmid (either hSERT or C109A/G338C hSERT mutant) for 24 hr before experiments. The DNA plasmid containing the C109A/G338C hSERT gene was kindly provided by Randy Blakely of Vanderbilt University.

Solutions For All Experiments Using hSERT-HEK Cells

Krebs-Ringer Hepes (KRH) buffer consists of (in mM): 120 NaCl, 1.3 KCl, 2.2 $CaCl_2$, 1.2 $MgSO_4$, 10 HEPES, and 1 g/L glucose, pH 7.4. For the ionic-dependence

experiments, Na^+ is replaced with equimolar choline and Cl^- is replaced with equimolar gluconate.

Fluorescence Image Acquisition

Experiments are performed at room temperature (RT, 23-25°C) unless otherwise noted. hSERT-HEK or HEK293 cells are mounted on a Zeiss 510 confocal laser scanning microscope (LSM, Zeiss, Germany) and are focused with differential interference contrast (DIC). The culture medium is discarded, and the cells are immediately mounted on the microscope, and re-focused. As soon as image acquisition begins, the desired treatment is applied. An argon laser tuned to 488 nm was used to excite APP^+, its analogs, and ASP^+. Emission filters used were 505-550 nm for APP^+ and its analogs and 585-615 nm for ASP^+. Gain (contrast) and offset (brightness) of the photomultiplier tube (PMT) was set to avoid saturation at the highest fluorophore concentration. Microscopy was performed with a 10x 0.8 numerical aperture (NA) water objective, a 40x 1.3 NA water objective, or a 40x 1.4 NA oil objective.

Total Fluorescence Intensity

The cellular spectra were acquired under 'lambda' mode after exposure to each synthesized fluorescent compound for 5 min, in which emitted fluorescence was acquired at 10 nm intervals. To determine total fluorescence, the spectra curves are integrated (Excel, Microsoft).

Time-lapse Acquisition and Analysis

Time-lapses consist of a series of images taken over a defined period of time (from 30 s to 10 min as indicated) with acquisition rates ranging from one image every second to one image every five seconds (sample of images in a time-lapse shown in Figure 5, top panel). Fluorescent image analysis is performed using LSM software, AIM (Zeiss, Germany). Fluorescence accumulation is measured as average pixel intensity within specified regions of interest (ROI) identified in the DIC channel images, which represent individual cells. Fluorescence accumulation is averaged for at least 30 cells per time-lapse. The fluorescence intensity is plotted in arbitrary fluorescent units (AFU) over time (Figure 5, bottom panel). To determine V_{max}, V_{min}, k_m, and the Hill coefficient n, values are fit to the Hill equation $y = V_{max} + (V_{min} - V_{max}) * x^n / (k^n + x^n)$ using Origin 8 (OriginLab Corporation, Northampton, MA).

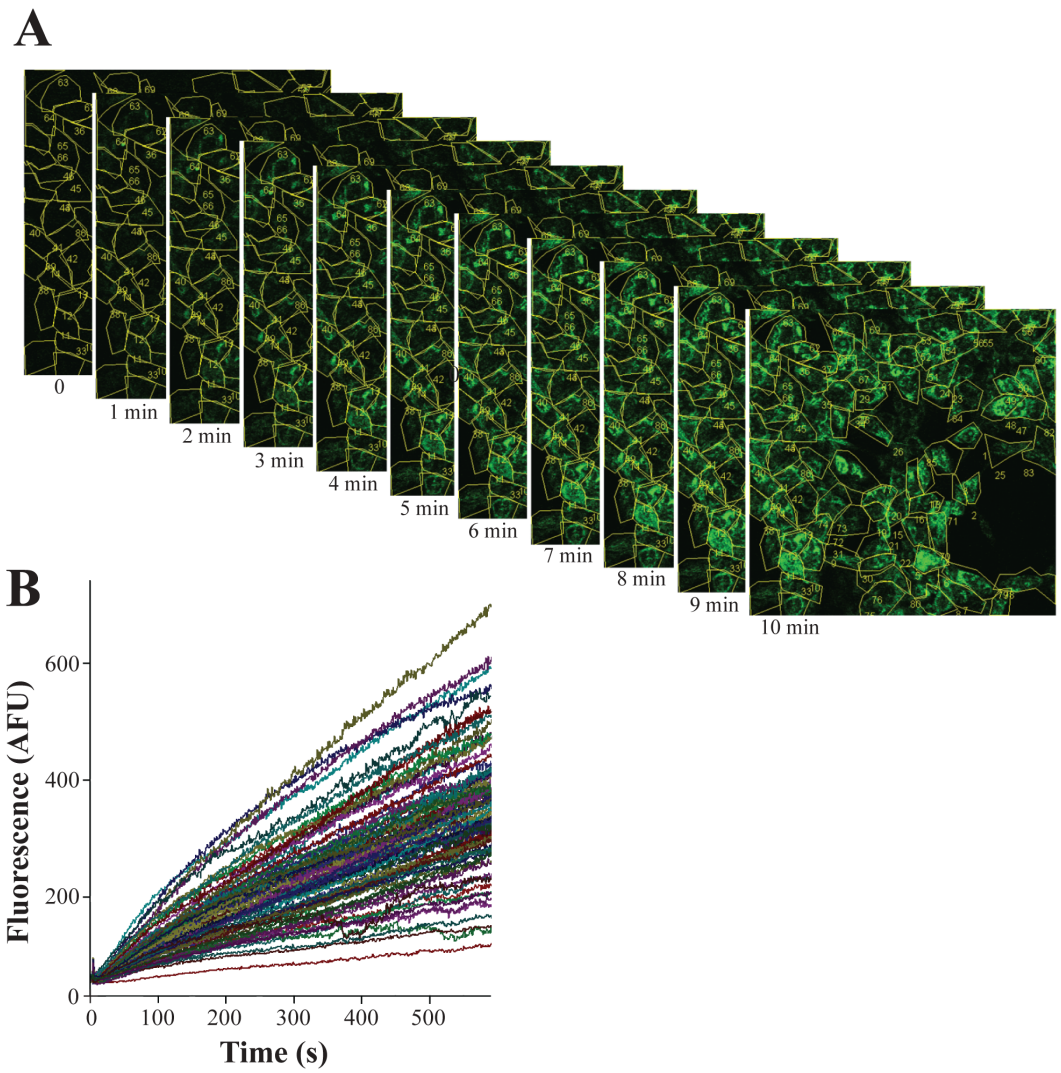

Figure 5. Time-lapse acquisition and image analysis. A time-lapse is a series of images taken over a defined period of time. Images are acquired at varying rates (rates typically range from one image per second). (A) Illustration of time-lapse images from a time-lapse in which images were acquired at a rate of one per second for 10 minutes (the total number of images for the entire time lapse was 1000). The images show fluorescence in hSERT-HEK cells at the indicated time point (1-10 min). (B) Quantitative fluorescence measurements for each cell in a time lapse. Fluorescent images were analyzed using AIM software (Zeiss, Germany). Fluorescence accumulation was defined from average pixel intensity of time-resolved fluorescent images within specified regions of interest (ROI, shown as numbered yellow circles in A) representing cells, which are identified in DIC images. The fluorescence intensity is plotted in arbitrary fluorescent units (AFU) over time.

Plasma Membrane Colocalization and Line Scans

Colocalization studies were performed by incubating cells at 37^{o}C for 15 min with 1,1'-dioctadecyl-3,3,3',3'-tetramethylindocarbocyanine perchlorate (DiI, Invitrogen) and co-applying 10 μM APP^{+} for 5 min. Then images were merged for the APP^{+} channel and DiI channel. DiI was excited with an argon laser tuned to 549 nm and the emission filter used was 560-615 nm. Line scans are performed by selecting regions from the outer edges of cells as determined by DiI labeling of the plasma membrane.

Statistics

Standard error of the mean (SEM) is calculated for fluorescence accumulation in all cells at each time point in a time-lapse, and SEM for each plot are shown as merged Y-error bars.

Colocalization of Subcellular Organelles

Colocalization studies were performed by incubating cells at 37^{o}C for 15 min with either SYTO-17 (Invitrogen) or MitoTracker Orange (Invitrogen) and co-applying 10 μM APP^{+} for 5 min. Then images were merged for the APP^{+} channel and either of the markers, which have emission at longer wavelengths.

Expression of hSERT in Xenopus Laevis Oocytes

Oocytes are harvested and prepared from adult *Xenopus laevis* females following standard procedures (Machaca and Hartzell 1998; Iwamoto, Blakely et al. 2006). We select stage V-VI oocytes for cRNA injection within 24 h of isolation. cRNA is

transcribed from the pOTV vector using mMessage Machine T7 kit (Ambion Inc., Austin, TX). Each oocyte is injected with 30 ng cRNA using a Nanoject AutoOocyteInjector (Drummond Scientific Co., Broomall, PA) and incubated at 18°C for 5-10 days in Ringers solution supplemented with NaPyruvate (550 μg/ml), streptomycin (100 μg/ml), tetracycline (50 μg/ml) and 5% dialyzed horse serum.

Electrophysiology

We performed two-electrode voltage-clamp (TEVC) experiments as previously described (Wang, Li et al. 2006). TEVC allows recordings of currents from proteins expressed on the plasma membrane that are electrogenic, such as monoamine transporters (Figure 6 describes the TEVC setup). Recordings were done at RT (23-25°C). Electrodes having resistances from 1-5 MΩ are filled with 3 M KCl. *Xenopus laevis* oocytes are voltage-clamped to –60 mV (unless otherwise noted) with a GeneClamp 500 (Axon Instruments), and the holding current is recorded using Clampex 10 (Axon Instruments). Standard extracellular buffer is perfused until stable baseline currents are obtained, followed by experimental drugs. Extracellular buffer consists of (in mM): 120 NaCl, 7.5 HEPES, 5.4 KGluconate, 1.2 CaGluconate, pH 7.4.

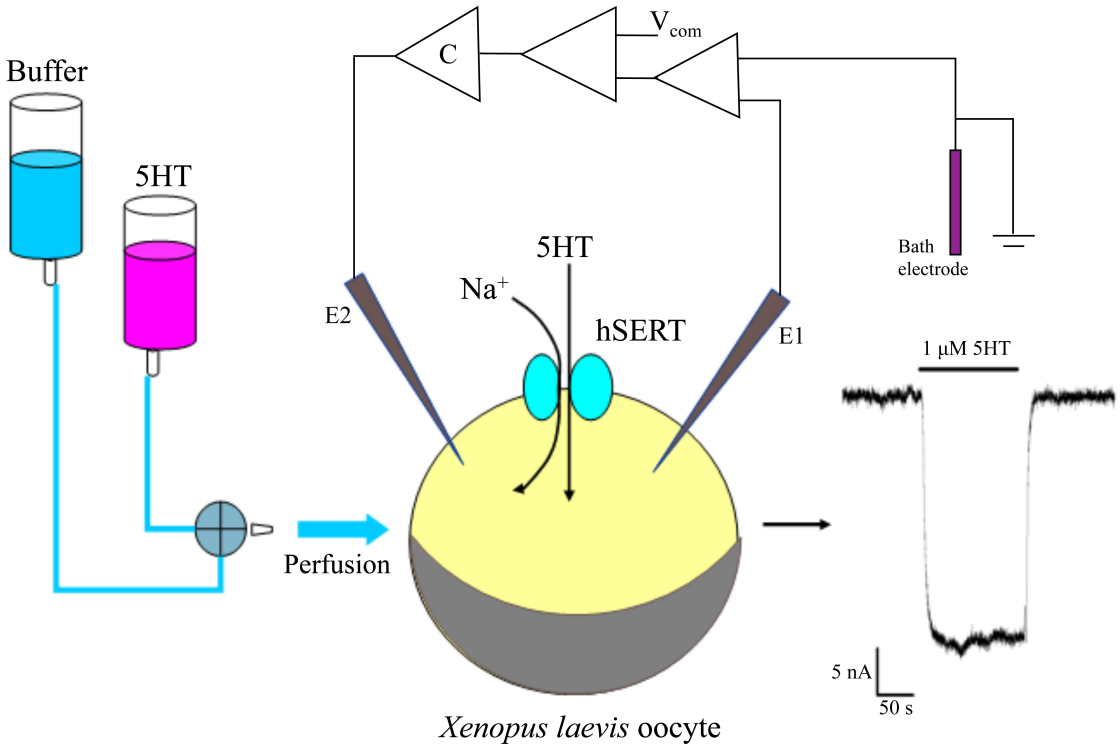

Figure 6. Two-electrode voltage-clamp (TEVC) of hSERT-expressing oocyte. The membrane of a *Xenopus laevis* oocyte is penetrated by two microelectrodes, one for voltage sensing (E1) and one for current injection (E2). The membrane potential as measured by the voltage-sensing electrode is compared with a command voltage (V_{com}), and the difference is brought to zero by a control amplifier (C), thus clamping the potential to V_{com}. The resultant current represents the conductance through hSERT. In our experiments, *Xenopus* oocytes expressing SERT are voltage-clamped to -60 mV and solutions are gently perfused (typically buffer is perfused until a stable baseline is obtained, then the experimental drug is perfused, followed by perfusion with buffer). The trace below shows perfusion with 1 µM 5HT. Adapted from figure by Hideki Iwamoto.

Competition Assay

Radiolabeled assay protocols were performed as described previously (Barker, Moore et al. 1999; Henry, Adkins et al. 2003). First, hSERT-HEK cells are plated on poly-L-lysine coated, 24-well tissue culture plates at 10,000 cells per well for 2-3 days to obtain about 90% cell confluence. Then, medium is removed by aspiration and the hSERT-HEK cells are washed with RT KRH buffer. Cells are incubated for 10 min at 37^{o}C with mixtures of radiolabeled substrate and the compounds tested at a broad range of concentrations. The assay mixture is aspirated and cells are washed three times with ice-cold (4ºC) KRH buffer. Lastly, cells are solubilized with ice-cold Ecoscint H (National Diagnostics) and [^{3}H]-5HT remaining is measured using a scintillation counter.

Competition Assay Analysis and Cheng-Prusoff Correction

Concentration-response curves for APP^{+} and ASP^{+} inhibition of [^{3}H]-5HT uptake into hSERT-HEK cells are used to obtain the IC_{50}. Briefly, [^{3}H]-5HT accumulation is measured in hSERT-HEK cells in the presence of increasing APP^{+} and ASP^{+} concentrations and these values are normalized to the highest [^{3}H]-5HT reading, which is the value in the absence of competing compound. The data are fit to the Hill equation $y = V_{max} + (V_{min} - V_{max}) * x^{n} / (k^{n} + x^{n})$ (Origin 8), and to correct for substrate concentration the Cheng-Prusoff equation is employed: $k_i = IC_{50} / (1 + [S] / k_m)$, where k_i is the binding affinity of the inhibitor, IC_{50} is the functional strength of the inhibitor, [S] is the substrate concentration, and k_m is the affinity of the substrate for the enzyme.

Torsional Scans and Energy Minimization

Prior to docking, conformations of the substrates were optimized by performing energy minimization on each compound using hybrid density functional B3LYP with split-valence 6-31G* basis set (Gaussian03). The torsional surface of the molecules has been examined using protocols developed before for force-field parametrization (Guvench and MacKerell 2008). Energy was calculated at increments of 18° rotation around the dihedral angle linking the two rings providing a torsional scan. The coordinate files created in Molden and optimized in Gaussian03, provided us with the most energetically favorable structure *in vacuo* and the most physiological relevant structure.

Substrate Models in Ligand Docking Studies

First, the energy grid for the transporter was created and each of the ligands docked individually. A square volume with a length of 14 Å around the location of the active site was designated for allowed insertions of the ligands. The center of the insertion region was defined around the known substrate-binding site in the leucine transporter (LeuT). There is a strong line of evidence that this binding pocket is preserved in hSERT (Kaufmann, Dawson et al. 2009; Field, Henry et al. 2010). The docking was performed on the basis of a rigid protein approximation and a flexible ligand. Extra precision docking (Friesner, Murphy et al. 2006) was subsequently used and the top ten potential docks were further optimized. The hSERT homology model was obtained from the Meiler lab (Kaufmann, Dawson et al. 2009), and is based on the crystallized structure of the leucine transporter ($LeuT_{Aa}$) reported by Yamashita et al. PBDID 2A65 (Yamashita, Singh et al. 2005). The ranking of each pose and its energy was calculated using the G-Score. The G-Score is a sum of the most significant energy constants including hydrophobic, van der Waals, and coulomb interactions. Once re-minimized, each dock is assigned a G-Score as a sum of interactions and the docks are ranked from most negative (favorable) to least. The ligand in each dock is allowed full degrees of motion, within its optimal conformation. Hindrance with the transporter or unfavorable torsional angles are penalized in the G-Score.

RESULTS

Fluorescent MPP^+ Analogs

Addition of an electron donating dimethyl amino group to the phenyl ring of MPP^+ results in the compound called 4-(4-(dimethylamino)phenyl)-1-methylpyridinium (APP^+) (Figure 4A, top row) that is transported by hSERT-expressing HEK293 (hSERT-HEK) cells and fluoresces inside cells after the 2 rings immobilize by adopting a co-planar conformation at organelle membranes (Figure 7A). APP^+ colocalizes with MitoTracker and SYTO-17, indicating APP^+ stains mitochondria and nucleoli, respectively (Figure 8). The fluorescence intensity for APP^+ and a series of APP^+ analogs was measured in hSERT-HEK cells. APP^+ and compound 321 emitted the most fluorescence, whereas compounds 326, 330, and 375 emitted the weakest fluorescence (Figure 7B). All tested APP^+ analogs displayed similar fluorescence localization inside hSERT-HEK cells, and peak emission was measured at 520-525 nm, with the highest emission peak seen with APP^+ (Figure 9). We pursued characterization of APP^+ to assess its utility to study hSERT activity in single cells.

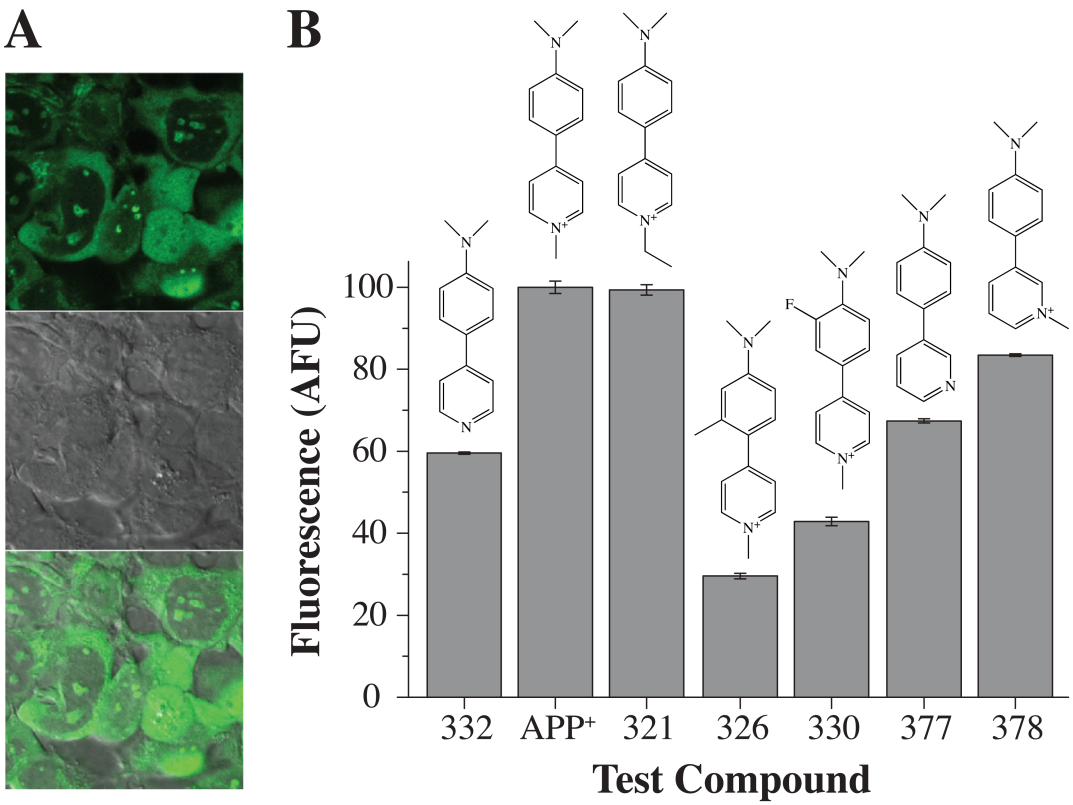

Figure 7. Screening for a fluorescent substrate of hSERT. (A) Images of hSERT-HEK cells exposed to fluorescent compounds (from top to bottom: APP^+ only, DIC, and APP^+ and DIC merged). (B) Fluorescence intensity is calculated by integrating emission spectra curves for each compound. Fluorescence is normalized to the brightest compound, APP^+. Structure nomenclature: 332, *N,N*-dimethyl-4-(pyridin-4-yl)aniline; APP^+, 4-(4-(dimethylamino)styryl)-N-methylpyridinium; 321, 4-(4-(dimethylamino)phenyl)-1-ethylpyridinium; 326, 4-(4-(dimethylamino)-2-methylphenyl)-1-methylpyridinium; 330, 4-(4-(dimethylamino)-3-fluorophenyl)-1-methylpyridinium; 377, *N,N*-dimethyl-4-(pyridin-3-yl)aniline; 378, 3-(4-(dimethylamino)phenyl)-1-methylpyridinium. Adapted from Solis, Zdravkovic et al. 2012. Compounds provided by Ian D. Tomlinson and Sandra Rosenthal.

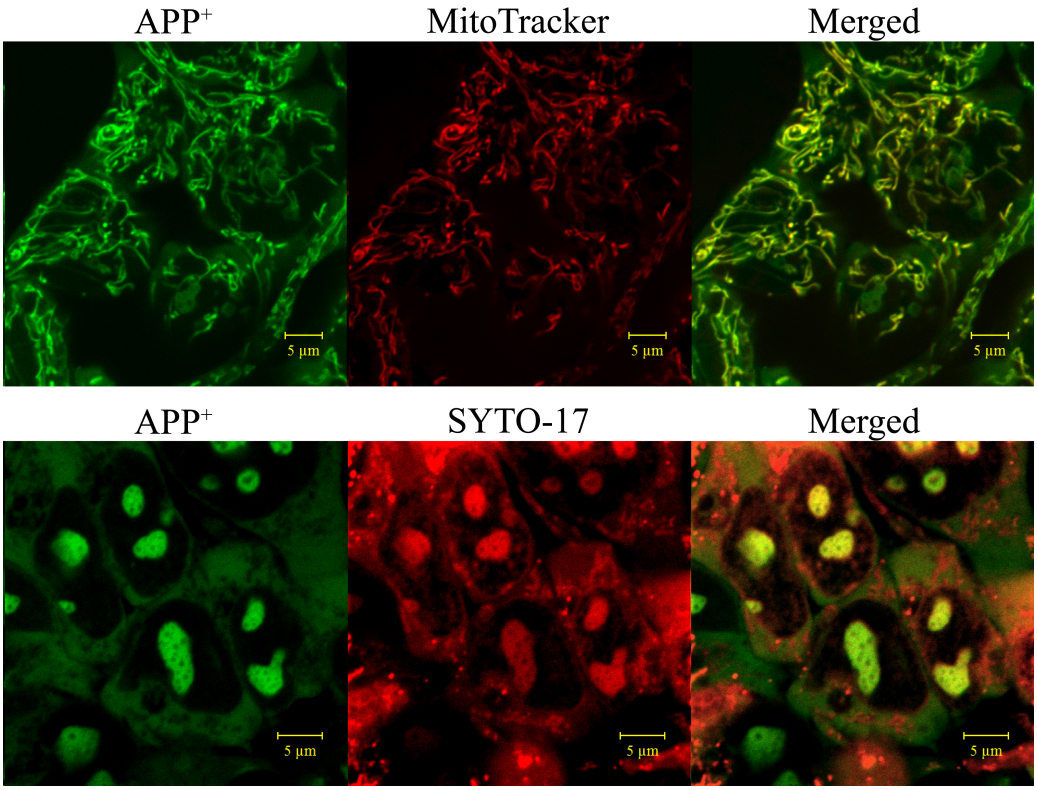

Figure 8. APP$^+$ subcellular fluorescence pattern. hSERT-HEK cells are incubated for 15 min with either MitoTracker or SYTO-17, and then APP$^+$ (10 µM) is added for 5 min. APP$^+$ colocalizes with the mitochondria marker MitoTracker (top), and with nucleoli labeled with SYTO-17 (bottom). Note: when SYTO-17 is employed, APP$^+$ staining of the mitochondria disappears as soon as cells are exposed to the laser. Adapted from Solis, Zdravkovic et al. 2012.

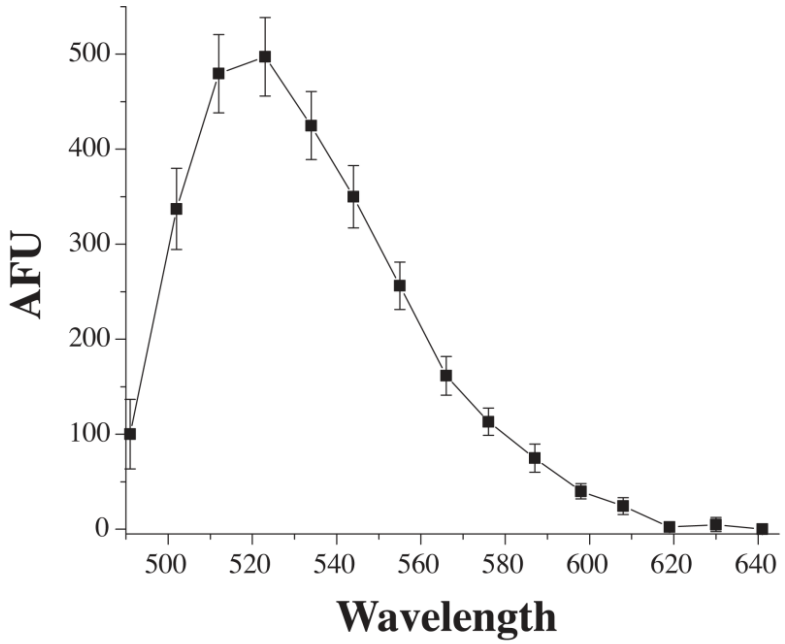

Figure 9. APP$^+$ emission spectra. hSERT-HEK cells were exposed to 2 μM APP$^+$ for 5 minutes and images were acquired with lambda mode to determine emission spectra at 10-11 nm intervals. Maximum emission peak for APP$^+$ was 520-525 nM. Adapted from Solis, Zdravkovic et al. 2012.

APP^+ Displays Two Distinct Fluorescence Accumulation Rates

We first established a concentration-response curve of APP^+ by performing time-lapses of hSERT-HEK cells exposed to APP^+ at concentrations ranging from 250 nM to 10 μM (Figure 10A). APP^+ fluorescence accumulation yielded a biphasic plot that corresponds with two distinct rates of fluorescence accumulation, an initial "fast" phase and a secondary "slow" phase, indicated by dotted lines over the 10 μM APP^+ accumulation curve (Figure 10A). To compare the rates of APP^+ fluorescence accumulation, we fit straight lines to the slow and fast components for each concentration, plotted these slope values against concentration, and then fit to the Hill equation. The V_{max} and k_m for the fast phase were 0.65 ± 0.07 AFU/s and 2.29 ± 0.65 μM, respectively, and for the slow phase the V_{max} and k_m were 0.38 ± 0.04 AFU/s and 2.36 ± 0.55 μM, respectively (Figure 10B). The Hill coefficient was 2.91 ± 1.09 for the fast component and 2.53 ± 0.68 for the slow component.

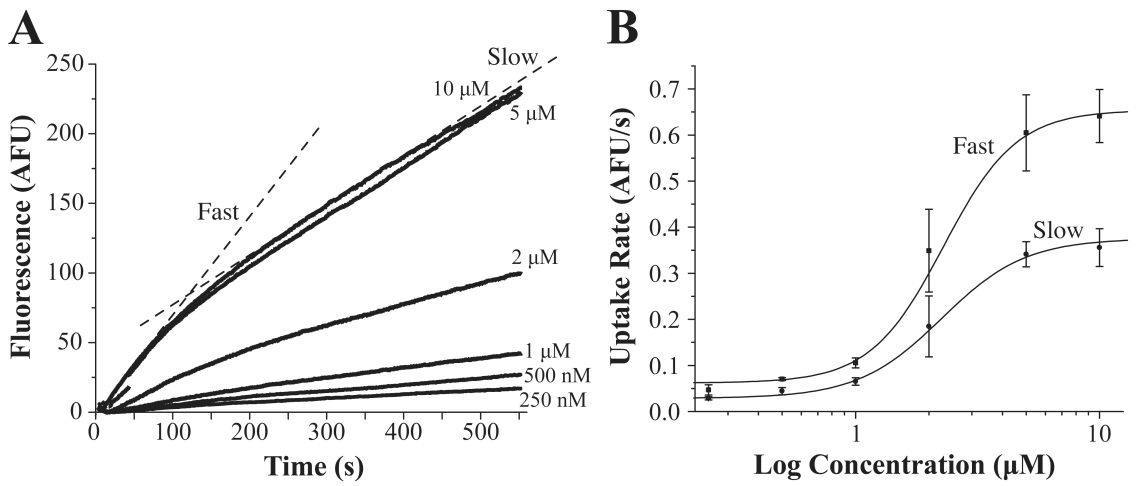

Figure 10. APP$^+$ displays two rates of uptake. (A) APP$^+$ accumulation depends on concentration. Time-lapses of hSERT-HEK cells exposed to different concentrations of APP$^+$ (from 250 nM to 10 µM) were acquired at a rate of 1 image per second for 10 min. Dotted lines represent the 2 rates observed, the initial (slow) and subsequent (fast) components. (B) To determine the V_{max} and k_m, straight lines were fitted and slopes obtained for both the slow and fast phases acquired at each concentration. For the fast phase, measurements from 20-100 s were used, and for the slow phase, the measurements from 200 s to the end of the acquisition were used. Slopes were plotted against concentration and these values were fit to the Hill equation $y = V_{min} + (V_{max} - V_{min}) * x^n / (k^n + x^n)$. The V_{max}, V_{min}, and k_m for the fast phase were 0.65 ± 0.07 AFU/s, 0.062 ± 0.008 AFU/s, and 2.29 ± 0.65 µM, respectively, and for the slow phase the V_{max}, V_{min}, and k_m were 0.38 ± 0.04 AFU/s, 0.029 ± 0.003 AFU/s, and 2.36 ± 0.55 µM, respectively. The Hill coefficient was 2.91 ± 1.09 for the fast component and 2.53 ± 0.68 for the slow component. Adapted from Solis, Zdravkovic et al. 2012.

APP^+ is an hSERT Substrate

To characterize APP^+ as a suitable substrate to study hSERT activity in single cells, we performed a series of time-lapse experiments measuring 2 μM APP^+ accumulation. Because monoamine transporter uptake is temperature sensitive (Chang, Frnka et al. 1989), we measured APP^+ accumulation at 20°C, 27°C, and 37°C. As expected, temperature induced altered APP^+ accumulation by hSERT, which was more noticeable for the initial "fast" uptake rate (Figure 11A). Removal of Na^+ or Cl^- eliminated APP^+ accumulation in hSERT-expressing cells (Figure 11B), which is in agreement with the ionic dependence for monoamine transporter uptake (Hoffman, Hansson et al. 1998; Nelson 1998). Furthermore, application of the endogenous hSERT substrate 5HT (10 μM) while measuring APP^+ accumulation induced an immediate decrease in APP^+ accumulation, which suggests APP^+ uptake is mediated by hSERT (Figure 11C). Lastly, to verify that APP^+ is specifically transported through hSERT, we measured APP^+ accumulation in the presence of the specific hSERT inhibitor fluoxetine. Whereas the low FLX concentration (1 μM) only partially diminished the APP^+ signal, the higher FLX concentrations (5-10 μM) completely abolished APP^+ uptake (Figure 11D). We further studied the effect on extracellular ionic concentration on APP^+ uptake through hSERT by substituting Na^+ with choline (from 0 to 120 mM) and Cl- with gluconate (from 0 to 120 mM) (Figure 12). Although hSERT-mediated APP^+ accumulation requires values near 120 mM Na^+ (Figure 12A), a concentration of 60 mM Cl- is enough to display maximal APP^+ accumulation (Figure 12B). By fitting the slopes from straight lines overlapping time-lapse measurements from 100-300 s at each Na^+ and Cl^- concentration to the Hill 1 equation, we obtained a k_m for Na^+ of 62.52 ± 20.53 mM with Hill coefficient of 1.47 ±

0.69 (Figure 12C), and a k_m for Cl^- of 38.04 ± 26.93 mM with a Hill coefficient of 1.15 ± 0.59 (Figure 12D).

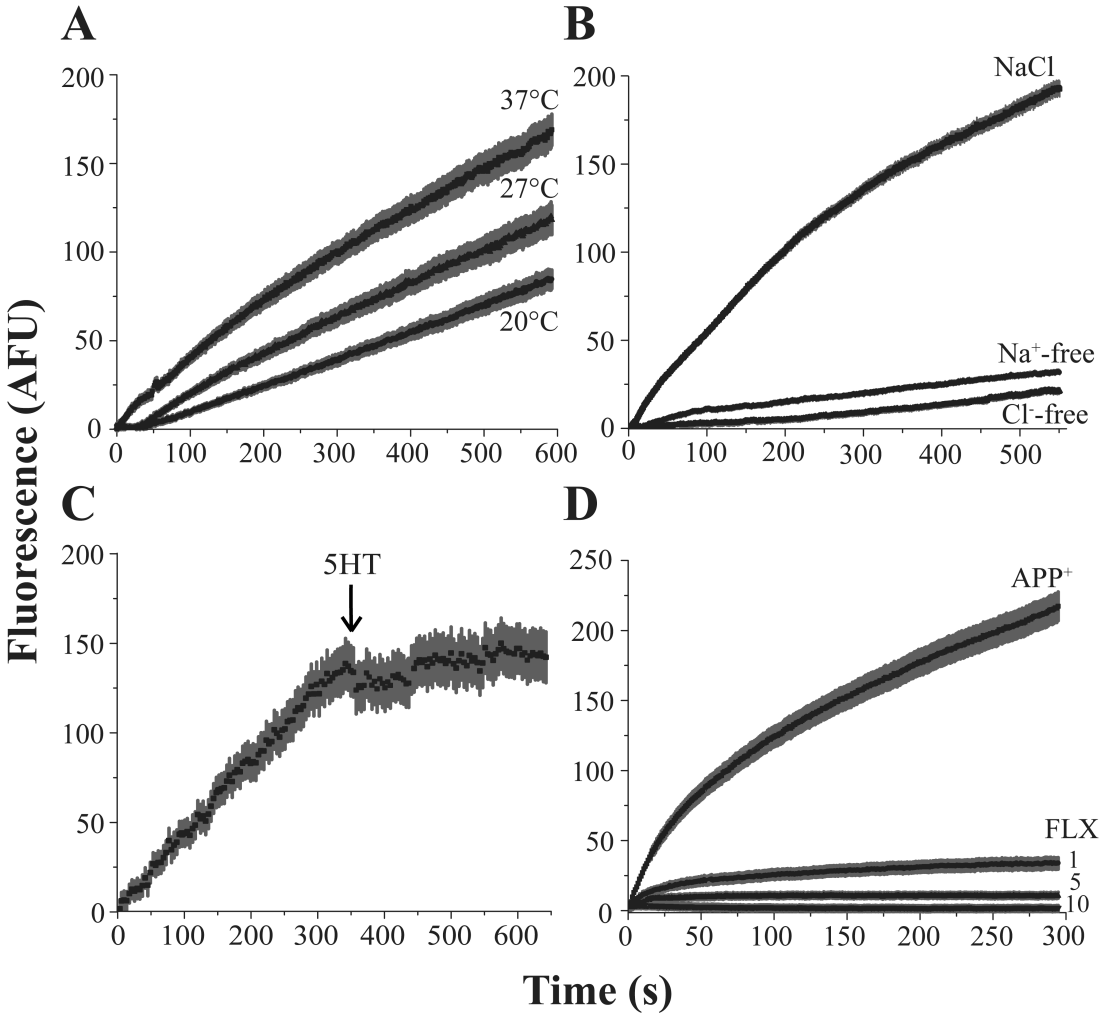

Figure 11. APP^+ is a fluorescent substrate of hSERT. Time-lapses of hSERT-HEK cells exposed to 2 μM APP^+. (A) Temperature regulates APP^+ accumulation. APP^+ fluorescence accumulation is greater when measured under physiological (37°C) temperature, and much lower at 20°C as compared to the moderate (27°C) temperature. (B) Removal of both Na^+ and Cl^- diminished APP^+ accumulation. (C) An immediate decrease in APP^+ accumulation occurs when 5HT (10 μM) was added 6 min into the time-lapse (indicated by arrow). (D) Co-treatment with fluoxetine (from 1-10 μM) abolishes APP^+ fluorescence accumulation. Adapted from Solis, Zdravkovic et al. 2012.

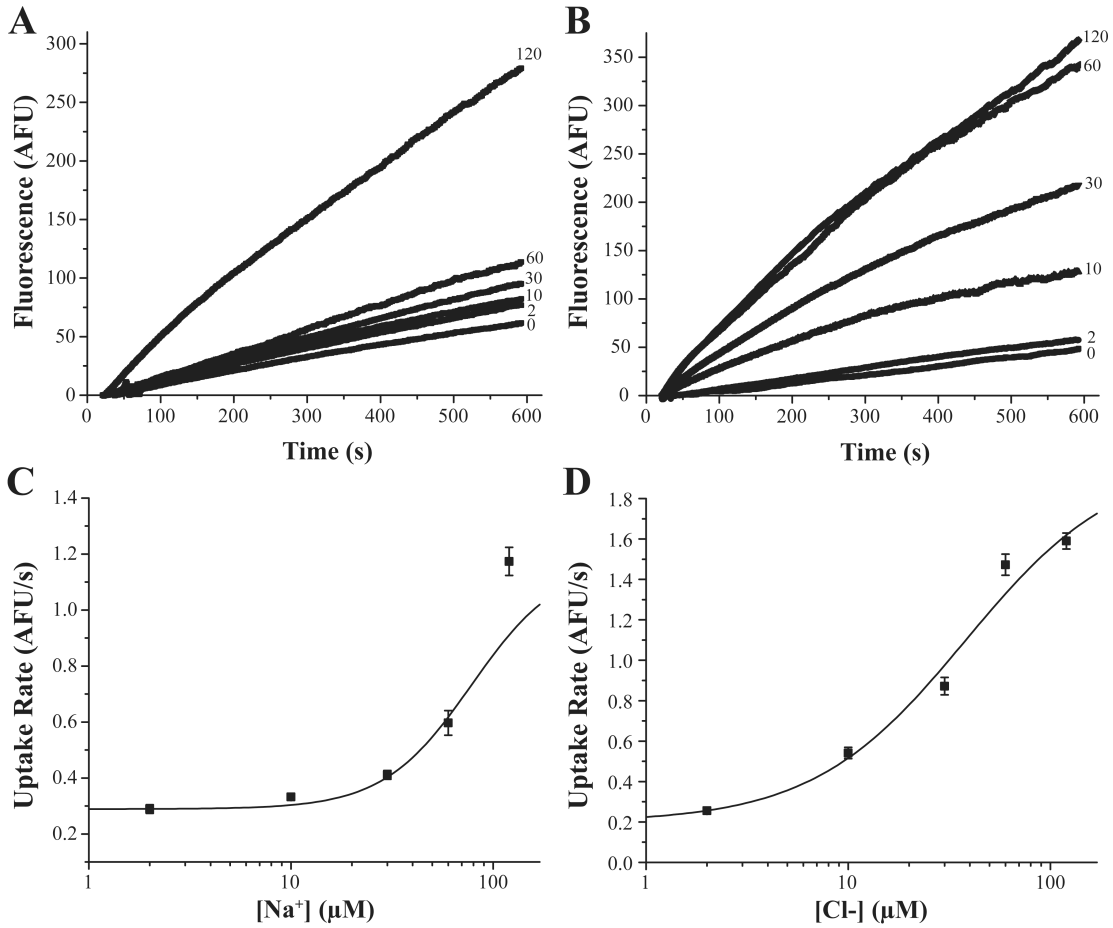

Figure 12. Effect of ionic concentration replacement on APP^+ uptake by hSERT. (A) To determine Na^+-dependence of APP^+ accumulation, Na^+ was replaced with ChCl from full replacement (120 mM ChCl) to increasing NaCl and proportional decreases in ChCl. Concentrations of Na^+ tested were 0, 2, 10, 30, 60, and 120 mM. (B) To determine Cl^--dependence of APP^+ accumulation, NaCl was replaced with NaGluconate from full replacement (120 mM NaGluconate) to increasing NaCl and proportional decreases in NaGluconate. Concentrations of Cl^- tested were 0, 2, 10, 30, 60, and 120 mM. To determine the k_m, straight lines were fitted to time-lapse measurements from 100-300 s. Slopes were plotted against (C) Na^+ and (D) Cl^- concentration and these values were fit to the Hill equation $y = V_{min} + (V_{max} - V_{min}) * x^n / (k^n + x^n)$. The k_m for Na^+ was 62.52 ± 20.53 mM with Hill coefficient (n) 1.47 ± 0.69, and for Cl^- the k_m and n were 38.04 ± 26.93 mM and 1.15 ± 0.59, respectively. Personal unpublished data.

ASP^+ is Less Efficient than APP^+ at Targeting hSERT

We have demonstrated that APP^+ is an adequate fluorescent substrate for hSERT in single-cells. However, because ASP^+ has not been thoroughly studied as an hSERT fluorescent substrate, we sought to test APP^+ against ASP^+ under similar conditions. ASP^+ did not elicit visible levels of fluorescence in hSERT-HEK cells until 10 μM or higher concentrations were employed; however, the signal elicited at these ASP^+ concentrations is similarly bright in both hSERT-HEK and parental cells, and falls within the noise for all time points measured (Figure 13A, [ASP^+] = 10 μM). In addition, ASP^+ fluorescence accumulation rates were parallel between hSERT-HEK and parental cells for all concentrations tested (1-30 μM), indicating non-specific ASP^+ uptake (Figure 14A, [ASP^+] = 10 μM). Conversely, APP^+ (10 μM) signal appears much brighter in hSERT-HEK cells than in parental cells (Figure 13B), and APP^+ (2 μM) fluorescence uptake is greater in hSERT-HEK cells as compared to parental cells (Figure 14B). These discernable differences are clearly observed at APP^+ concentrations from 1-10 μM (data not shown). To assess the affinity of APP^+ and ASP^+ at hSERT we produced concentration-response curves for inhibition of [^{3}H]-5HT uptake in hSERT-HEK cells with increasing APP^+ or ASP^+ concentrations (Figure 15). Fitting to the Hill equation and subsequent correction for substrate concentration with the Cheng-Prusoff equation yielded k_i of 19.7 ± 2.23 μM for APP^+ and a weaker k_i of 180.1 ± 20.3 μM for ASP^+. For comparison the k_i for 5HT is reported as 1.7 ± 1 μM (Talvenheimo, Nelson et al. 1979). The Hill coefficients for inhibition of [^{3}H]-5HT uptake were 1.23 ± 0.08 for APP^+ and 0.91 ± 0.15 for ASP^+.

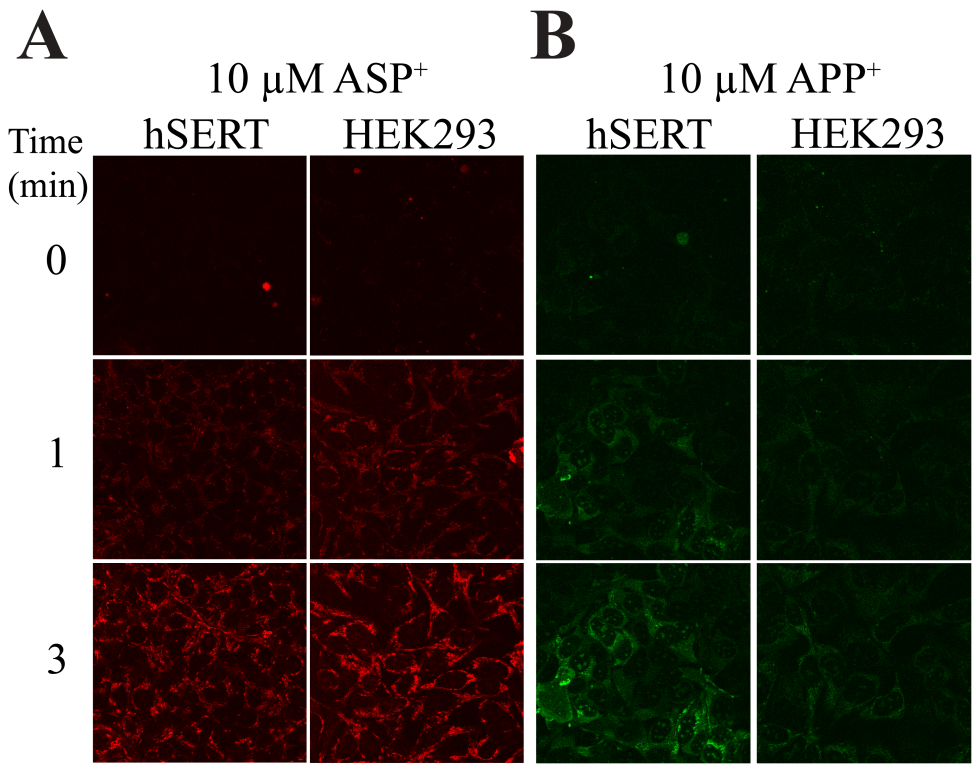

Figure 13. Comparing fluorescence of ASP^+ and APP^+ in hSERT-expressing cells. Images of hSERT-HEK or parental HEK293 cells before (row labeled with 0) and after exposure to 10 μM (A) ASP^+ or (B) APP^+ for 1 or 3 min. ASP^+ fluoresces red and labels the exterior membrane of cells in both hSERT-HEK and parental cells, while APP^+, which fluoresces green, seems to accumulate only inside of hSERT-HEK cells. Adapted from Solis, Zdravkovic et al. 2012.

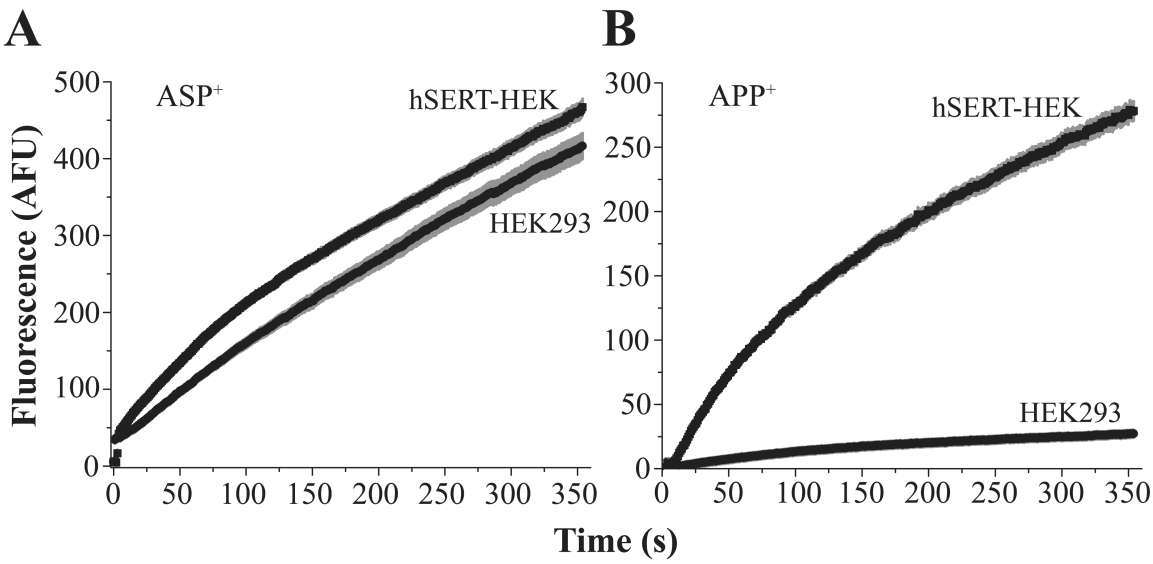

Figure 14. APP$^+$ is better suited than ASP$^+$ to report hSERT uptake. Time-lapses comparing fluorescence accumulation rates between hSERT-HEK and HEK293 cells for (A) ASP$^+$ (30 μM) and (B) APP$^+$ (5 μM). ASP$^+$ exhibits similar uptake rates in both hSERT-HEK and parental cells, whereas APP$^+$ accumulation rate is much greater in hSERT-HEK cells than in parental cells. Adapted from Solis, Zdravkovic et al. 2012.

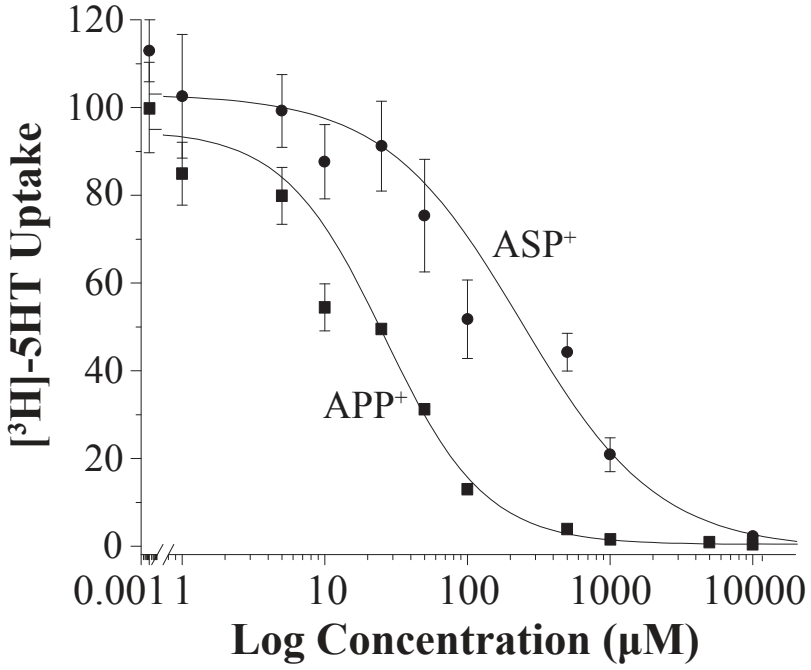

Figure 15. APP^+ and ASP^+ inhibit 5HT uptake by hSERT. Concentration curve for APP^+ and ASP^+ inhibition of [^{3}H]-5HT uptake into hSERT-HEK cells. [^{3}H]-5HT accumulation was measured in hSERT-HEK cells in the presence of increasing APP^+ and ASP^+ concentrations and normalized to data in the absence of the competing substrate. The data were fit to the Hill equation $y = V_{max} + (V_0 - V_{max}) * x^n / (k^n+x^n)$, and k_i values were determined using the Cheng-Prusoff equation to correct for substrate concentration. The fits yield k_i (APP^+) = 19.7 ± 2.23 µM and k_i (ASP^+) =180.1 ± 20.3 µM. Values are represented as means ± S.E., N = 3. The Hill coefficients for ASP^+ and APP^+ are 0.91 ± 0.15 and 1.23 ± 0.08, respectively. Adapted from Solis, Zdravkovic et al. 2012.

APP^+ Acts as an hSERT Substrate, Whereas ASP^+ Behaves Like an hSERT Inhibitor

Since transporter currents reflect the effect of substrates and inhibitors, we employed TEVC and measured hSERT currents in *Xenopus* oocytes in response to 10 μM 5HT, APP^+, ASP^+, and 1 μM fluoxetine (holding potential = –60 mV). Whereas APP^+ induced an hSERT-mediated inward current, similar in effect to hSERT's endogenous substrate 5HT, ASP^+ induced an hSERT-mediated outward current, which is similar to the effect the hSERT inhibitor fluoxetine exerts on hSERT (Figure 16A). Control oocytes (not expressing hSERT) do not induce currents when exposed to 5HT, ASP^+, APP^+ or fluoxetine (data not shown). Voltage-dependence was assessed by stepping the holding potential in oocytes (from -100 to 0 mV), and measuring APP^+ and ASP^+ induced inward and outward hSERT-mediated currents, respectively, which are plotted as drug-induced currents relative to baseline set to 0 (Figure 16B). A concentration-response curve of hSERT currents in response to APP^+ was produced by applying from 0.1 to 25 μM APP^+ to hSERT-expressing oocytes (Figure 17A), and average data from several recordings were fit to the Hill equation, which yielded k_m = 1.13 ± 0.28 μM and n = 1.23 ± 0.60 (Figure 17B). The hSERT inhibitor fluoxetine (1 μM) blocked inward currents produced in response to 2 μM 5HT and 10 μM APP^+ (compare Figure 17C and Figure 17D). A concentration-response curve for ASP^+ was determined using concentrations from 0.5 to 100 μM (Figure 18A) and fitting average data from several recordings yielded k_m = 12.25 ± 2.71 μM and n = 1.34 ± 0.31 (Figure 18B). Since the hSERT-mediated outward current induced by ASP^+ resembles the action of transporter inhibitors, we tested its utility as an inhibitor. Application of ASP^+ (1-250 μM) inhibited 5HT-induced hSERT-mediated

currents in a dose-dependent manner, and notably, ASP^+ imposed an outward current at the highest ASP^+ concentration tested (Figure 18C and Figure 18D).

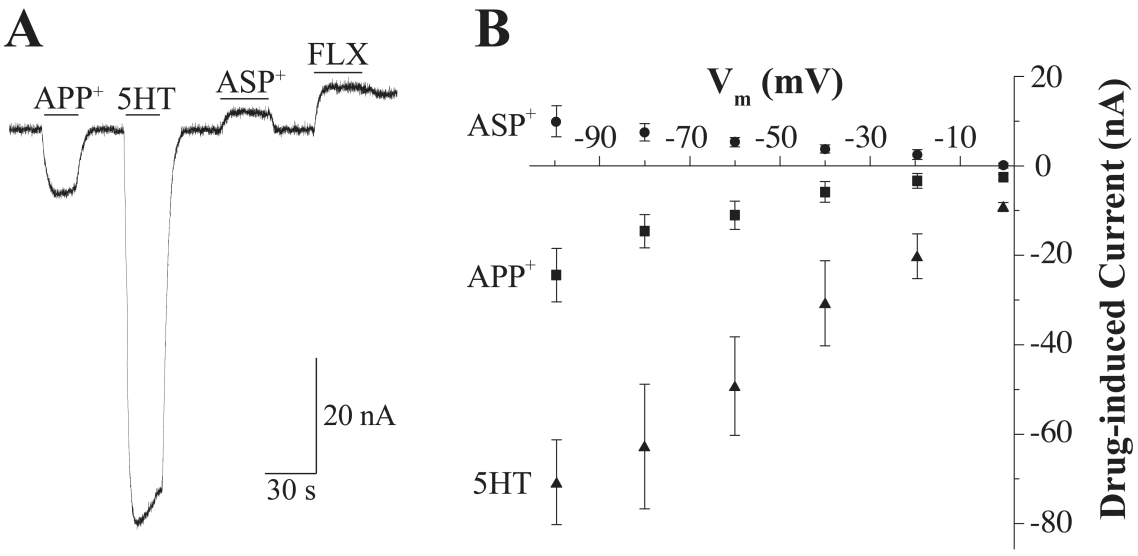

Figure 16. Electrophysiological effect of substrates on hSERT. (A) Currents in an hSERT-expressing *Xenopus laevis* oocyte clamped to -60 mV are measured in response to 10 μM 5HT, APP^+, ASP^+, and 1 μM fluoxetine. Bars display perfusion duration of each compound. Control (uninjected) oocytes show no response to 5HT, ASP^+, or APP^+ (not shown). (B) The effect of voltage (from 0 to -100 mV) on hSERT-induced currents. Currents induced by 5HT, APP^+, ASP^+ are plotted relative to the baseline set as 0 at each potential (N = 4). Adapted from Solis, Zdravkovic et al. 2012.

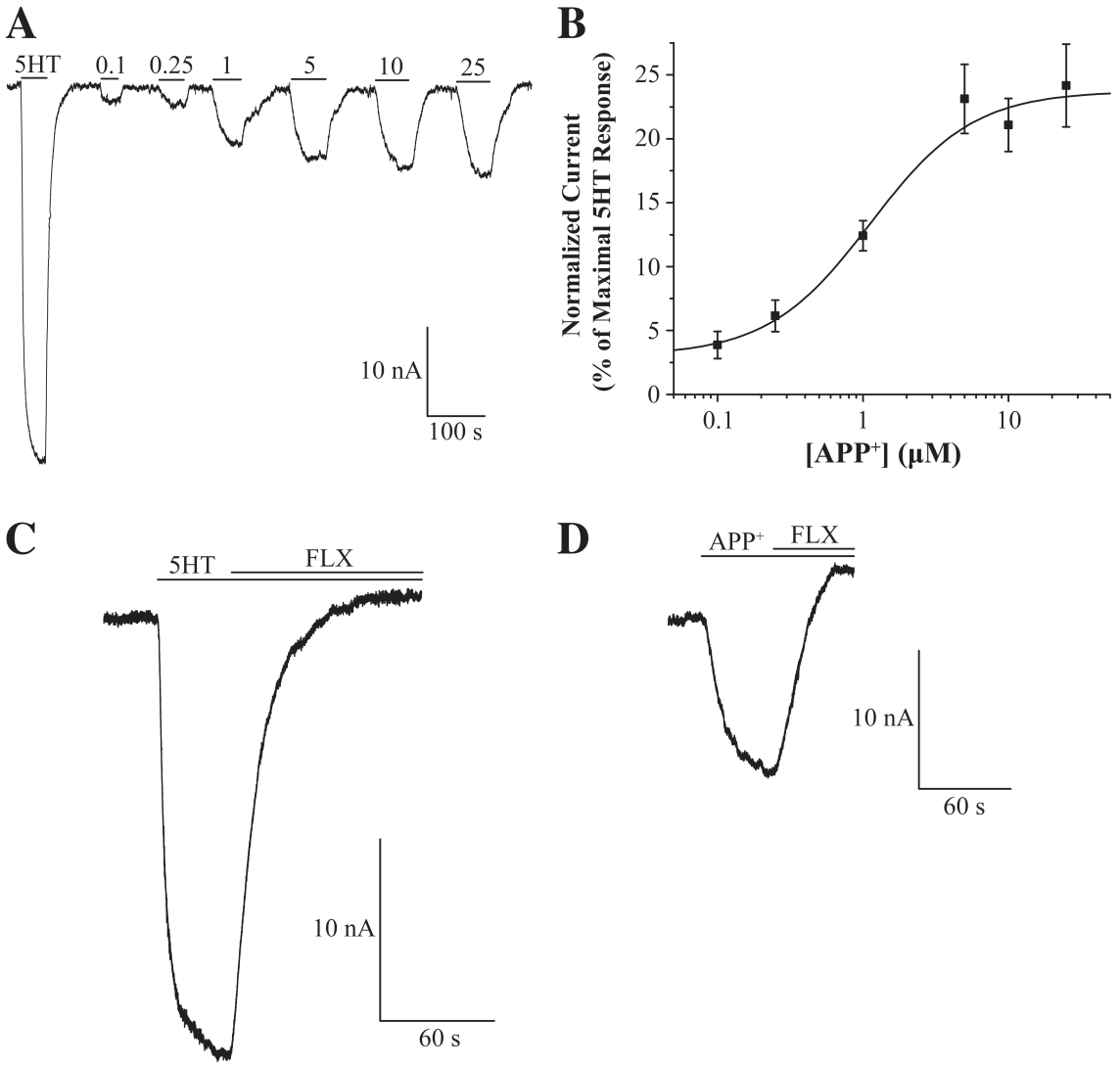

Figure 17. APP$^+$ exhibits substrate-like activity at hSERT. (A) APP$^+$ concentration-response curve. Representative trace of hSERT currents are measured in response to APP$^+$ (0.1-25 μM) applied to hSERT-expressing *Xenopus laevis* oocyte clamped to –60 mV. (B) Summary data were normalized to 5 μM 5HT-induced currents and fit to the Hill equation $y = I_{max} + (I_{min} - I_{max}) * x^n / (k^n+x^n)$, (N = 8). The I_{max}, I_{min}, k_m, and Hill coefficient were 23.75 ± 2.51, 3.02 ± 2.08, 1.13 ± 0.28 μM, and 1.23 ± 0.60, respectively. (C) Application of fluoxetine (1 μM) blocks the 5HT-induced hSERT current ([5HT] = 2 μM). (D) Application of fluoxetine (1 μM) blocks the APP$^+$-induced hSERT current ([APP$^+$] = 10 μM). Adapted from Solis, Zdravkovic et al. 2012.

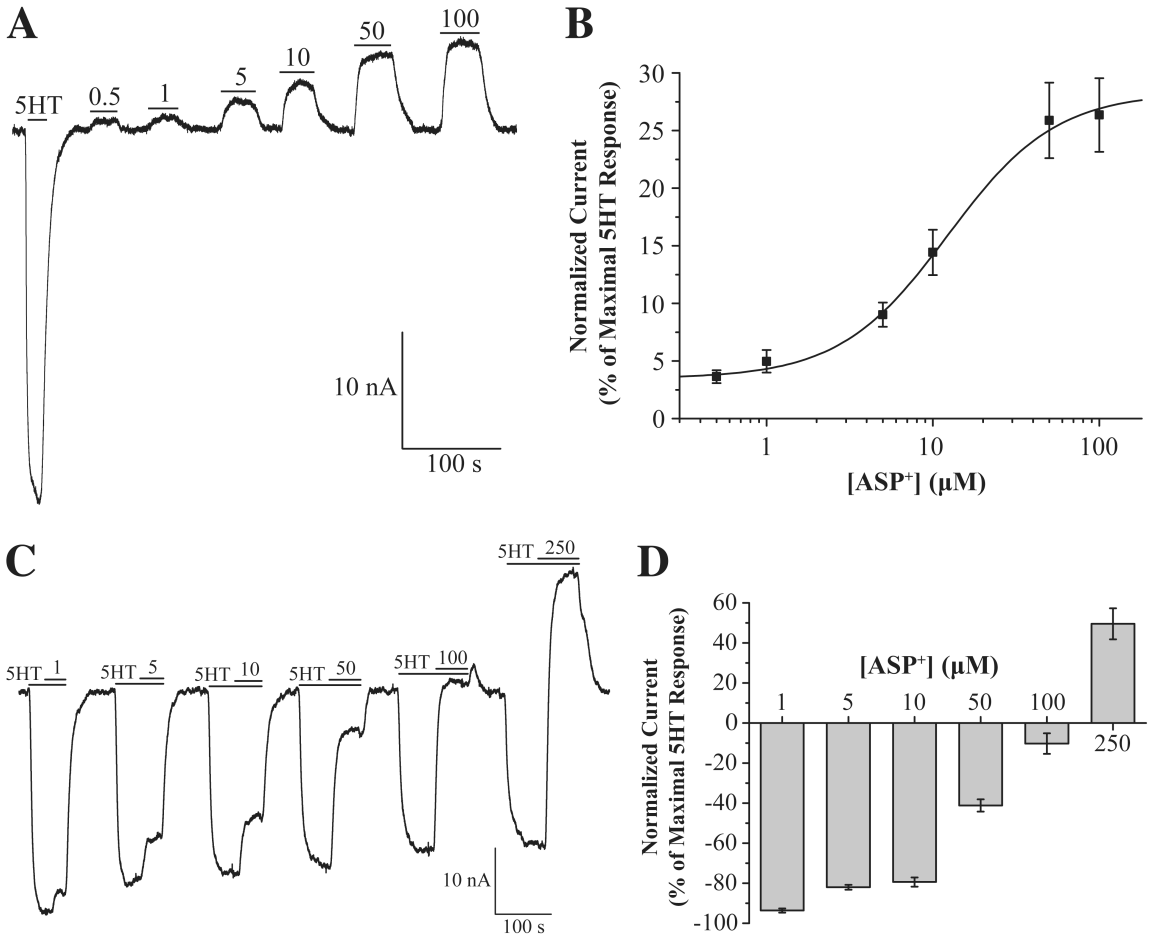

Figure 18. ASP^+ exhibits inhibitor-like activity at hSERT. (A) ASP^+ concentration-response curve. Representative trace of hSERT currents are measured in response to APP^+ (0.5-100 μM) applied to hSERT-expressing *Xenopus laevis* oocyte clamped to -60 mV. (B) Summary data were normalized to 2 μM 5HT-induced currents and fit to the Hill equation $y = I_{max} + (I_{min} - I_{max}) * x^n / (k^n + x^n)$, (N = 8). The I_{max}, I_{min}, k_m, and Hill coefficient were 28.32 ± 2.17, 3.48 ± 0.44, 12.25 ± 2.71 μM, and 1.34 ± 0.31, respectively. (C) ASP^+ inhibits 5HT-induced hSERT currents. During currents induced by 5HT (2 μM) ASP^+ is co-applied at indicated concentrations (from 1-250 μM, as indicated above upper bars in traces) (N = 8). (D) Summary data of ASP^+ inhibition of 5HT-induced hSERT currents (from currents in C). Adapted from Solis, Zdravkovic et al. 2012. Adapted from Solis, Zdravkovic et al. 2012.

Neither APP$^+$ Nor ASP$^+$ Display Measureable Fluorescence on hSERT

Due to the inherent ability of ASP$^+$ to fluoresce while interacting at hNET, we were previously able to take advantage of ASP$^+$ to study ASP$^+$-hNET stoichiometry and measure the residence time of ASP$^+$ on hNET before being transported (Schwartz, Novarino et al. 2005). These studies were successful because the ASP$^+$ signal displayed on the plasma membrane of hNET-expressing cells was sensitive and specific over parental cells (Schwartz, Blakely et al. 2003; Schwartz, Novarino et al. 2005). Although we were able to mimic the initial rapid ASP$^+$ binding phase (previously observed in hNET-expressing cells) in hSERT-HEK cells (labeled with arrow in Figure 19A, and clearly seen in high-resolution images 10 s after ASP$^+$ application in Figure 20A), these ASP$^+$ concentrations that elicited signal on the plasma membrane (10 μM and higher) displayed comparable fluorescence binding in parental cells (Figure 13A and Figure 14A). Furthermore, pre-treatment of hSERT-HEK cells with the hSERT inhibitor paroxetine did not quell ASP$^+$ plasma membrane fluorescence (Figure 21). These data strongly imply that ASP$^+$ is not suitable to discern plasma membrane labeling in hSERT-HEK cells solely attributed to specific ASP$^+$ interaction on hSERT.

We moved on to see whether APP$^+$ would elicit specific signal at the plasma membrane of hSERT-HEK cells. Since we had noticed APP$^+$ time-lapses (at a rate of 1 Hz) displayed no rapid fluorescent signal associated with membrane binding (Figure 11A, Figure 12, and Figure 14B), we tried to resolve a potential initial binding phase on the plasma membrane that may not be discernable at slow image acquisition rates; however, even increasing the image acquisition rate to 5 Hz failed to yield a plasma membrane binding phase (arrow in Figure 19B). Interestingly, APP$^+$ fluorescence

increased diffusely inside the cells without any visible APP^+ fluorescence while being transported by hSERT (seen as lack of a fluorescence accumulation peak in Figure 19B, and shown in a high-resolution image in Figure 20B after 10 s APP^+ exposure). Another attempt to determine whether APP^+ yields any visible fluorescence at the plasma membrane was to establish APP^+ Colocalization with the lipophilic plasma membrane marker DiI in hSERT-HEK cells; however, no overlap between the two signals was detected (Figure 22A). To look for APP^+/DiI colocalization in more detail, dual-channel line-scans through individual cells were performed, but no discernable colocalization was obtained, as indicated by asynchronous peaks (Figure 22B, plot) corresponding to APP^+ and DiI fluorescence intensity along a line-scan through an individual hSERT-HEK cell (Figure 22B, red arrow). Subsequently, we sought colocalization of DiI to additional APP^+ analogs that had been shown to induce hSERT-mediated outward currents in TEVC recordings (data not shown), which suggests they bind to hSERT in a manner similar to inhibitors. However, neither compound produced signal at the plasma membrane as shown by their lack of colocalization with DiI (Figure 23). In another effort to detect APP^+ binding at hSERT, we employed the hSERT mutant C109A/G338C that has been shown to lack 5HT transport while maintaining similar substrate binding affinity (Field, Henry et al. 2010). Since the strong intracellular fluorescence due to APP^+ transport would be absent, any fluorescent signal measured would be attributed to APP^+-mutant hSERT interaction. Following exposure to 3 μM APP^+ for 5 min, cells transiently-transfected with wild-type hSERT cells exhibited bright fluorescence signal; conversely, hardly any APP^+ signal was observed in parental cells or in cells transiently-transfected with C109A/G338C hSERT (Figure 24, top row). The lack of APP^+ uptake in the

C109A/G338C SERT is consistent with its reported inability to transport substrate (Field, Henry et al. 2010). Further, the fact that APP^+ displays no discernable fluorescence on the plasma membrane in the mutant SERT suggests APP^+ does not abide to a co-planar conformation amenable to exhibit fluorescence during its transport. Lastly, increasing APP^+ concentration to 50 μM did not elicit fluorescent signal on the plasma membrane in either parental cells or cells transiently-transfected with wild-type or C109A/G338C hSERT (Figure 24, bottom row). As expected, 50 μM APP^+ entry was comparable in all conditions tested, which is explained by non-specific diffusion or by the presence of endogenous organic cation transporters, which transport substrates, such as MPP^+ and ASP^+, with low affinity and high capacity (Busch, Quester et al. 1996; Gorboulev, Ulzheimer et al. 1997; Hohage, Stachon et al. 1998; Mehrens, Lelleck et al. 2000; Daws 2009).

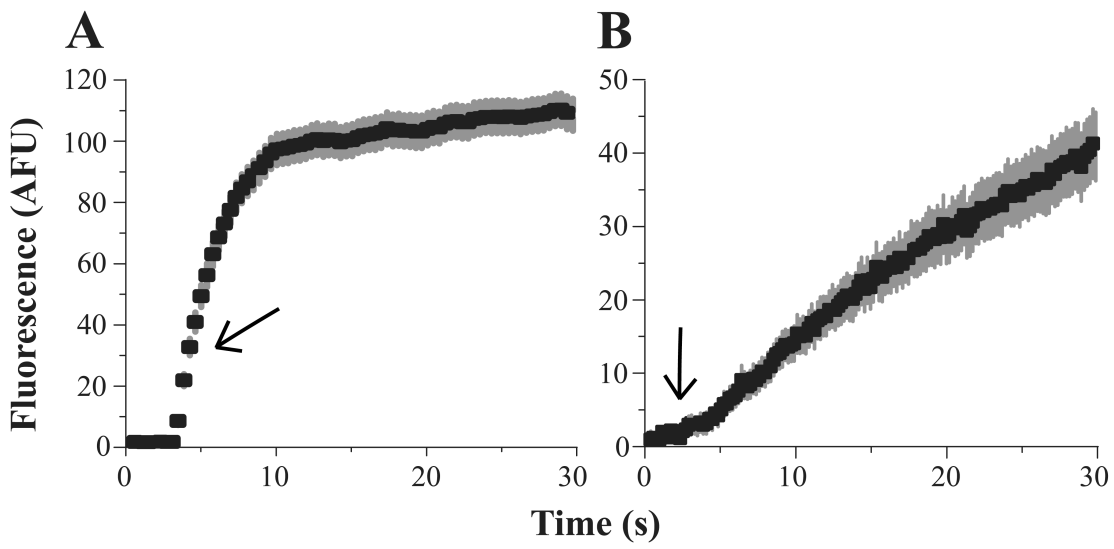

Figure 19. APP$^+$ does not display a plasma membrane-associated fluorescent binding phase like ASP$^+$ in hSERT-HEK cells. (A) ASP$^+$ (20 μM) displays rapid fluorescence accumulation (indicated by arrow) associated with plasma membrane binding in hSERT-HEK cells. (B) APP$^+$ (20 μM) application at a rate of 5 images per second does not reveal a fluorescent binding phase (indicated by arrow) associated with plasma membrane binding. Adapted from Solis, Zdravkovic et al. 2012.

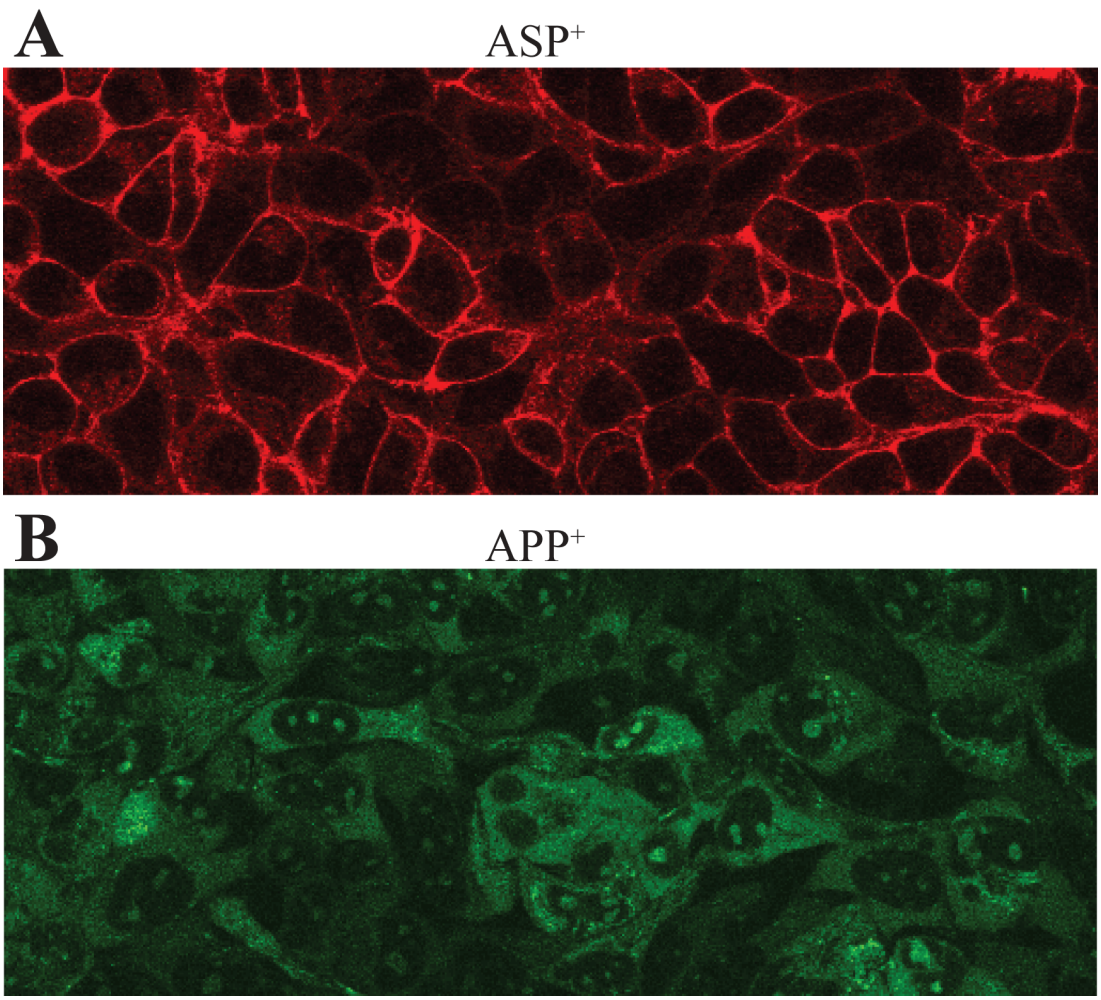

Figure 20. Fluorescent pattern of ASP^+ and APP^+ in hSERT-HEK cells. (A) Immediately following application, ASP^+ displays rapid plasma membrane binding on hSERT-HEK cells. (B) APP^+ fluorescence accumulation is diffuse within hSERT-HEK cells, and plasma membrane fluorescence is not apparent. Adapted from video from Solis, Zdravkovic et al. 2012.

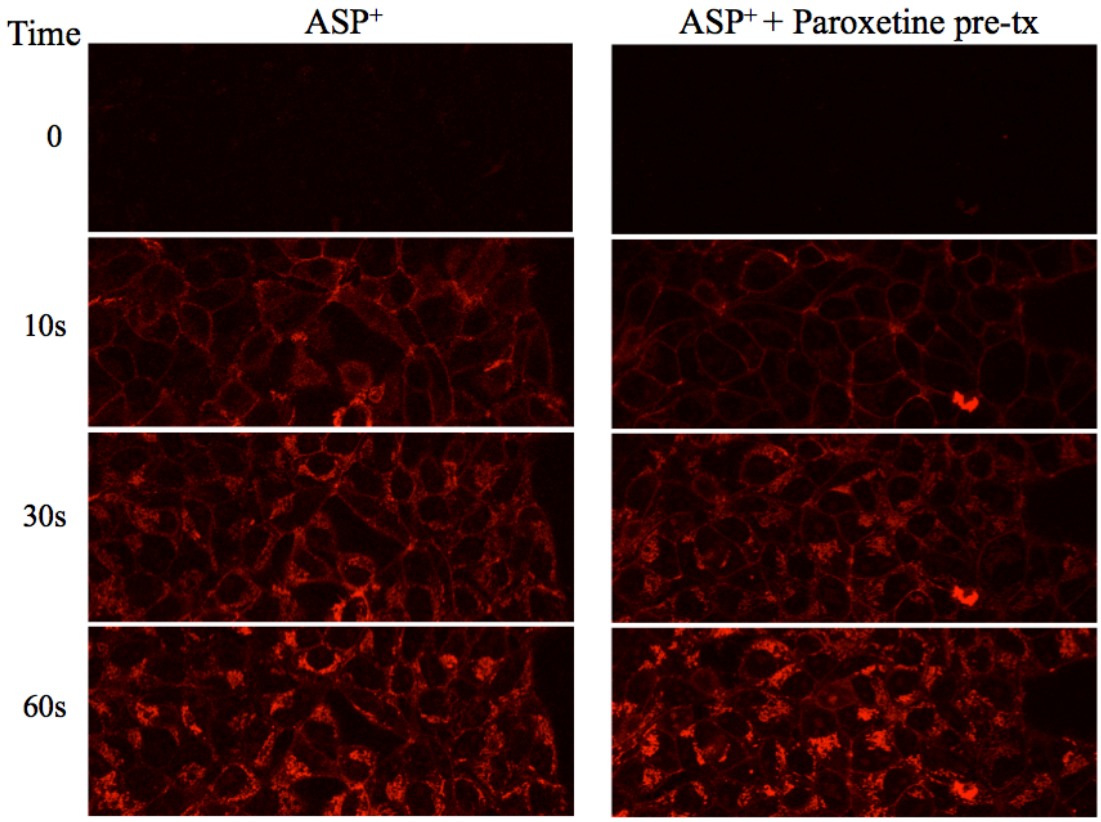

Figure 21. Paroxetine pre-treatment does not inhibit ASP^+ fluorescence accumulation. hSERT-HEK cells are untreated (left column) or pre-treated with paroxetine (right column). Paroxetine pre-treatment (10 μM) did not prevent fluorescence accumulation in hSERT-HEK cells. Adapted from Solis, Zdravkovic et al. 2012.

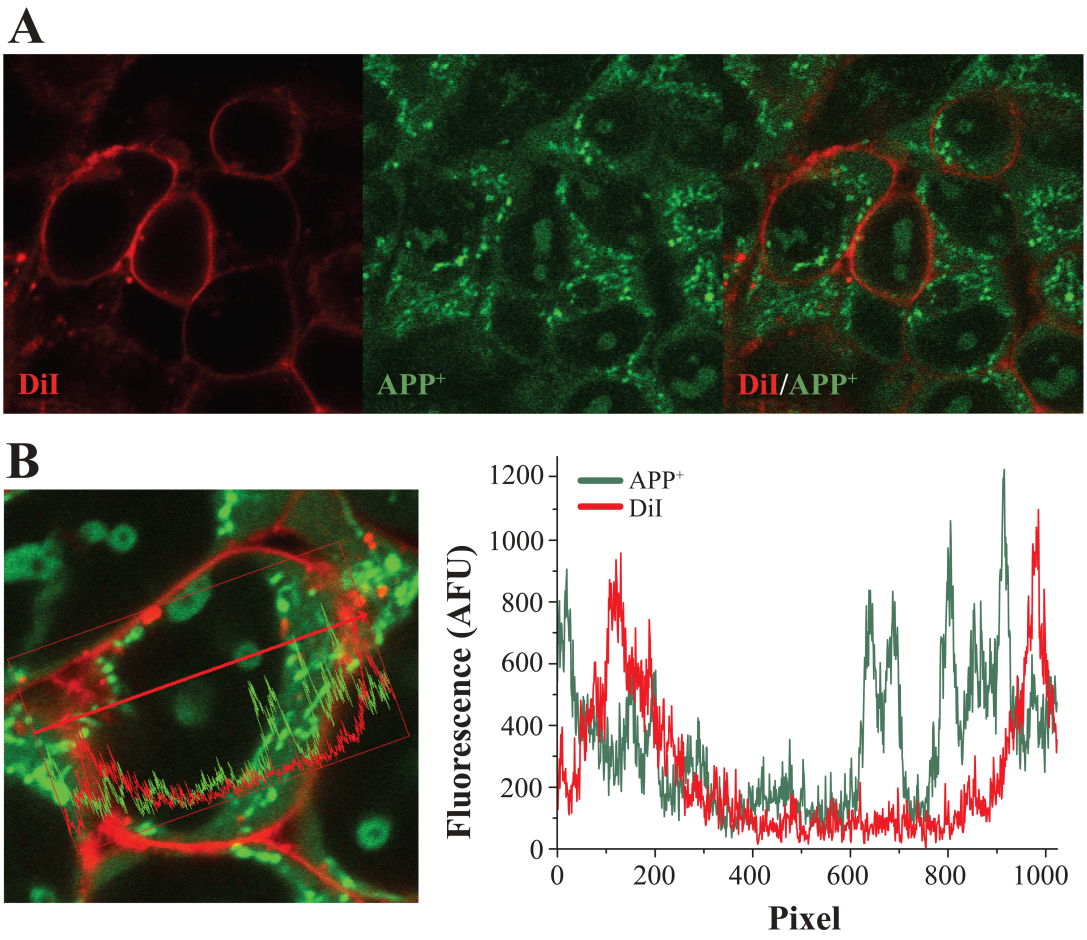

Figure 22. APP$^+$ is not fluorescent at the plasma membrane. (A) Plasma membrane of hSERT-HEK cells is labeled with DiI (red, left image) and APP$^+$ (green, middle image) is added to cells to determine colocalization (DiI and APP$^+$ merged in right image). (B) Line scan (red arrow) through an hSERT-HEK cell with APP$^+$/DiI (left), and plotted fluorescence intensity of line scan through cell (right). Adapted from Solis, Zdravkovic et al. 2012.

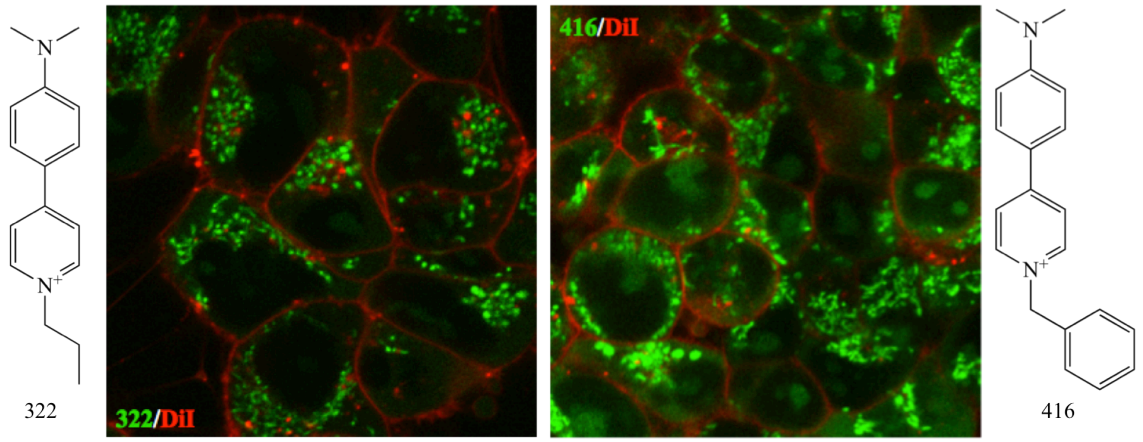

Figure 23. APP$^+$ analogs do not display fluorescence accumulation at the plasma membrane. Images of DiI-labeled hSERT-HEK cells exposed to 10 µM of either compound 322 or 416 show no colocalization between the red-labeled plasma membrane and the APP$^+$ analogs, which emit green fluorescence. Structure nomenclature: 322, 4-(4-(dimethylamino)phenyl)-1-propylpyridinium; 416, 1-benzyl-4-(4-(dimethylamino)phenyl)pyridinium. Adapted from Solis, Zdravkovic et al. 2012.

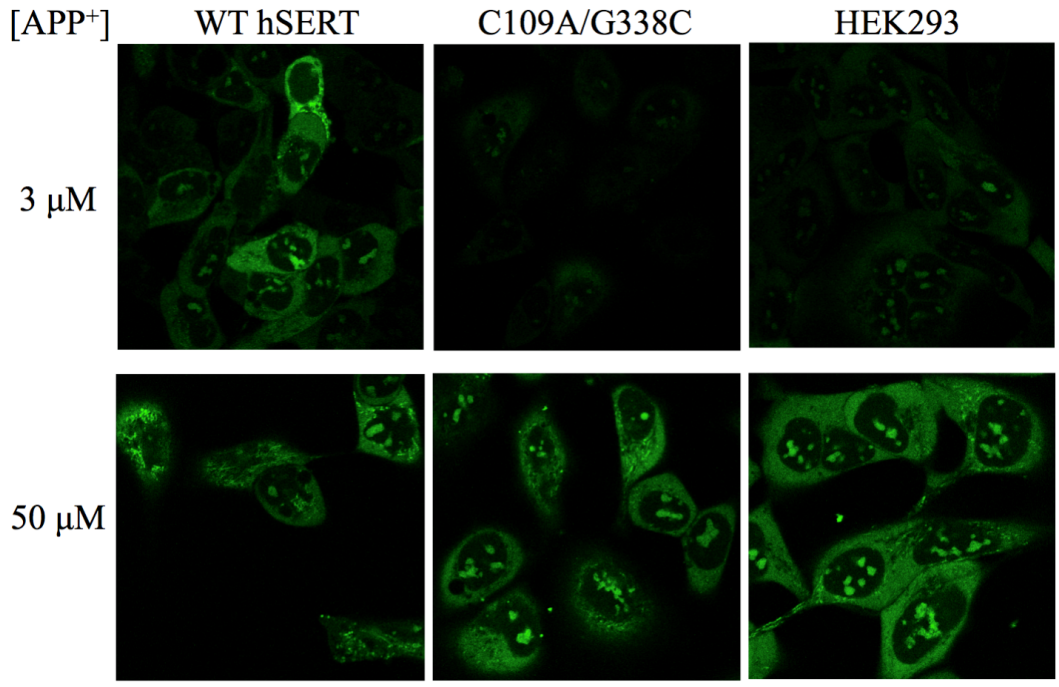

Figure 24. Non-transporting hSERT mutant did not exhibit plasma membrane fluorescence with APP$^+$. HEK293 cells transiently-transfected with WT hSERT or C109A/G338C hSERT mutant were exposed to either 3 or 50 μM APP$^+$, and no condition exhibited plasma membrane fluorescence. Representative images acquired 5 min post-APP$^+$ application. Field, Henry et al. 2010 demonstrated the C109A/G338C hSERT mutant lacks 5HT transport while maintaining similar substrate binding affinity. The C109A/G338C hSERT mutant was kindly provided by Randy Blakely. Adapted from Solis, Zdravkovic et al. 2012.

Docking of APP^+ and ASP^+ to hSERT

We sought to examine how the structural difference between APP^+ and ASP^+ affects their interaction with hSERT by utilizing a homology model of hSERT based on the crystal structure of $LeuT_{Aa}$ (Yamashita, Singh et al. 2005), and employing extra-precise ligand-receptor docking, which yields information about how tightly compounds dock within the active region of hSERT. Docking was performed with APP^+ and ASP^+ at their low-energy state (Figure 25, energy-minimized structures are shown in Figure 4, bottom row). All three compounds tested (5HT, APP^+ and ASP^+) displayed most favorable docking at the same place (Figure 26A-C shows docking of the compounds individually and Figure 26D shows they overlap within the active region of hSERT). Whereas 5HT, APP^+, and ASP^+ all docked favorably within the established active region of hSERT (Figure 27A-C) with respective G-scores of -10.95, -7.61, and -8.90 kcal/mol (values for energies measured are shown in Table 1), only 5HT displays significantly improved docking over both APP^+ and ASP^+. The difference in binding scores between APP^+ and ASP^+ is within uncertainty of the method. Zoomed images display interactions of docked 5HT, APP^+ and ASP^+ at their most energetically favorable positions to residues within the active region of hSERT (Figure 27D-F). The hSERT amino acids whose side chains are within 3 Å or less of docked compounds (listed in Table 2) are mostly from transmembrane helices 1, 3, 6 and 8, which have been shown to form the active region where substrates bind (Yamashita, Singh et al. 2005).

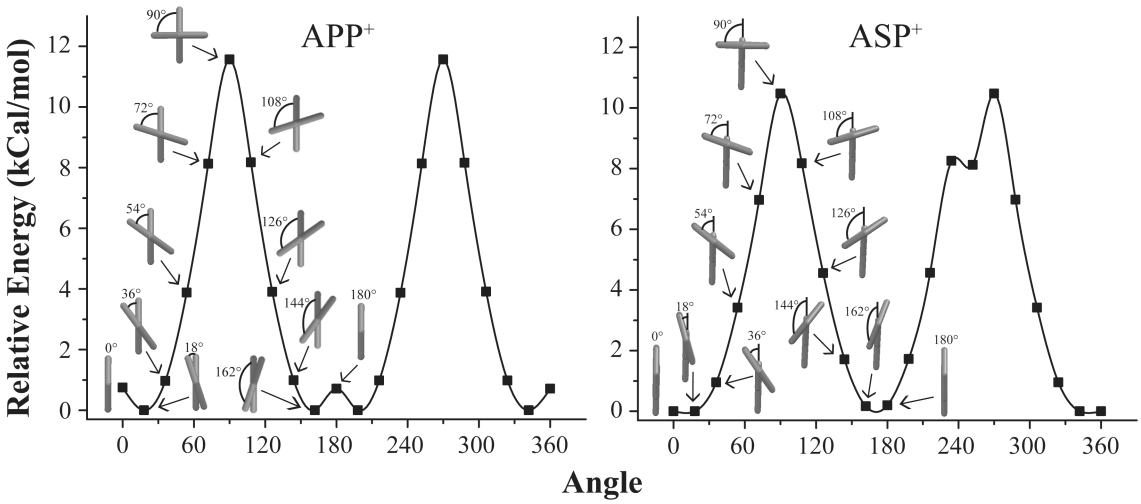

Figure 25. Energy minimization of APP^+ and ASP^+. Relative energies were calculated for torsional conformations at 18º rotation increments around the dihedral angle for APP^+ (left) and ASP^+ (right). The conformations with the lowest energy were used to dock to the homology model. The conformation with the lowest energy for APP^+ was a twisted conformer at 18º and 162º (due to symmetry 198º and 342º exhibit the same energy minima), and the conformation with the lowest energy for ASP^+ was at 0º. Adapted from Solis, Zdravkovic et al. 2012.

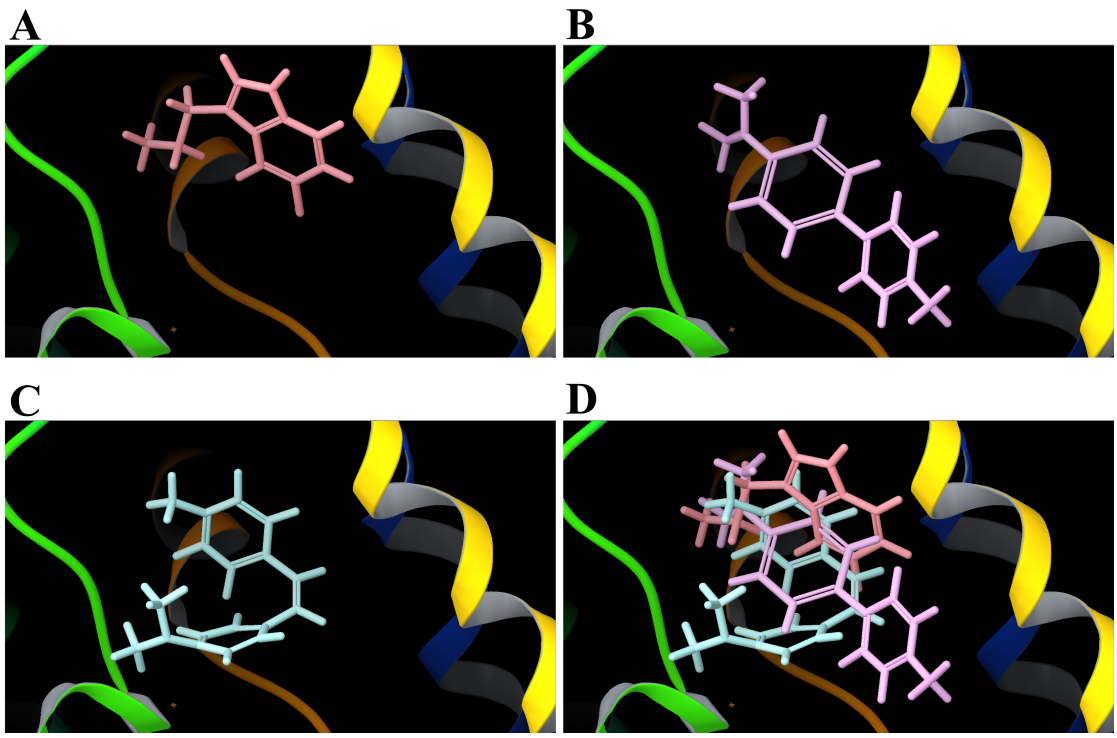

Figure 26. Most favorable position of docked substrates within the active region of the hSERT homology model. To validate the homology model of hSERT (A) 5HT, (B) APP^+, (C) ASP^+ were allowed to dock within hSERT and (D) all three compounds (5HT, APP^+, and ASP^+) displayed interactions within the active region of hSERT. Homology model based on the Yamashita, Singh et al. 2005 leucine transporter crystal structure and obtained from Igor Zdravkovic.

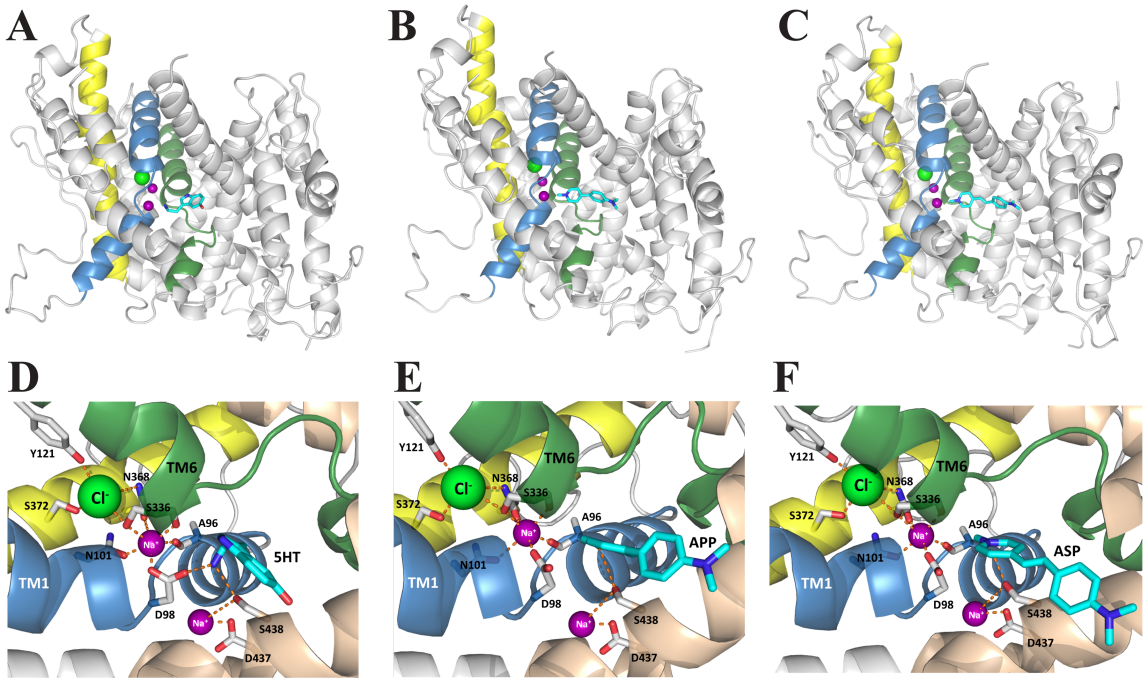

Figure 27. An hSERT homology model favors docking of APP^+ and ASP^+ in the active region. (A, D) Most favorable docking position for 5HT within the hSERT active region. (D) Relationship between 5HT and side chains of amino acids and coordinating ions (2 Na^+ and a Cl^-). (B, E) Most favorable docking position for APP^+ within the hSERT active region. (E) Relationship between APP^+ and side chains of amino acids and coordinating ions (2 Na^+ and a Cl^-). (C, F) Most favorable docking position for ASP^+ within the hSERT active region. (F) Relationship between ASP^+ and side chains of amino acids and coordinating ions (2 Na^+ and a Cl^-). Homology model based on the Yamashita, Singh et al. 2005 leucine transporter crystal structure and obtained from Igor Zdravkovic. Adapted from Solis, Zdravkovic et al. 2012.

	G-Scr	vdW	Lipo	Hbond	Clmb
5HT	-10.95	-24.35	-1.82	-0.06	-10.22
APP^+	-7.61	-34.20	-2.01	0.00	-6.48
ASP^+	-8.90	-35.34	-2.23	0.00	-5.76

Table 1. Docking values for 5HT, APP^+, and ASP^+ in the hSERT active region. The docking study was performed using GLIDE. The energy grid for the receptor was created and each of the ligands docked individually. A square volume with a length of 14 Å around the location of the active site was designated to allow insertions of the ligands. The center of the insertion region was defined around the known substrate-binding site in the leucine transporter (LeuT). The docking was performed on the basis of a rigid protein approximation and a flexible ligand. Extra precision docking (Friesner, Murphy et al. 2006) was subsequently used and the top ten potential docks were further optimized. The ranking of each pose and its energy was calculated using the G-Score. Once re-minimized, each dock is assigned a G-Score as a sum of interactions and the docks are ranked from most negative (favorable) to least. The ligand in each dock is allowed full degrees of motion, within its optimal conformation. The hSERT homology model was obtained from the Meiler lab (Kaufmann, Dawson et al. 2009), and is based on the crystallized structure of the leucine transporter ($LeuT_{Aa}$) reported by Yamashita et al. PBDID 2A65 (Yamashita, Singh et al. 2005). Abbreviations: G-scr (G-score), vdW (van der Waals energy), Lipo (lipophilic energy), Hbond (H-bond energy), Clmb (coulombic energy). Adapted from Solis, Zdravkovic et al. 2012.

		5HT	APP^+	ASP^+
TM1	95 Tyr	+	+	+
	96 Ala	+	+	-
	98 Asp	+	+	-
TM3	164 Ala	-	-	+
	165 Ile	-	+	+
	168 Ile	-	+	+
	169 Ala	+	+	+
	172 Ile	+	+	+
	176 Tyr	+	+	+
TM6	337 Leu	+	+	-
	338 Gly	+	+	-
	341 Phe	+	+	+
	343 Val	+	+	+
	344 Leu	+	-	-
TM8	438 Ser	+	+	+
	441 Ala	+	+	+
TM10	496 Ala	-	-	+
	500 Ala	-	-	+
	501 Val	-	+	+

Table 2. hSERT residues interacting with 5HT, APP^+, and ASP^+. APP^+ and ASP^+ dock within the same region as for the endogenous ligand 5HT, and all amino acids are located near the active region of hSERT. The amino acids listed were in proximity to either 5HT, APP^+ or ASP^+. Residues that are less than 3 Å away from the docked compound are indicated by a +. Adapted from Solis, Zdravkovic et al. 2012.

DISCUSSION

Rationale of Study

Fluorescent monoamine transporter substrates provide a significant technical improvement to study substrate transport and binding over traditional radiolabeled substrate uptake assays. Fluorescent substrates in conjunction with confocal microscopy enable the measurement of real-time activity in individual cells. When we first established the fluorescent compound ASP^+ as a substrate for monoamine transporters, we determined the substrate-to-transporter stoichiometry and the residence time of ASP^+ on hNET before being transported (Schwartz, Blakely et al. 2003; Schwartz, Novarino et al. 2005; Schwartz, Piston et al. 2006). Subsequently, ASP^+ was successfully utilized to study the regulation of DAT activity by several DA receptors (Bolan, Kivell et al. 2007; Zapata, Kivell et al. 2007). In addition, further studies validated the use of ASP^+ as a useful fluorescent substrate amenable for high-throughput methods for which ASP^+ uptake by hNET was effective with low μM affinity (Mason, Farmer et al. 2005; Haunso and Buchanan 2007). However, ASP^+ had marginal effectiveness as an hSERT substrate; in fact, to see substantial hSERT-mediated uptake incubation for long time-periods was required. In one instance, measurements taken 10-60 min after hSERT-expressing cells were incubated with ASP^+ yielded an uptake k_m between 9.9 and 20 μM (Fowler, Seifert et al. 2006). Our previous research also indicated ASP^+ was very weak at labeling hSERT-expressing cells (Schwartz, Blakely et al. 2003). Therefore, it was unknown what the utility of ASP^+ as a fluorescent hSERT reporter would be in real-time measurements, and the development for improved fluorescent hSERT substrates was evident.

In this study we identified APP^+ (also known as IDT307) from a series of fluorescent MPP^+ analogs synthesized by Ian D. Tomlinson and Sandra Rosenthal, and thoroughly characterized its utility as an hSERT substrate. The fluorescent APP^+ uptake rate by hSERT resembles the ASP^+ uptake phase by hNET previously observed (Schwartz, Blakely et al. 2003). Furthermore, APP^+ uptake k_m values at hSERT are 5 to 10 times better than the reported k_m for ASP^+ as an hSERT substrate (Fowler, Seifert et al. 2006). This difference in affinity is consistent with TEVC recordings where APP^+ induces hSERT-mediated inward currents with a k_m that is roughly 10 times better than the k_m for ASP^+-induced hSERT-mediated outward currents. In agreement, the radiolabeled substrate uptake competition assay we performed shows APP^+ has nearly a 10-fold better k_i than ASP^+ when inhibiting [^{3}H]-5HT uptake through hSERT. By all our measures APP^+ is superior to ASP^+ at targeting hSERT.

The Action of APP^+ on hSERT

Consistent with activity as an hSERT substrate, APP^+ behaves similarly to the endogenous hSERT substrate 5HT. The k_m for APP^+ fluorescence uptake by hSERT is comparable to the reported k_m for [^{3}H]-5HT uptake (Hilber, Scholze et al. 2005; Andersen, Taboureau et al. 2009). In agreement, 5HT and APP^+ display similar affinity when evoking hSERT-mediated currents. Since inward currents by hSERT are observed only in response to transported substrates, such as 5HT, MPP^+, or MDMA, the presence of APP^+-induced hSERT-mediated inward currents supports that APP^+ is a substrate of hSERT. While the k_m values for APP^+ fluorescence uptake and APP^+-induced hSERT currents are comparable (~2.3 and 1.13 μM, respectively), the APP^+ k_i for [^{3}H]-5HT uptake inhibition is much weaker (nearly 20 μM). This discrepancy in affinity can be explained by the assay employed. Both APP^+ uptake and APP^+-induced currents are measured with only the substrate present; on the other hand, the [^{3}H]-5HT inhibition assay requires the presence of 5HT, which could confer an alternate conformational state of hSERT, and in turn alter the interaction between APP^+ and hSERT.

Source of APP^+ Fluorescence

To perform biophysical studies for hSERT similar to ones we previously performed for hNET, the fluorescent substrate for hSERT should display fluorescence on the plasma membrane while interacting with the transporter. Hence, we sought to identify APP^+ fluorescence on the plasma membrane of hSERT-HEK cells, but were unsuccessful in all our attempts, which included colocalization studies using DiI and additional APP^+ analogs, and experiments employing an hSERT mutant. The absence of fluorescence of APP^+ and its analogs while interacting with the transporter may be explained by the physical properties of this class of compounds. APP^+ and its analogs are twist-intramolecular-charge-transfer-state-forming (TICT) compounds (Murali and Rettig 2006), which display energy emission under specific structural conditions. In order for APP^+ to be fluorescent, the phenyl and pyridyl rings must assume a co-planar conformation. Molecular modeling studies have suggested that the lowest energy conformer of APP^+ is in the twisted conformation (Figure 4 and Figure 25), and it is likely that this conformation is the most abundant conformer in an aqueous environment. Since the co-planar conformer may become more energetically favorable when the molecule binds to intracellular biomolecules such as proteins or DNA, APP^+ will fluoresce only after entering cells. It is likely that the co-planar APP^+ conformer intercalates between the base pairs of DNA and RNA because this conformer would produce π-π stacking interactions with nucleic acid base pairs, and confer π-π stacking interactions among nucleic acid base pairs. Intriguingly, the lack of APP^+ fluorescence on the plasma membrane of hSERT-expressing cells suggests the co-planar fluorescent state of APP^+ is not achieved during transport by hSERT. Instead, APP^+ fluorescence

accumulation in hSERT-HEK cells seems diffuse in the cytosol and gathers preferentially at mitochondria and nucleoli. It is well known that MPP^+ and its analogs exert their neurotoxic effects by disrupting the electron transport chain at mitochondria (Krueger, Sablin et al. 1993; Gluck, Youngster et al. 1994; Desai, Feuers et al. 1996), which supports the preference APP^+ (an MPP^+ analog) has to stain mitochondria. In addition, since the membrane potential of mitochondria is highly negative (Johnson, Walsh et al. 1980; Johnson, Walsh et al. 1981), positively charged compounds such as APP^+ would display favorable mitochondrial accumulation. Nucleoli are the most dense compartments in the nucleus consisting of tightly packed DNA, RNA, and proteins, and were recently shown to exhibit the slowest rate of protein diffusion, which implies limited mobility (Bancaud, Huet et al. 2009). Perhaps this dense and spatially restricted environment within nucleoli favors APP^+ accumulation and subsequent binding to nucleic acids in its fluorescence-emitting conformation.

It is worth noting that we observed minimal reversal of APP^+ signal in response to 5HT application (Figure 11C). As mentioned, for APP^+ to display fluorescence, it must abide to a rigid co-planar conformation, which occurs when it binds to specific regions in the cell. Thus, in order for transported hSERT substrates, such as 5HT, or releasing-agents like MDMA, to induce hSERT-mediated APP^+ efflux, they would need to displace bound APP^+, which requires affinity at the same binding sites. Furthermore, if APP^+ intercalates the base pairs in DNA and RNA it would form strong hydrophobic interactions between the base pairs of DNA and RNA. The intrinsic positive charge of APP^+ might form charge-charge interactions between the positively charged pyridyl nitrogen and the phosphate backbone of these polymers. Since these interactions are

energetically favorable, they would result in strong binding making it very difficult for APP^+ to be displaced from nucleic acids. Lastly, if bound APP^+ could be displaced, it might bind to other subcellular compartments before undergoing hSERT-mediated efflux. Further studies employing strong releasing compounds are warranted.

The Hill coefficient for APP^+ fluorescence accumulation through hSERT ranged from 2.5 to 2.9 (depending on accumulation rate), which is in contrast to the Hill coefficient obtained from TEVC recordings and the [^{3}H]-5HT uptake inhibition assay (1.23). APP^+ fluorescence accumulation consists of several processes that could influence the Hill coefficient, including rate of uptake through hSERT, distinct accumulation sites within the cell that are at different distances from the entry point (besides displaying fluorescence at nucleoli and mitochondria, APP^+ emits diffuse fluorescence in the cytosol), manner of APP^+ incorporation into subcellular compartments, and the mechanism whereby APP^+ abides to the co-planar conformation. On the other hand, TEVC recordings and the [^{3}H]-5HT uptake inhibition assay measure single processes by hSERT (currents mediated primarily by Na^+ or [^{3}H]-5HT uptake), which are the limiting step. Since these measures are solely dependent on hSERT activity, a Hill coefficient near unity seems reasonable.

The Action of ASP^+ on hSERT

Although ASP^+ does not report specific hSERT uptake or binding, our study demonstrates that ASP^+ interacts with hSERT. Most strikingly is the result in TEVC oocyte recordings showing ASP^+ induce hSERT-mediated outward currents, which resemble the outward currents induced by hSERT inhibitors, such as fluoxetine (Li, Zhong et al. 2006), and are usually interpreted as the inhibition of the constitutive inward leak current seen by many transporters (Mager, Min et al. 1994; Adams and DeFelice 2003). However, ASP^+ proves to be very poor when acting as an inhibitor, as demonstrated by the high ASP^+ concentrations required to inhibit 5HT-induced hSERT currents, and the poor k_i obtained for ASP^+ inhibition of [^{3}H]-5HT uptake. Still, we cannot rule out that ASP^+ is transported through hSERT and that its interaction with hSERT is distinct from bona fide hSERT inhibitors. ASP^+ could even serve dual functions at hSERT, as both an inhibitor (in electrophysiology measurements) and a substrate (in uptake measurements), albeit likely having a very slow uptake rate. To determine if a fraction of ASP^+ is taken up through hSERT, radiolabeled ASP^+ could be employed in uptake assays. Interestingly, ASP^+ is effectively transported by hNET and electrophysiology experiments show ASP^+ elicits inward currents through hNET (Schwartz, Novarino et al. 2005). The distinct effect of ASP^+ as an inhibitor on hSERT and as a substrate on hNET highlights the structural and functional differences between these two monoamine transporters.

The difference observed in affinity for ASP^+ on hSERT in the [^{3}H]-5HT competition assay versus TEVC oocyte recordings could be explained by the existence of two distinct binding sites, the established substrate-binding active region and the recently discovered

secondary antidepressant binding site in the extracellular vestibule of the homologous LeuT (Singh, Yamashita et al. 2007; Zhou, Zhen et al. 2007; Zhou, Zhen et al. 2009), which has been further substantiated for SERT (Andersen, Taboureau et al. 2009; Sarker, Weissensteiner et al. 2010). ASP^+ might not be readily accessible to the substrate-binding site, and hence, it is weak at displacing 5HT, whereas it can induce an hSERT-mediated outward current at a much lower concentration possibly because in the absence of 5HT, hSERT is at a conformation that provides easy access for ASP^+ at the outer antidepressant-binding site. Supporting this possibility are recent studies showing that two structurally dissimilar classes of drugs, the TCAs and the SSRIs, interact at this promiscuous binding site (Zhou, Zhen et al. 2009; Sarker, Weissensteiner et al. 2010).

Docking to an hSERT Homology Model

To understand the interaction of APP^+ and ASP^+ with hSERT, we performed a docking study, which yielded favorable docking scores for 5HT, APP^+, and ASP^+ at the active region of hSERT, and agrees well with the electrophysiology data, in which, when applied individually, 5HT, APP^+ and ASP^+ induce visible hSERT-mediated currents at low μM concentrations. The hSERT model predicts amino acid side chains in proximity to docked substrates within the active region. Of interest are residues that displayed interactions with the three compounds tested in our model that are involved in substrate or antidepressant affinity to hSERT, including Tyrosine 95, Isoleucine 172, Alanine 169, and Serine 438 (Barker and Blakely 1996; Henry, Field et al. 2006; Celik, Sinning et al. 2008; Andersen, Taboureau et al. 2009). Additionally, while 5HT shares 80% of hSERT interacting residues with APP^+, it only shares ~57% residues to docked ASP^+ (Table 2). The similarity between 5HT and APP^+ interaction with hSERT is consistent with comparable affinity at hSERT, and their action as transported substrates. On the other hand, ASP^+, which interacts with distinct residues than 5HT in the hSERT model, has the weakest affinity for hSERT in all the assays performed in this study and it exhibits minimal transport. We speculate that the interactions a docked compound makes to residues in this model can help predict whether the compound will function as a substrate or inhibitor.

Conclusions

Despite exhibiting no measureable fluorescence on the plasma membrane, we have established that APP^+ is a suitable fluorescent substrate to study hSERT uptake activity in single cells, which may introduce new protocols to study hSERT transport in real-time. ASP^+, on the other hand, is not adequate to study hSERT activity.

CHAPTER III

S(+)AMPHETAMINE INDUCES A PERSISTENT LEAK IN THE HUMAN DOPAMINE TRANSPORTER: MOLECULAR STENT HYPOTHESIS

Parts of Chapter 3 are adapted from Rodriguez-Menchaca, A. A., E. Solis, Jr., K. Cameron and L. J. De Felice (2012). "S(+)amphetamine induces a persistent leak in the human dopamine transporter: molecular stent hypothesis." Br J Pharmacol **165**(8): 2749-2757.

STUDY OVERVIEW

Background and Purpose

Wherever they are located, DA transporters (DATs) clear DA from the extracellular milieu to help regulate dopaminergic signaling. Exposure to amphetamine (AMPH) increases extracellular DA in the synaptic cleft, a process that has been ascribed to DAT reverse transport. Increased extracellular DA prolongs postsynaptic activity and reinforces abuse and hedonic behavior. The mechanisms underlying AMPH-induced DA release are only partially understood.

Experimental Approach

Currents were recorded from *Xenopus laevis* oocytes expressing hDAT and voltage-clamped to –60 mV in response to exposure to DA, R(–)AMPH, or S(+)AMPH externally and internally by injection.

Key results and Conclusions

Here we report a hitherto unknown action of S(+)AMPH on hDAT that potentially impacts AMPH-induced DA release. At –60mV, near the resting potential of neurons, S(+)AMPH induces a depolarizing current through hDAT that surprisingly, after removing the drug, persists for up to 30 minutes. This persistent leak current in the absence of substrate (shown in Figure 27) is in contrast to the R(–)AMPH- and DA-induced currents, which return to baseline immediately after their removal. In addition, the persistent current depends on Na^+ and is blocked by cocaine. Our data suggests that

S(+)AMPH and Na^+ carry the initial S(+)AMPH-induced current, whereas Na^+ and Cl^- carry the persistent leak current. We propose that the persistent current results from the internal action of S(+)AMPH on hDAT because the temporal effect is consistent with S(+)AMPH transport influx and intracellular injection of S(+)AMPH produces the effect. Remarkably, following S(+)AMPH injection into the oocyte, external application with DA can induce the persistent leak current.

Implications

We propose that S(+)AMPH acts as a molecular stent that holds the transporter open even after it is removed externally. AMPH-induced persistent currents, if found in DA neurons, are likely to impact dopaminergic signaling, DA release mechanisms, and AMPH abuse.

INTRODUCTION

The Dopamine Transporter

Cocaine (COC) and AMPH profoundly influence dopaminergic neurotransmission through their action on DAT. In response to prolonged exposure to these drugs, DAT displays reduced capacity for DA transport (Iversen 2006; Samuvel, Jayanthi et al. 2008). In contrast to the DAT inhibitor COC, AMPH acts as a DAT substrate that fluxes into cells through the transporter (Volz, Hanson et al. 2007; Erreger, Grewer et al. 2008). Thus, COC and AMPH both increase extracellular DA by diminishing uptake, but they do so by entirely different mechanisms. Whereas COC blocks DA uptake, AMPH replaces DA as a substrate and, in addition, releases DA into the synaptic cleft (Iversen 2006). In striatal slices, as one example, AMPH causes a gradual increase in extracellular DA that lasts for over 30 min in normal mice, whereas no analogous increase exists in -/- DAT mice (Giros, Jaber et al. 1996). Although DAT is required for the DA releasing action of AMPH, its presence is not necessary for the vesicle-depleting action of AMPH; furthermore, in the absence of AMPH, cytoplasmic DA is considered insufficiently concentrated to reverse DAT, implying that AMPH releases DA from vesicular stores prior to DA efflux (Jones, Gainetdinov et al. 1998). In some cases, however, as in dendrodendritic autoinhibition, DAT block abolishes DA efflux even in the absence of AMPH (Falkenburger, Barstow et al. 2001).

AMPH as a Therapeutic Agent

Because AMPH releases DA from terminals in the frontal lobe and limbic system, it has been used clinically to treat medical conditions such as attention-deficit hyperactivity disorder and narcolepsy (Burnette, Bailey et al. 1996; Fleckenstein, Volz et al. 2007). Due to the higher potency of the dextroamphetamine isomer (S(+)AMPH) over levoamphetamine (R(–)AMPH) (Phillips, Brooke et al. 1975; Holmes and Rutledge 1976; Kuczenski, Segal et al. 1995), therapeutic agents are composed primarily of S(+)AMPH. For example, Adderall is composed of 3:1 S(+)AMPH to R(–)AMPH (Cody, Valtier et al. 2003), and Vyvanse (lisdexamphetamine) is a pro-drug that is metabolized entirely to S(+)AMPH (Najib 2009). Clinical manifestations associated with the abuse of AMPH or its precursors or derivatives, such as phenethylamine or METH, are well documented (Potkin, Karoum et al. 1979; Romanelli and Smith 2006; Winslow, Voorhees et al. 2007).

AMPH as an Abused Substance

AMPH is a homologue of phenethylamine and the parent compound of a wide range of psychoactive derivatives, from the *N*-methylated methamphetamine (METH) to 3,4-Methylenedioxy-N-methamphetamine (MDMA, commonly known as ecstasy). AMPH is widely abused and the clinical manifestations associated with the abuse of AMPH, its precursors, or its derivatives, such as phenethylamine or METH, are well documented (Potkin, Karoum et al. 1979; Romanelli and Smith 2006; Winslow, Voorhees et al. 2007). Because DAT is the primary target for AMPH, DAT is most frequently implicated in the reinforcing properties and abuse potential of AMPH (Sulzer, Maidment et al. 1993; Sulzer, Chen et al. 1995; Seidel, Singer et al. 2005). The reward and addiction properties of AMPH rely on its ability to increase extracellular DA levels by mechanisms as yet only partially understood.

Findings of Study

The principal mechanisms proposed for AMPH-induced increases in extracellular DA are the facilitated exchange model (Fischer and Cho 1979), the DAT efflux channel and reverse transport model (Kahlig, Binda et al. 2005), and the vesicular depletion model, which is also called the weak-base model (Sulzer, Maidment et al. 1993; Sulzer, Chen et al. 1995). Here we introduce a mechanism garnered from electrophysiological data that is based on a novel action of S(+)AMPH. In our model, hDAT transports S(+)AMPH inside the cell where it is available to bind hDAT at an internally accessible site. S(+)AMPH transport and induced current depend on extracellular Na^+, which also carries part of the current. S(+)AMPH binding to an internal site maintains hDAT in a constitutively-active state long after removing external S(+)AMPH. The state defines a use-dependent leak named for the previously described substrate-independent leak (Sonders, Zhu et al. 1997). Once hDAT has been exposed to S(+)AMPH, subsequent exposure to DA also results in a persistent leak. In a free running cell, the persistent leak current, if carried by Na^+, would depolarize the presynaptic terminal and increase the likelihood of vesicular fusion and DA release. Future studies are warranted to elucidate the relationship between the persistent leak current and the AMPH-induced DAT-mediated DA efflux, as well as determining whether the required players in DAT efflux, such as Ca2+, protein kinase B, and CaMKII, play a role to produce the persistent leak current.

EXPERIMENTAL PROCEDURES

Expression of hDAT in Xenopus Laevis Oocytes

Oocytes are harvested and prepared from adult *Xenopus laevis* females following standard procedures (Machaca and Hartzell 1998; Iwamoto, Blakely et al. 2006). We select stage V-VI oocytes for cRNA injection within 24 h of isolation. cRNA is transcribed in the pOTV vector (gift of Mark Sonders, Columbia University) using Ambion mMessage Machine T7 kit (Ambion Inc., Austin, TX). Each oocyte is injected with 50 nl of 1 μg/μl hDAT cRNA (final amount 50 ng) (Nanoject AutoOocyteInjector, Drummond Scientific Co., Broomall, PA) and incubated at 18^{o}C for 4-8 days in Ringers solution supplemented with NaPyruvate (550 μg/ml), streptomycin (100 μg/ml), tetracycline (50 μg/ml) and 5% dialyzed horse serum.

Electrophysiology

We performed two-electrode voltage-clamp (TEVC) experiments as previously described (Wang, Li et al. 2006). Electrodes have resistances from 1-5 MΩ. *Xenopus laevis* oocytes expressing hDAT are voltage-clamped to -60 mV (unless otherwise noted) and buffer is gently perfused until a stable baseline is obtained. Then, the experimental substrates are perfused until stable currents are obtained for time periods indicated.

Oocyte Injection With S(+)AMPH

We injected a small volume of concentrated drug and calculated the final concentration by dilution in the oocyte volume. For example, 50 nl of 0.5 mM

S(+)AMPH diluted into an oocyte with estimated cytoplasmic volume of 1 µl (stage V-VI oocytes are 1-1.2 mm in diameter) gives a 25 µM final concentration. Repeated injections at the same concentration, or a single injection at a higher concentration produced a range of S(+)AMPH inside the oocyte from 0 to 180 µM.

Solutions

Extracellular (in mM): 120 NaCl, 7.5 HEPES, 5.4 K gluconate, 1.2 Ca^{2+} gluconate, pH 7.4 with KOH. For Na^{+}-free solution, 120 NaCl is replaced with 120 mM NMDG-Cl. Intracellular: 3 M KCl.

RESULTS

Structures of DA and AMPH Stereoisomers

Racemic AMPH consists of equal amounts of S(+)amphetamine (S(+)AMPH) and R(–)amphetamine (R(–)AMPH). The AMPH stereoisomers share similarity with the unique structure of DA (Figure 28). Although DA, S(+)AMPH, and R(–)AMPH have similar structures, they have markedly distinct effects on hDAT with regard to the current they induce under voltage clamp of hDAT-expressing oocytes (Figure 29).

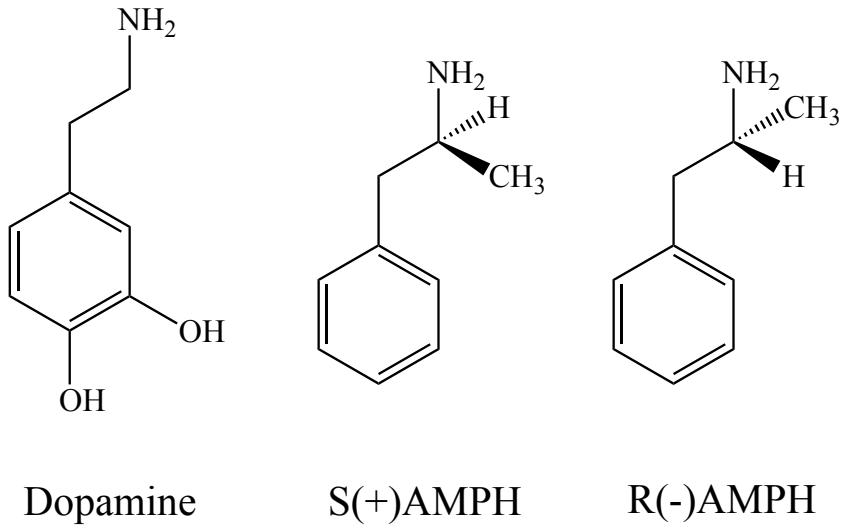

Figure 28. Structures of DA and stereoisomers of AMPH. Chemical composition of DA, S(+)amphetamine, and R(–)amphetamine (labeled S(+)AMPH and R(–)AMPH, respectively), showing their structural similarity. Adapted from Rodriguez-Menchaca, Solis et al. 2012.

DA and S(+)AMPH Affect hDAT Differentially

Xenopus laevis oocytes expressing hDAT were exposed to DA or S(+)AMPH (10 μM, –60 mV) for time periods ranging from 20-200 s (Figure 29). Adding 10 μM DA elicits an inward current ranging from 10 to 70 nA at –60 mV, depending on the level of hDAT expression. We confined ourselves to expression levels in this range. Control oocytes (not expressing hDAT) display no currents in response to substrate (DA or AMPH) exposure (data not shown). In hDAT-expressing oocytes, when DA is removed, the DA-induced current returns to baseline (Figure 29A) regardless of exposure time. As with DA, a brief exposure to 10 μM S(+)AMPH (30 s or less) elicits currents that return to baseline following S(+)AMPH removal. However, for exposures greater than 30 s, the hDAT current induced by 10 μM S(+)AMPH persists despite removal of external S(+)AMPH. Furthermore, the amplitude of the persistent current depends on the length of exposure to S(+)AMPH (Figure 29B). S(+)AMPH-induced persistent currents, also referred to as 'shelf' currents, may last as long as 30 min. The relationship between the amplitude of the shelf current and the duration of S(+)AMPH exposure (normalized to the initial hDAT-mediated peak current) shows that the shelf current amplitude saturates as a function of S(+)AMPH exposure time (Figure 29C). The existence of a shelf after removal of S(+)AMPH is tied not only to the duration of S(+)AMPH, but also to extracellular S(+)AMPH concentration. If the concentration of external S(+)AMPH is elevated from 10 to 30 μM, an exposure time that is too brief to elicit a *bona fide* shelf current (10 s) is now capable of doing so (Figure 29D).

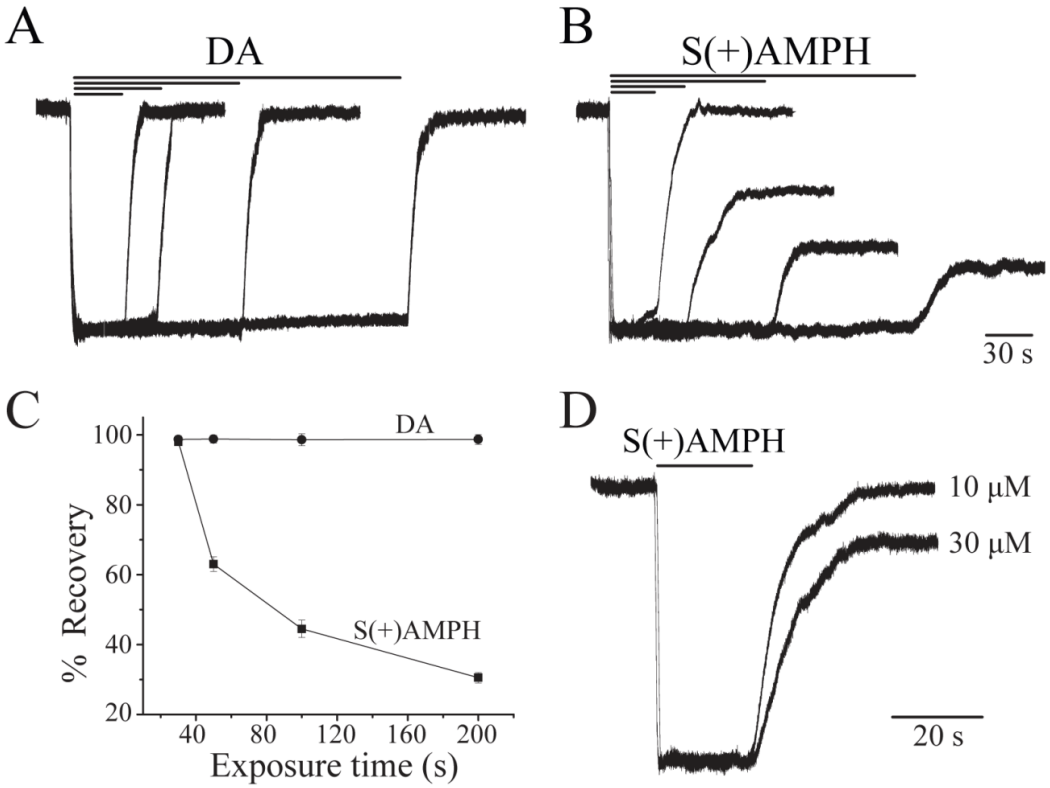

Figure 29. S(+)AMPH induces a persistent "shelf" current through hDAT. (A) External DA (10 μM) induces a large inward 'peak' current at V = –60 mV that returns to baseline when DA is removed, regardless of DA exposure time. DA peak currents are normalized to the briefest exposure time. (B) S(+)AMPH (10 μM) induces a similar inward peak current for exposures less than 30 s; however, for longer exposure times a current that we term 'leak' or 'shelf' remains long after S(+)AMPH is removed, and the amplitude of the shelf is proportional to the length of exposure. S(+)AMPH peak currents are normalized to the briefest exposure time. (C) Amplitude of the shelf current relative to the initial peak current plotted against exposure time of external S(+)AMPH, compared with the corresponding DA currents (n = 4, ± SEM). (D) A relatively brief and initial exposure to S(+)AMPH (20 s), which ordinarily would not produce a shelf current, does so if the concentration of S(+)AMPH increases from 10 to 30 μM. For the same exposure range of times and concentrations, neither DA nor S(+)AMPH induce peak or shelf currents in mock-injected oocytes (data not shown). Adapted from Rodriguez-Menchaca, Solis et al. 2012.

The Current-voltage Relationship of DA- and S(+)AMPH-induced Currents

At –60 mV, R(–)AMPH consistently induces a peak current slightly smaller than DA, whereas S(+)AMPH induces a slightly larger current; these differences diminish below –60 mV and exaggerate above –60 mV. Strikingly, R(–)AMPH has no authentic shelf compared with S(+)AMPH, but at –60 mV always meanders to its pre-stimulus value (Figure 30). For sufficiently long exposure, however, S(+)AMPH induces a prominent shelf current that is blocked by subsequent exposure of the hDAT inhibitor, COC (Figure 30). COC also blocks the peak currents for DA, R(–)AMPH, and S(+)AMPH (not shown) and in all cases returns the current to positive values compared with the pre-stimulus baseline, as shown in Figure 30. Thus hDAT, like other co-transporters in this family, has cocaine sensitive DA- and AMPH-induced currents and cocaine sensitive leak currents (Sonders, Zhu et al. 1997; Amara and Sonders 1998), to which we have added the cocaine sensitive shelf current. Because Na^+ plays a major role in the transport of substrate by monoamine transporters (Nelson 1998; Rudnick 1998), we investigated its effect on DA- and S(+)AMPH-induced currents. The peak currents induced by DA, S(+)AMPH, and R(–)AMPH are abolished when external Na^+ is replaced with $NMDG^+$, as well as the shelf current, suggesting all these currents are dependent on Na^+. We generated I(V) curves of initial current and shelf current for DA, S(+)AMPH peak, and S(+)AMPH shelf (Figure 31). The I(V) for DA bends downward (toward more negative currents) at more positive potentials. This is due to blockade of the endogenous leak current for DAT (Sonders, Zhu et al. 1997; Ingram and Amara 2000), similar to SERT (Galli, Petersen et al. 1997), and NET (Galli, Blakely et al. 1998). When external S(+)AMPH is present, the I(V) curve shifts to the left (between –20 and +20 mV),

possibly reflecting the co-conductance of Na^+ and S(+)AMPH cations. The shelf current I(V) is further shifted to the left, which implies not only the absence of S(+)AMPH, since at physiological conditions S(+)AMPH is protonated, but the likely presence of Cl^- ions which are known to carry current in DAT (Ingram, Prasad et al. 2002; Carvelli, Blakely et al. 2008). In addition, the fact that the reversal potential for the shelf current is different than the reversal potential for the peak currents suggests a change in hDAT trafficking does not play a role in producing the shelf current.

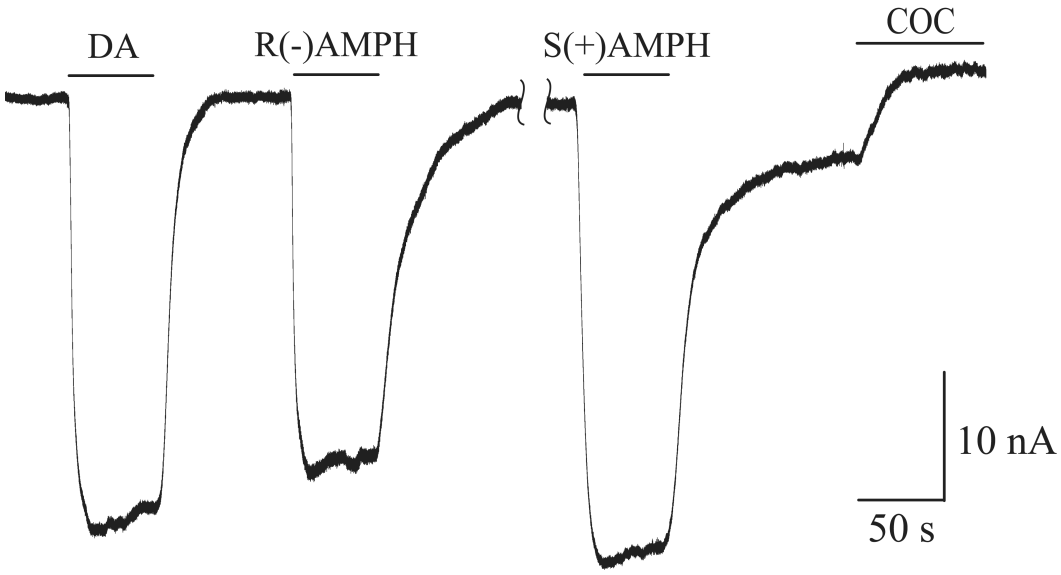

Figure 30. Effect of AMPH enantiomers on hDAT. At –60 mV, neither 10 μM DA nor 10 μM R(–)AMPH induce a shelf but always return to baseline after their removal. S(+)AMPH on the other hand induces a prominent shelf current that is blocked by cocaine (10 μM). The peak currents are approximately the same at -60 mV for 10 μM DA, R(–)AMPH, or S(+)AMPH. Note that 10 μM cocaine returns the current to values positive to the initial baseline, indicating the presence of an endogenous leak current. Adapted from Rodriguez-Menchaca, Solis et al. 2012.

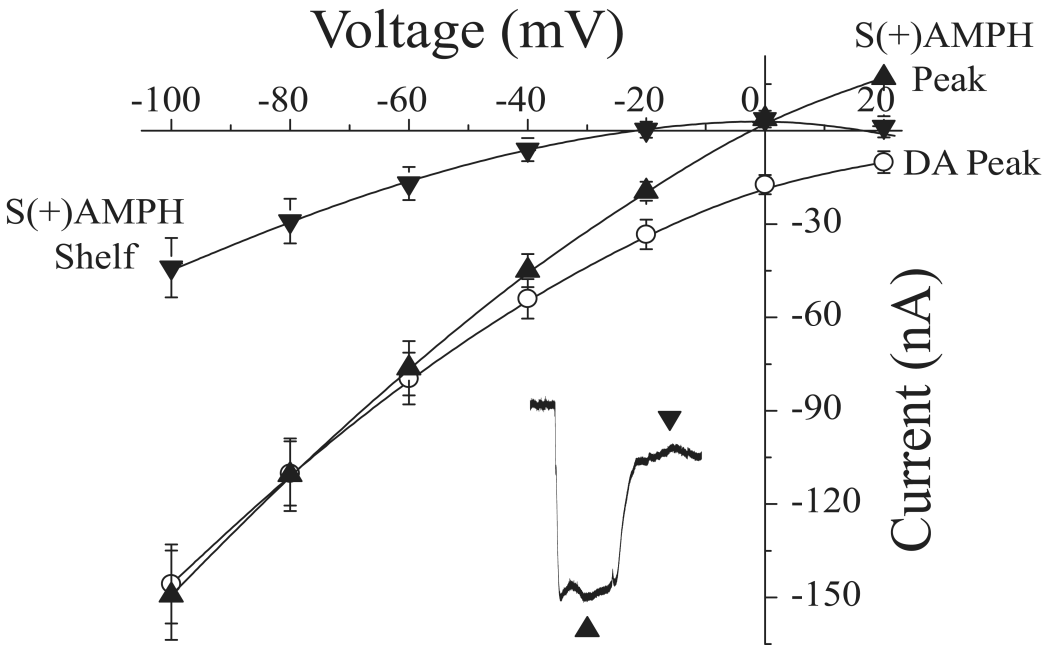

Figure 31. DA- and S(+)AMPH-induced I(V) curves. Cocaine subtracted I(V) curves for DA, S(+)AMPH peak, and S(+)AMPH shelf. The S(+)AMPH peak I(V) is left shifted above -60 mV compared with the DA peak, consistent with the conductance of both Na^+ and S(+)AMPH through hDAT. The S(+)AMPH shelf I(V) is further shifted to the left, consistent with the absence of S(+)AMPH and presence of Cl^- ions flowing through hDAT. Adapted from Rodriguez-Menchaca, Solis et al. 2012.

S(+)AMPH Operates on hDAT From the Inside

Until now, we had applied S(+)AMPH externally and shown that an exposure of 50 s or more (at 10 μM, –60 mV) activates the shelf current. Because of this relatively long time to elicit an effect, and because increasing S(+)AMPH concentration reduces the time required to activate a shelf current (Figure 29D), we suspected that S(+)AMPH was being transported into the cell to exert its effect internally. To test this possibility we injected S(+)AMPH into the oocyte to obtain a range of internal concentrations (see Methods) and correlated the internal concentration with the degree of persistent leak current. Whereas a brief application (10 s) of 10 μM external S(+)AMPH is insufficient to induce a shelf current, after injecting S(+)AMPH into the oocyte the same application induced a prominent shelf (Figure 32A). Remarkably, using external DA instead of S(+)AMPH also resulted in a shelf current (Figure 32B, center trace) and increasing internal S(+)AMPH (in a different oocyte) generates a larger shelf (Figure 32B, right most trace). Injecting DA or water into the oocyte had no similar effect for either external S(+)AMPH or DA (data not shown). These data suggest that S(+)AMPH is a use-dependent drug, and the ability to elicit the shelf current depends on its accessibility to hDAT from the inside. Thus, when hDAT has been previously exposed to S(+)AMPH, either external S(+)AMPH or external DA have the potential to generate persistent currents, though for the same external and internal concentrations, S(+)AMPH has a stronger effect (Figure 32C). Following the protocol in Figure 32B in different oocytes, we methodically titrated internal S(+)AMPH by repeated injections at the same concentration or stronger concentrations in different oocytes (see Experimental Procedures). Application with 10 μM external DA for 10 s after S(+)AMPH has been injected shows that the greater the

internal S(+)AMPH concentration the greater the shelf current (i.e., less recovery). The shelf saturates at 80% full recovery, with a Hill coefficient n = 1.7 and k_m = 37 μM.

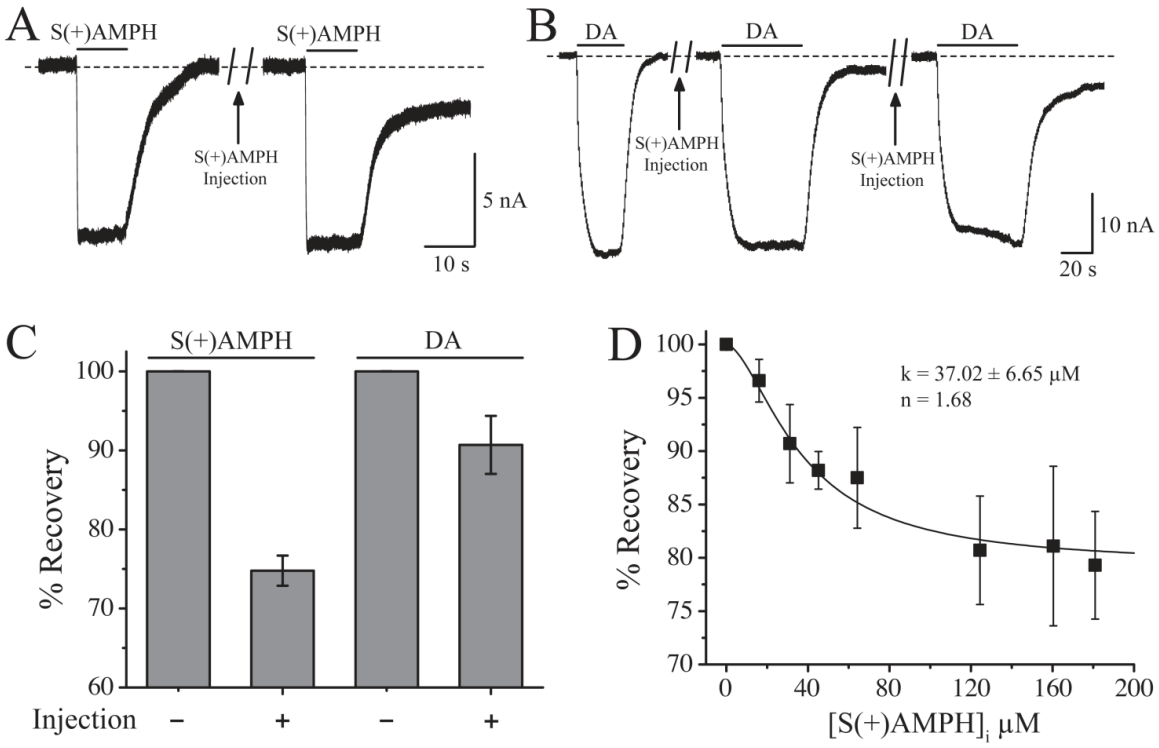

Figure 32. S(+)AMPH injection promotes the shelf current. (A) A brief exposure of external S(+)AMPH (10 s) does not elicit a shelf current as previously shown; however, after injection of 25 µM S(+)AMPH, the same external exposure reveals a prominent shelf current. (B) DA exposure does not elicit a shelf current; however, after injections of 25 µM S(+)AMPH, DA now elicits a shelf similar to the S(+)AMPH-induced shelf current. Increasing internal S(+)AMPH with repeated injections generates a larger shelf (right trace). Injecting DA into the oocyte had no similar effect for external S(+)AMPH or DA (data not shown). (C) Percent recovery after external exposure to 25 µM S(+)AMPH or DA for 10 s with (+) or without (–) S(+)AMPH injection. (D) Baseline recovery following S(+)AMPH injections at increasing concentrations. Pooled data for 10 µM external DA applied for 10 s: the greater the internal S(+)AMPH concentration the greater the DA-induced shelf current, i.e., in the presence of internal S(+)AMPH, less of the DA-induced current is able to return to baseline after external DA is removed. For a DA challenge, the shelf current saturates at 80% full recovery, with a Hill coefficient n = 1.7 and k_m = 37 µM. Adapted from Rodriguez-Menchaca, Solis et al. 2012.

Internal S(+)AMPH is Silent Without External S(+)AMPH and Na^+

Based on our experiments, we formulated a model of the S(+)AMPH-induced persistent current based on two gates in the hDAT protein: an external gate operated by S(+)AMPH and Na^+ and blocked by cocaine, and an internal gate operated by S(+)AMPH (Figure 33). Previous work suggests that Na^+ plays a regulatory role at the internal face of hDAT (Khoshbouei, Wang et al. 2003); however, this possibility was not explicitly tested in the present work. In stage (1) of Figure 33, we would expect hDAT to maintain a small leak current even in the absence of substrate. This endogenous leak, which can be revealed by cocaine, is present even without prior exposure to substrate (Figure 30) as had been shown previously (Sonders and Amara 1996). Here we ignore this background leak and focus only on the substrate-induced currents. In our model opening the outer gate requires both Na^+ and S(+)AMPH; however, R(–)AMPH or DA can also operate the gate. Opening the gate generates the peak (or steady state) current in phase (2), which is likely carried by Na^+ and S(+)AMPH cations though Cl^- is also implicated (Figure 31), which is substantiated by previous work (Ingram, Prasad et al. 2002; Carvelli, Blakely et al. 2008). As transport ensues, the inner gate becomes exposed to S(+)AMPH and, once occupied, remains open and holds the outer gate open even though external S(+)AMPH has been removed. This allosteric action between the inner and outer gate acts as a molecular stent that holds the transporter in an open state (3). The molecular stent requires external Na^+, and removing Na^+ returns the current to baseline (4). However, merely reintroducing Na^+ does not restore the current (5); rather, S(+)AMPH and Na^+ must both be present to regenerate the peak (6) and shelf (4). Unless this dual condition is fulfilled, internal S(+)AMPH is silent.

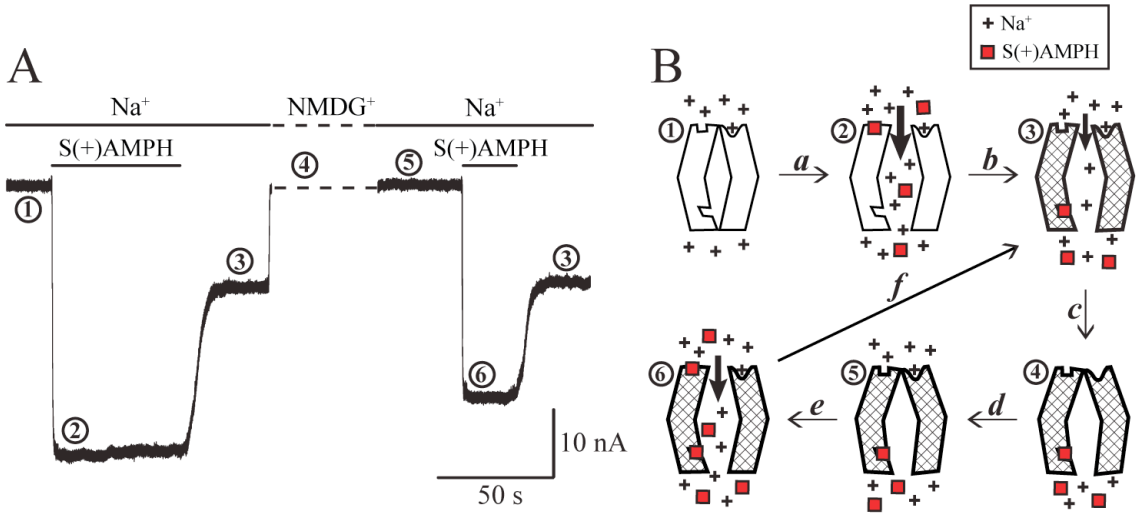

Figure 33. Model for S(+)AMPH-induced, hDAT-mediated peak and shelf currents. (A) Phase ①: The baseline current at V_{hold} = –60 mV in standard external physiological solution containing Na^+. Phase ②: In the presence of external Na^+, S(+)AMPH (10 µM) induces an initial peak current. Also, S(+)AMPH is transported and accumulated in the cell. Phase ③: Removing external S(+)AMPH reduces the S(+)AMPH-induced current to a fraction of its initial peak value (the shelf current). At a fixed voltage, the shelf amplitude depends on exposure time and concentration of external S(+)AMPH. Phase ④: Replacing Na^+ with NMDG introduces a shift in baseline that was removed from the figure (dashed line); however, reintroducing Na^+ during phase ④ (Phase ⑤) does not restore the shelf current but returns the current to the original baseline. Phase ⑥: Reintroducing external S(+)AMPH in the presence of Na^+ induces a new peak current. Note that the second application of S(+)AMPH is normally too brief to elicit a shelf current; however, S(+)AMPH is already present inside the cell from the first application. After removing S(+)AMPH for the second time, the shelf current again manifests itself. The new peak is smaller than the first peak, possibly due to hDAT internalization. (B) States of hDAT during S(+)AMPH-induced shelf current. The hatched transporter indicates internal occupancy by S(+)AMPH and a long lasting 'molecular stent' configuration. The numbers above each state of the transporter correspond to the traces in part (A). Transition (***a***) opens the top and bottom gates, which for brief external S(+)AMPH exposures would close. Transition (***b***) occurs after longer exposures and S(+)AMPH has built up inside to the extent that the inner S(+)AMPH site remains occupied and holds both gates open (molecular stent hypothesis), even in the absence of external S(+)AMPH. Transition (***c***) Removing external Na^+ closes the outer gate, which does not reopen without external Na^+ and S(+)AMPH both present (transitions ***d*** and ***e***), rendering the transporter capable of (and indeed more prone to) forming the molecular stent (transition ***f***), because internal S(+)AMPH is still present. Adapted from Rodriguez-Menchaca, Solis et al. 2012.

DISCUSSION

Novel Mechanism of Action of S(+)AMPH on hDAT

In this work, we present a novel finding for the action of S(+)AMPH on hDAT. Our results suggest a model in which S(+)AMPH is transported into the cell through hDAT, whereupon the drug has access to an internal site on the transporter that induces a persistent "shelf" current. Bound to the internal site, S(+)AMPH induces a molecular stent in hDAT that holds the transporter open long after external AMPH is removed. The internally accessible site is in addition to an external site for S(+)AMPH, which initiates the transport of the drug to the inside. Although, the existence of two substrate binding sites for neurotransmitter transporters is controversial, with evidence for (Shi, Quick et al. 2008; Shan, Javitch et al. 2011; Zhao, Terry et al. 2011) and against (Piscitelli, Krishnamurthy et al. 2010), our model (Figure 33) is consistent with two binding sites for S(+)AMPH.

S(+)AMPH is a Use-Dependent Drug

Regardless of the specific mechanism, the existence of the shelf current has physiological consequences for synaptic transmission. At rest, the persistent leak current could depolarize the presynaptic membrane and increase the probability of transmitter release. Furthermore, once it is exposed to S(+)AMPH, the presynaptic membrane would respond to DA abnormally for as long as S(+)AMPH remains inside the terminal (30 min) at a significant concentration (30 μM). S(+)AMPH is therefore a use-dependent drug that could pre-condition hDAT to generate a persistent leak when subsequently challenged by endogenous transmitter DA, or exogenous AMPH. The half-life of AMPH inside cells is not well known (Seiden, Sabol et al. 1993), but it ranges from 2 hours up to 12 hours if measured from body fluids (Mofenson and Greensher 1975; Verstraete 2005; Verstraete and Heyden 2005).

Composition of the Persistent Leak Current

The persistent leak flows in the absence of external S(+)AMPH or DA and must therefore be entirely composed of co-transported ions, most likely Na^+ and Cl^-. We explicitly tested the dependence of S(+)AMPH-induced currents on external Na^+, and the results are consistent with well-known criteria for coupled co-transport (Gu, Caplan et al. 1998; Rudnick 1998; Rudnick 1998). Near the resting potential of most cells (–60 mV), the persistent leak current is constant as long as the voltage is held constant. In a free running cell, however, the depolarizing leak current would be self-quenching as the voltage becomes more positive.

Implications of AMPH-induced Shelf Current on Synaptic Neurotransmission

It was already known that DA acting on DAT elicits inward currents through a channel-like mechanism that can depolarize dopaminergic neurons and increase their excitability (Ingram, Prasad et al. 2002; Carvelli, McDonald et al. 2004; Carvelli, Blakely et al. 2008). Ingram and colleagues suggest that tonic activity excites dopaminergic neurons by activating an uncoupled Cl^- conductance mediated by DAT. In this study, the increase in cell excitability induced by DA or AMPH in voltage-clamped neurons was tested during the external perfusion that corresponds to the peak or steady state current in our model (illustrated in Figure 34 as "acute depolarization"). As discussed above, in addition to the established peak current, in which S(+)AMPH and DA both participate, a persistent leak current exists, which in similar conditions would prolong depolarization and increase midbrain dopaminergic neuron excitability long after AMPH is removed (shown in Figure 34 as "prolonged depolarization"). This additional experiment is warranted to validate the concept that the AMPH-induced hDAT-mediated persistent leak current has a physiological role in the brain. As postulated, prolonged depolarization of the presynaptic membrane (as illustrated in the model of shelf-induced prolonged synaptic depolarization in Figure 34) is expected to further increase the excitability of neurons and the probability of neurotransmitter release (Ingram, Prasad et al. 2002).

A full understanding of this effect and its magnitude is at present unknown and would require a complete knowledge of current-generating channels and receptors on the presynaptic membrane. In particular, D_2 DA receptors are known to be involved in transmitter release (Schmitz, Lee et al. 2001). It has been suggested that released DA may feed back onto D_2 autoreceptors to depress neuronal activity (Sulzer and Galli 2003). In

addition, AMPH may regulate hDAT indirectly by targeting or modulating proteins that then impact DAT function. These possible responses extend the range of synaptic states regulated by neurotransmitters, to which the newly discovered leak current will undoubtedly contribute for a more complete understanding of AMPH action. One caveat that should be noted is that oocyte experiments lack associated proteins that alter transporter currents, such as syntaxin, which eliminates SERT currents (Quick 2003). If DAT requires a protein, such as syntaxin, to produce currents, persistent leak currents might not be produced in neurons; however, studies have shown the presence of uncoupled depolarizing currents in neurons (Ingram, Prasad et al. 2002; Carvelli, McDonald et al. 2004).

The density of DAT expression would also be a contributing factor to the relative effect of DA- or AMPH-induced currents. Rapid treatment of rat striatal synaptosomes with low-doses of AMPH increases surface expression of DAT. Either DA or AMPH increased surface DAT within 10 s of substrate addition and steadily increased surface DAT until removal 2 min later. In these experiments exocytosis of DAT was blocked with tetanus and botulinum neurotoxins. These data demonstrate that DA and AMPH can rapidly increase surface DAT possibly to respond rapidly during DA secretion (Furman, Chen et al. 2009). However, it is also known that long-term exposure to AMPH can decrease surface DAT expression (Saunders, Ferrer et al. 2000; Galici, Galli et al. 2003). Thus, increase in surface DAT occurs within a minute and has a fairly short life of a few minutes, whereas longer treatments of AMPH, especially at doses equal to or greater than 10 μM, cause down-regulation. We believe that a decrease in surface hDAT is responsible for the consistently observed decrease in the second application of

S(+)AMPH, as seen in Figure 33. Nevertheless, even a brief exposure to AMPH, normally too brief to elicit a shelf current, readily demonstrates a shelf current due to the previous exposure and S(+)AMPH pre-conditioning of the cell.

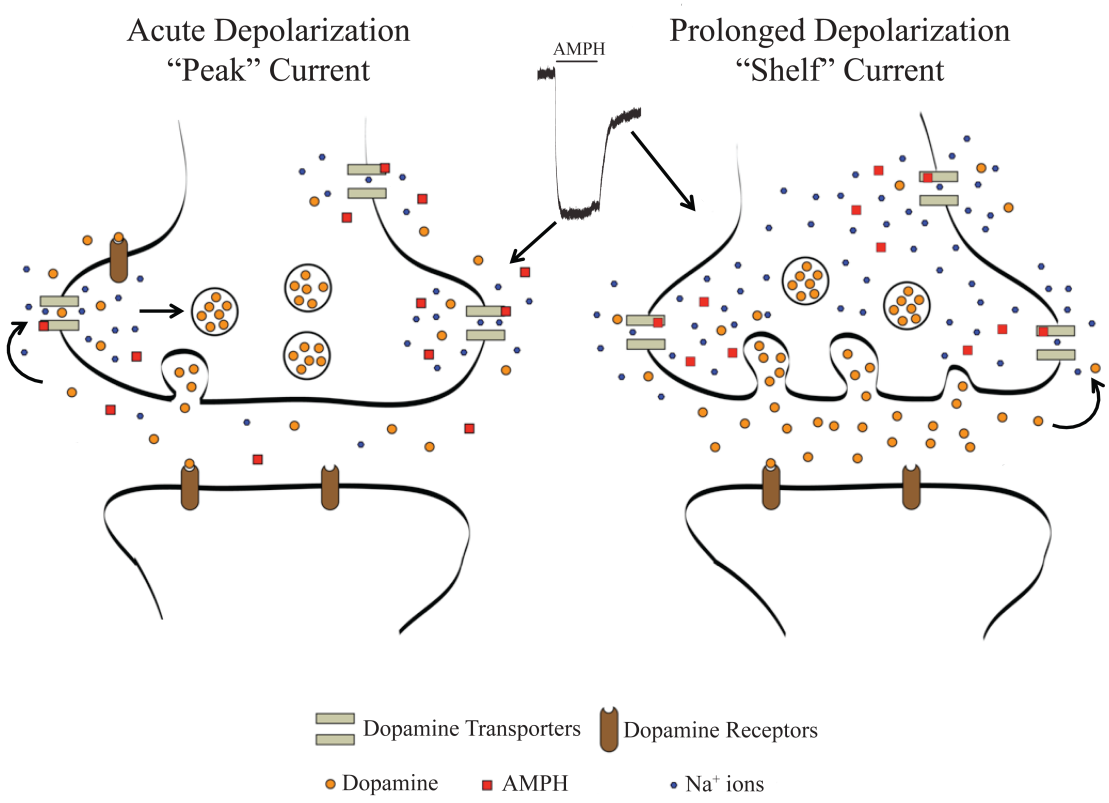

Figure 34. Model of shelf-induced prolonged synaptic depolarization. In this work, we present a new model for the action of AMPH on DAT in which AMPH is transported through DAT and concentrates inside the cell (at the presynaptic terminal) over time, where it is becomes available to bind at an internal site in the transporter. This produces a sustained inward "shelf" current under voltage clamp that remains even after the external substrate is removed. Our data support a model of an acute AMPH-induced depolarization (left synapse) and a chronic shelf current that leads to prolonged depolarization (right synapse). Acute depolarization by AMPH elicits inward currents in DAT via a channel-like mechanism that depolarizes dopaminergic neurons and increases neuronal firing. Prolonged depolarization would lead to further increased excitability and firing of dopaminergic neurons.

Conclusions

Persistent depolarizing currents following AMPH exposure would be relevant to any model of presynaptic physiology and transmitter release. The resulting persistent depolarization of dopaminergic neurons caused in particular by S(+)AMPH, a component of street AMPH and prescription drugs, could play an important role in behavioral effects, including craving, withdrawal, and relapse, as well as the pleasurable effects of AMPH, such as rush and euphoria.

CHAPTER IV.

A COMPARISON OF PEAK AND PERSISTENT LEAK CURRENTS INDUCED BY METHAMPHETAMINE AND 3,4-METHYLENE-DIOXYMETHAMPHETAMINE IN THE HUMAN DOPAMINE AND SEROTONIN TRANSPORTERS

STUDY OVERVIEW

Background and Purpose

Despite their structural similarities methamphetamine (METH) and 3,4-methylenedioxy-methamphetamine (MDMA or ecstasy) elicit distinct behavioral responses in rodents and humans. METH is a psychoactive stimulant that increases the levels of DA, NE, and 5HT in the brain reward pathways, and thus, has a high potential for abuse and addiction. Since MDMA can induce euphoria in humans, it has become a widely abused recreational drug; however, MDMA offers therapeutic benefit to some individuals presumably through an increase in serotonergic signaling. Furthermore, many studies have shown differences in behaviors elicited by the stereoisomers of both METH and MDMA.

Experimental Approach

We record electrical currents mediated by hDAT or hSERT expressed in *Xenopus laevis* oocytes in response to S(+)MDMA, R(–)MDMA, S(+)METH, or R(–)METH. Each compound induces an inward (depolarizing) current when the oocyte is held near rest at –60 mV and each acts as an hDAT or hSERT agonist.

Key Results and Conclusions

In both hDAT and hSERT the METH and MDMA stereoisomers induce inward peak currents. In hDAT, out of the four compounds tested (METH and MDMA stereoisomers), only S(+)METH results in a persistent leak current after it is removed. In hSERT,

S(+)METH, S(+)MDMA, and R(–)MDMA (but not R(–)METH) induce a persistent leak current.

Implications

Structurally similar METH and MDMA stereoisomers induce electrophysiological responses in hDAT and hSERT that correlate with the known effects of these drugs to release specific neurotransmitters in the brain.

INTRODUCTION

Amphetamine

Amphetamine (AMPH) is a prototypical phenylisopropylamine stimulant. AMPH-like psychostimulants interact with multiple monoamine transporters as releasing agents or as transmitter reuptake competitors (Sulzer, Sonders et al. 2005; Chen, Tilley et al. 2006). The behavioral effects associated with these agents are closely linked to enhanced dopaminergic activity (Howell, Carroll et al. 2007; Howell and Kimmel 2007). Particularly, an increase in DA levels in the *nucleus accumbens* by the actions of AMPH on DAT produces rewarding and hyperlocomotor effects (Sellings and Clarke 2003; Williams and Galli 2006). Interestingly, it is known that the S(+)AMPH enantiomer is a stronger stimulant than the R(–)AMPH enantiomer (Mendelson, Uemura et al. 2006). Furthermore, S(+)AMPH is more potent at inducing release of extracellular DA in the brain than R(–)AMPH (Kuczenski, Segal et al. 1995). Consequently, since S(+)AMPH has higher potency than R(–)AMPH (Phillips, Brooke et al. 1975; Holmes and Rutledge 1976; Kuczenski, Segal et al. 1995), therapeutic agents used clinically to treat medical conditions, such as attention-deficit hyperactivity disorder and narcolepsy (Burnette, Bailey et al. 1996; Fleckenstein, Volz et al. 2007), are composed primarily of S(+)AMPH. For example, Adderall is composed of 3:1 S(+)AMPH to R(–)AMPH (Cody, Valtier et al. 2003), and Vyvanse (lisdexamphetamine) is a pro-drug that is metabolized entirely to S(+)AMPH (Najib 2009).

METH

The AMPH analog METH is a potent locomotor stimulant (Van der Schoot, Ariens et al. 1961; Biel and Bopp 1978) and a widespread drug of abuse (Mendelson, Uemura et al. 2006) that possesses a monoamine transporter release profile similar to AMPH and a potency for DA release nearly identical to that for AMPH (Rothman and Baumann 2006). Interestingly, in humans S(+)METH is a stronger stimulant than R(–)METH (Mendelson, Uemura et al. 2006). In fact, in the United States illicit METH is predominately distributed as the S(+) enantiomer (Mendelson, Uemura et al. 2006). Also, similarly to AMPH, the S(+) isomer for METH is more potent at inducing release of extracellular DA in the brain than the R(–) counterpart (Kuczenski, Segal et al. 1995). In addition, in humans, the S(+) enantiomers of AMPH and METH are 2 to 10 times more potent in producing CNS stimulation than the corresponding R(–) enantiomers (Mendelson, Uemura et al. 2006).

MDMA

The "club drug" 3,4-methylenedioxy-methamphetamine (MDMA, also known as "ecstasy") belongs to the AMPH family of compounds. MDMA is commonly used as a recreational drug and is thought to produce neurotoxic effects (Lyles and Cadet 2003). MDMA is similar in structure to METH (it is a ring-substituted analog of METH), but like DA it bears oxygen moieties at the *meta*- and *para*- ring-positions (see Fig. 1 for a comparison of chemical structures). MDMA can produce AMPH-like effects in various animal species (Green, Mechan et al. 2003), yet in humans, unlike AMPH or METH, MDMA induces a sense of euphoria, feelings of well-being, and diminished anxiety leading to the therapeutic potential of MDMA for post-traumatic stress disorder (Johansen and Krebs 2009; Mithoefer, Wagner et al. 2011). It is thought that the unique psychopharmacological profile of MDMA is derived from its property to promote the release of DA and 5HT in the brain (Gudelsky and Yamamoto 2008). Similar to AMPH and METH, the stimulant actions of MDMA are believed to involve the release of DA in the *nucleus accumbens* (Gold, Hubner et al. 1989); however, MDMA has higher potency (than METH) to induce 5HT release through hSERT (Rothman and Baumann 2006). In rats, the motor actions of racemic MDMA have been correlated with increased levels of both 5HT and DA in specific brain regions (Baumann, Clark et al. 2008). In addition to evoking an acute release of DA, which is reduced in the striatum, MDMA also causes release of DA metabolites, homovanillic acid (HVA), and dihydroxyphenylacetic acid (DOPAC), 3 h after the last administration of the drug (O'Shea, Esteban et al. 2001). However, the rise in DA concentration elicited by acute application of MDMA is modest

unless followed by subsequent doses of MDMA (Colado, Camarero et al. 2001; Sanchez, Camarero et al. 2001).

MDMA Stereoisomers Display Pharmacological Differences

MDMA is normally a racemic mixture; however, the S(+) and R(–) stereoisomers have different pharmacological properties. S(+)MDMA is a potent psychomimetic compared to R(–)MDMA, and studies have suggested only S(+)MDMA is neurotoxic causing long-term depletion of 5HT and SERT (Lyles and Cadet 2003; Baumann, Clark et al. 2008). Differences in the effect of each MDMA enantiomer may be related to differences in metabolism and it may not be surprising that the stereoisomers have different pharmacokinetic properties (Fantegrossi, Murai et al. 2009). Although S(+)MDMA is nearly equipotent at the DA, NE, or 5HT transporters, the R(–)MDMA enantiomer is 5-fold less potent than S(+)MDMA at releasing NE or 5HT, and more than 25-fold less potent at DAT (Setola, Hufeisen et al. 2003).

MDMA Stereoisomers Elicit Distinct Behavioral Effects in Rodents

The hyperlocomotor effects of racemic MDMA were first described in mice (Glennon, Yousif et al. 1988) and rats (Gold, Koob et al. 1988; Gold, Hubner et al. 1989) more than 20 years ago. The behavioral effects of MDMA isomers in mice have shown variability across studies, but S(+)MDMA is generally more potent than the R(–)MDMA enantiomer (Glennon, Yousif et al. 1988; Young and Glennon 2008). For example, S(+)MDMA and racemic MDMA were more potent than R(–)MDMA at stimulating many different measurements of motor activity in mice (Young and Glennon 2008). Another study in mice, showed that S(+)MDMA, but not R(–)MDMA, produces hyperthermia and increased locomotor activity that is reversed with fluoxetine and $5HT_{2A}$ receptor antagonists (Fantegrossi, Godlewski et al. 2003).

Drug Discrimination Studies Using Rodents Elucidate Distinct Effects of the MDMA Stereoisomers

Several elegant drug discrimination studies have been performed to elucidate the reason the stereoisomers of MDMA produce distinct behavioral responses in rodents. These studies employ the high perceptive resolution rodents exhibit when exposed to different drugs to categorize them based on the effects they confer on the subject. The objective is to tease apart compounds that are related structurally, but may evoke distinct behavioral effects. In these studies, rodents are trained to respond to a specific drug (i.e. stimulant, hallucinogen), and the drug is substituted with the experimental drug. If responding is maintained, then it is inferred that the compound elicited a comparable effect; however, if the responding drops, it is interpreted as the compound eliciting distinct behavioral effects in the animal. In one such study, in which rats were taught to discriminate S(+)AMPH from vehicle, both S(+)METH and S(+)MDMA were able to substitute for the training drug (Glennon 1999), suggesting similarities in the stimulus effects these drugs elicit in the rats.

Another study sought to study discriminative stimulus effects of psychostimulants and hallucinogens in S(+)MDMA- and R(–)MDMA-trained mice (Murnane, Murai et al. 2009). The psychostimulant S(+)AMPH substitutes in S(+)MDMA-trained animals, but not in R(–)MDMA-trained animals, suggesting S(+)MDMA confers stimulant effects on mice. Both S(+)MDMA- and R(–)MDMA-trained animals respond to cocaine, but S(+)MDMA-trained animals respond to cocaine to a greater extent. While R(–)MDMA-trained mice generalize to hallucinogenic drugs, S(+)MDMA-trained mice do not respond to a dose of the hallucinogenic drug 2-[2,5-dimethoxy-4-(propylthio)phenyl]ethanamine

(2C-T-7). Both S(+)MDMA- and R(–)MDMA-trained animals respond to dipropyltryptamine (DPT), a drug with mixed hallucinogenic and stimulant actions. A reasonable conclusion from this study was that R(–)MDMA mediates effects of hallucinogenic drugs, whereas S(+)MDMA predominantly mediates stimulant behavior (Murnane, Murai et al. 2009).

MDMA Stereoisomers Induce Reinforcing Effects in Primates

In rhesus monkeys, the MDMA stereoisomers act as reinforcers; however, S(+)MDMA behaves as a more potent reinforcer than R(–)MDMA (Fantegrossi, Ullrich et al. 2002). Furthermore, in long-term self-administration protocols in rhesus monkeys, reinforcement effects of racemic and R(–)MDMA, but not of S(+)MDMA, are reduced over months of self-administration (Fantegrossi, Woolverton et al. 2004), implying weaker reinforcement effects for racemic and R(–)MDMA. Furthermore, the reinforcement effects of S(+)MDMA are more resistant to reduction than reinforcement effects for racemic and R(–)MDMA (Fantegrossi, Woolverton et al. 2004).

In addition, the R(–)MDMA reinforcing effect is abolished with $5HT_{2A}$ receptor antagonists, whereas the S(+)MDMA reinforcing effect can only be attenuated (Fantegrossi, Ullrich et al. 2002; Fantegrossi 2008), which implies a non-serotonergic mechanism underlying the reinforcing effect, presumably dopaminergic. Further work demonstrated that S(+)MDMA is less susceptible to tolerance after long term administration than racemic and R(–)MDMA (Fantegrossi 2008). Lastly, by employing positron emission tomography (PET) neuroimaging, it was found that R(–)MDMA does not display much DAT occupancy, whereas reasonable DAT interaction is seen with S(+)MDMA (Fantegrossi 2008).

In a different study in using non-human primates (rhesus and squirrel monkeys), behaviorally relevant doses of MDMA did not induce stimulant (DAT-mediated) effects (Fantegrossi, Bauzo et al. 2009). Also, at a certain dose of MDMA self-administration, responding is suppressed, and this effect seems to be mediated by the serotonergic system (Fantegrossi, Bauzo et al. 2009).

Comparing Relative Reinforcing Strength of METH and MDMA Stereoisomers

The difference METH and MDMA exhibit in their selectivity for monoamine neurotransmitters may explain why they differ in their relative reinforcing strength (Wang and Woolverton 2007). To compare their relative reinforcement, a long-term self-administration study was performed in which responses to racemic (+/-) METH, S(+)MDMA, R(–)MDMA, or racemic (+/-)MDMA by rhesus monkeys were measured using a progressive-ratio schedule (Wang and Woolverton 2007). This study showed that METH, racemic MDMA, and S(+)MDMA act as positive reinforcers with relative reinforcer strength (from strongest to weakest): METH > S(+)MDMA > racemic MDMA. In other words, racemic MDMA and S(+)MDMA were weaker reinforcers than METH, and R(–)MDMA was at best a weak reinforcer (Wang and Woolverton 2007). The reinforcing strength of racemic MDMA appears to derive from S(+)MDMA.

What Accounts for the Distinct Behavioral Effects Produced by AMPH-like Drugs of Abuse?

While drugs considered psychostimulants, such as AMPH and METH, possess high abuse potential and can cause hyperlocomotor activity, severe psychotic episodes, cardiovascular activation, increased energy and decreased need for sleep (Rothman and Baumann 2006; Rothman, Blough et al. 2008), drugs that are related structurally; in particular, MDMA, can elicit distinct behavioral effects, such as euphoria (feelings of elation), a sense of well-being, happiness, feelings of emotional closeness to others, and diminished aggression (Green, Mechan et al. 2003; Lyles and Cadet 2003; Baumann, Clark et al. 2008; Gudelsky and Yamamoto 2008). MDMA also has weaker reinforcement strength than AMPH and METH, and therefore, confers lower abuse potential (Fantegrossi, Ullrich et al. 2002).

Regardless of mechanism, ultimately, drugs of abuse, such as AMPH, METH, and MDMA lead to elevated levels of the endogenous monoamine neurotransmitters (DA, NE, 5HT) through actions on the monoamine transporters (DAT, NET, SERT) that are surmised to be responsible for the range of behavioral responses they induce. Furthermore, these agents (AMPH, METH, and MDMA) display different affinities at the monoamine transporters, which could be the main factor underlying the distinct behavioral effects they elicit. For example, METH is much more potent at releasing DA and NE (from DAT and NET, respectively) than at releasing 5HT through SERT (Rothman and Baumann 2006).

It has long been known that AMPH-induced reinforcing behavior, such as self-administration, is mediated by increases in DA concentrations in the mesolimbic reward

circuits, particularly, in the nucleus accumbens, which holds true for related AMPH-like stimulants (Wise 1996; Rothman and Baumann 2006). In contrast, MDMA-mediated behavioral effects are attributed to high-affinity transport of MDMA by SERT, which leads to 5HT release (Verrico, Miller et al. 2007). Interestingly, some evidence suggests that enhanced serotonergic activity is negatively associated with reinforcing effects, and compounds that selectively increase 5HT neurotransmission have been found neither to maintain self-administration by animals nor to have abuse liability in humans (Wang and Woolverton 2007), which would agree with the lower reinforcing strength MDMA (a primarily 5HT-releasing agent) possesses as relative to addictive agents such as METH and AMPH (Wang and Woolverton 2007).

Effect of AMPH Stereoisomers on the Persistent Leak Current

In previous work, we demonstrated that S(+)AMPH and R(–)AMPH both produce inward currents mediated by hDAT in *Xenopus laevis* oocytes voltage-clamped to –60 mV (Rodriguez-Menchaca, Solis et al. 2012). In this regard both AMPH isomers produce an effect similar to hDAT's endogenous substrate DA; however, only the S(+)AMPH enantiomer induced the recently characterized long-lasting inward leak current, which persists long after the drug is removed from the extracellular milieu (Rodriguez-Menchaca, Solis et al. 2012).

Purpose of Study

In the current study, we sought to determine whether the recently characterized AMPH-induced persistent leak current at hDAT (Rodriguez-Menchaca, Solis et al. 2012) would also be elicited by the stereoisomers of MDMA and METH in both hDAT and hSERT. We employed two-electrode voltage-clamp to measure the response to application of METH and MDMA stereoisomers in *Xenopus laevis* oocytes expressing either hDAT or hSERT. Although we expected the METH stereoisomers to behave similarly to the AMPH stereoisomers when applied to hDAT, we did not know what would happen if METH was applied to hSERT. Until now, there are no reports of the existence of a persistent leak current induced by hSERT; therefore, if successful, this study would demonstrate the persistent leak current induced by hSERT. We hypothesized that, in particular, S(+)MDMA would induce an hSERT-mediated persistent leak current since it has high potency at hSERT, and we had seen that S(+)AMPH, which has high potency at hDAT, does induce an hDAT-mediated persistent leak current.

In our studies we found that whereas hSERT exhibits the persistent leak current in response to S(+)METH and the MDMA stereoisomers, hDAT only shows a persistent leak current in response to S(+)METH. Since the persistent leak currents elicited by METH and MDMA would alter excitability differentially in distinct neuronal populations and evoke release of neurotransmitter by hSERT and hDAT, we posit these findings could contribute to the behavioral effects induced by MDMA and METH.

EXPERIMENTAL PROCEDURES

Expression of hDAT and hSERT in Xenopus Laevis Oocytes

Oocytes are harvested and prepared from adult *Xenopus laevis* females following standard procedures (Machaca and Hartzell 1998; Iwamoto, Blakely et al. 2006). We select stage V-VI oocytes for cRNA injection within 24 h of isolation. cRNA is transcribed from the pOTV vector using mMessage Machine T7 kit (Ambion Inc., Austin, TX). Oocytes are injected with either 50 ng hDAT cRNA or 30 ng hSERT cRNA (Nanoject AutoOocyteInjector, Drummond Scientific Co., Broomall, PA) and incubated at 18^{o}C for 4-8 days in Ringers solution supplemented with NaPyruvate (550 μg/ml), streptomycin (100 μg/ml), tetracycline (50 μg/ml) and 5% dialyzed horse serum.

Electrophysiology

We performed two-electrode voltage-clamp (TEVC) experiments as previously described (Wang, Li et al. 2006). Recordings were done at RT (23-25°C). Electrodes having resistances from 1-5 MΩ are filled with 3 M KCl. *Xenopus laevis* oocytes expressing hSERT or hDAT are voltage-clamped to -60 mV with a GeneClamp 500 (Axon Instruments), and the holding current is recorded using Clampex 10 (Axon Instruments). Extracellular buffer consists of (in mM): 120 NaCl, 7.5 HEPES, 5.4 KGluconate, 1.2 CaGluconate, pH 7.4. In a typical recording extracellular buffer is perfused until stable baseline currents are obtained, followed by experimental drugs (perfusion duration is indicated by a horizontal line on the trace).

Analysis

To control for transporter expression between different drugs (in the raw traces in Figure 36 and Figure 37), for hDAT we normalized each drug-induced trace (including DA) obtained in individual hDAT-expressing oocytes to the DA-induced current (recorded prior to application of each compound tested), and for hSERT we normalized each drug-induced trace (including 5HT) obtained in hSERT-expressing oocytes to the 5HT-induced current (recorded prior to application of each compound tested). To examine the persistent leak current among the different time point traces obtained in individual oocytes (in Figure 38, Figure 39, and Figure 40), the traces for each treatment (S(+)METH or S(+)MDMA) are normalized to the largest drug-induced response and aligned to start of drug perfusion. Concentration-response curves (in Figure 41 and Figure 42) are obtained by fitting values to the Hill 1 equation: $y = V_{max} + (V_{min} - V_{max}) * x^n / (k^n + x^n)$ (Origin 8). Values for peak amplitude of each drug–induced response are selected at time = 30 s during drug application, and values for persistent leak current are selected at time = 60 s during washout with extracellular buffer. For peak amplitude fit all concentration values recorded are used (0.1, 0.5, 1, 3, 10, 30 μM). For persistent leak current fit only values in response to 1, 3, 10, and 30 μM drug exposure were used because only these concentrations induced measurable persistent leak currents.

RESULTS

METH and MDMA Stereoisomers Produce Currents Through hDAT and hSERT

METH and MDMA both have a chiral center at the α-carbon, therefore, there are two enantiomers possible for each substrate (as shown in Figure 35). To test their effect on hDAT and hSERT, we first recorded currents from hDAT-expressing oocytes in response to application of 10 μM 5HT, DA, R(–)MDMA, S(+)MDMA, R(–)METH, and S(+)METH, and observed that all substrates induce inward currents (Figure 36). As expected, hDAT's endogenous substrate DA induced a larger inward current than 5HT, and all MDMA and METH stereoisomers induced substantial currents. Both S(+) enantiomers (S(+)METH and S(+)MDMA) induce larger currents than their R(–) counterparts (R(–)METH and R(–)MDMA, respectively).

Whereas S(+)METH yielded the persistent leak current (characterized by lack of return to baseline after removal of S(+)METH by wash out), neither MDMA enantiomer nor R(–)METH induced a discernable persistent leak current (Figure 36, unpublished). Next, we recorded currents from hSERT-expressing oocytes in response to application of 10 μM 5HT, DA, R(–)MDMA, S(+)MDMA, R(–)METH, and S(+)METH, and observed that hSERT produced inward currents in response to all substrates tested (Figure 37, Solis 2012, unpublished). The endogenous substrate for hSERT, 5HT, induced a larger inward current than DA. Although the inward current induced by 5HT is comparable to the R(–)METH-induced current, S(+)MDMA, R(–)MDMA, and S(+)METH produce hSERT-mediated inward currents that are much larger than the 5HT-induced currents (Figure 37).

In addition, R(–)METH induced a modest persistent leak current whereas S(+)MDMA, R(–)METH, and S(+)METH produced a stronger persistent leak current (Figure 37).

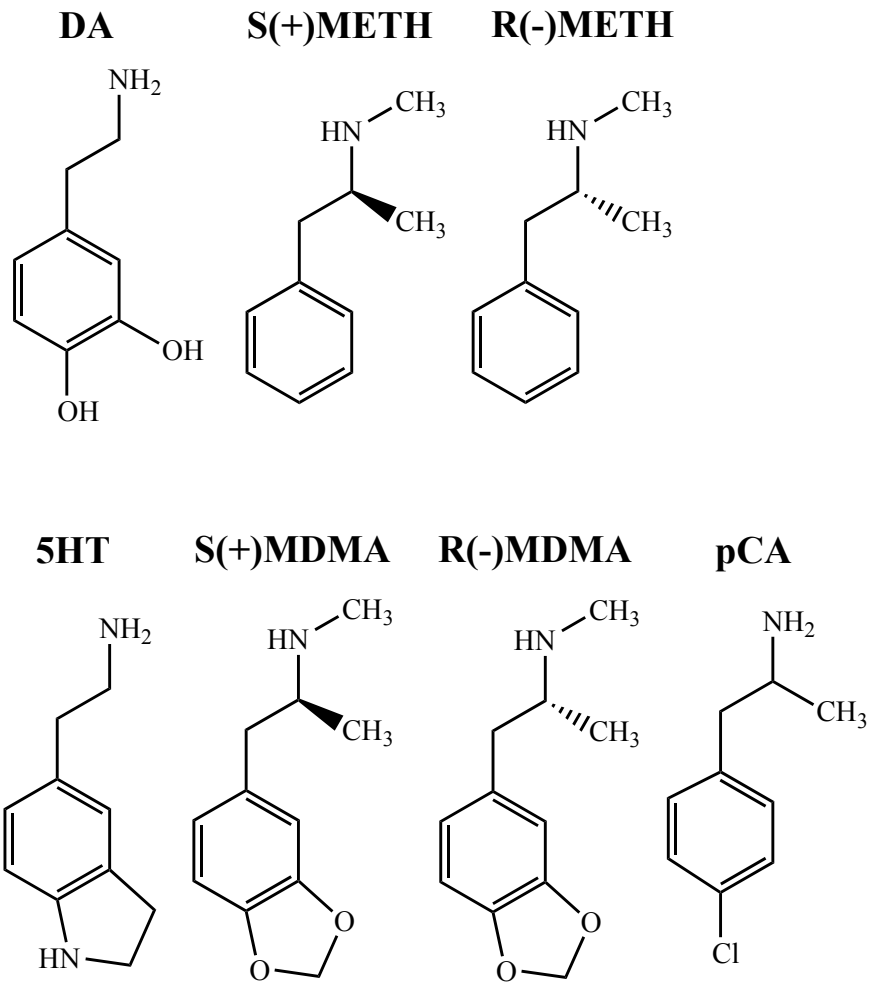

Figure 35. Structures of substrates acting on hDAT and hSERT. Abbreviations: dopamine (DA), S(+)amphetamine (S(+)AMPH), R(–)amphetamine (R(–)AMPH), S(+)methamphetamine (S(+)METH), R(–)methamphetamine (R(–)METH), serotonin (5HT), S(+)methylenedioxy-methamphetamine (S(+)MDMA), R(–)methylenedioxy-methamphetamine (R(–)MDMA), and *para*-chloroamphetamine (pCA).

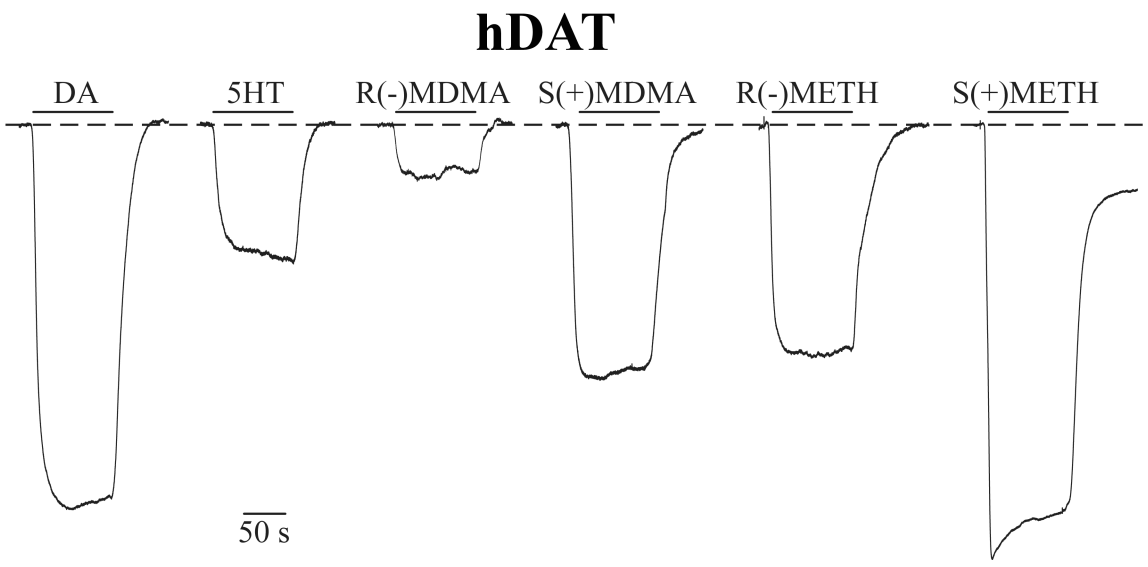

Figure 36. Currents generated by hDAT in response to METH and MDMA stereoisomers. Voltage-clamped (V_{com} = –60 mV) hDAT-expressing oocytes produce inward currents of varying magnitude and shape in response to application of 10 μM DA, 5HT, R(–)METH, S(+)METH, R(–)MDMA, and S(+)MDMA (100 s exposure, traces normalized to maximum 5HT response). Washing out the compound generally results in a complete return to baseline except for S(+) METH, which maintains a persistent current even after its removal.

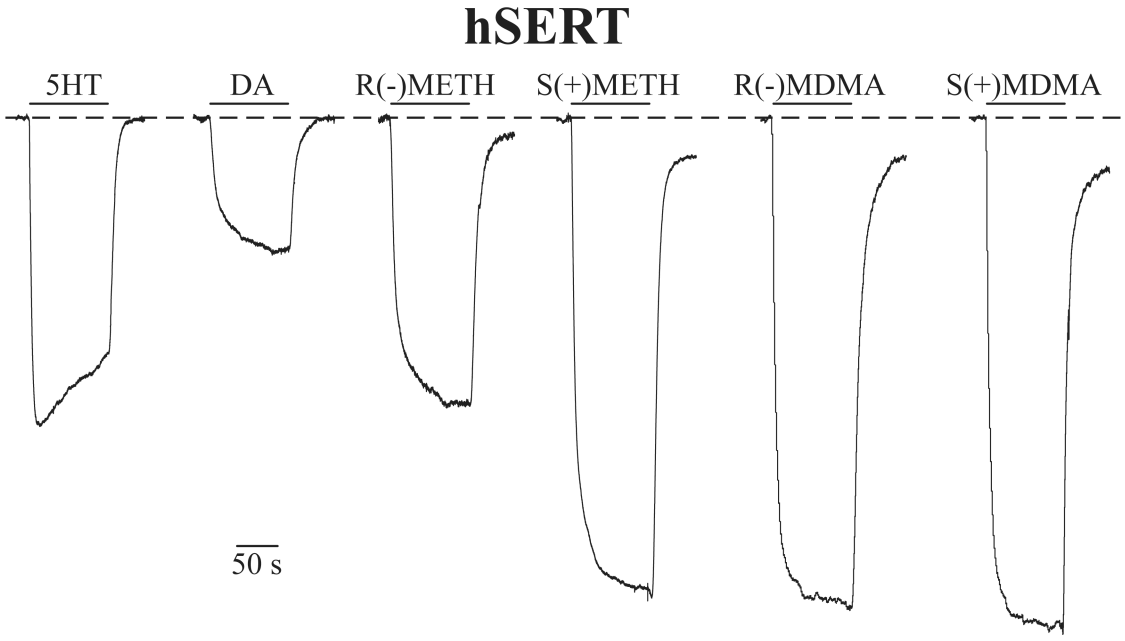

Fig. 37. Currents generated by hSERT in response to METH and MDMA stereoisomers. Voltage-clamped (V_{com} = –60 mV) hSERT-expressing oocytes produce inward currents of varying magnitude and shape in response to application of 10 μM 5HT, DA, R(–)METH, S(+)METH, R(–)MDMA, and S(+)MDMA (100 s exposure, traces normalized to maximum 5HT response). Washing out the compounds generally results in a complete return to baseline except for S(+) METH, R(–)MDMA, and S(+)MDMA, which even after their removal a persistent current remains. Unpublished data from Solis, 2012.

METH and MDMA Stereoisomers Produce hSERT-mediated Persistent Leak Currents that are Time-dependent

To further characterize the persistent leak current in hSERT, we tested the effect of varying time exposure of the stereoisomers of METH and MDMA (S(+)METH, R(–)METH, S(+)MDMA, and R(–)MDMA) on hSERT-mediated currents (Figure 38, Solis 2012, unpublished). To control for hSERT expression variability in different oocytes, we normalized each drug-induced inward current to a 5HT-induced exposure. The MDMA stereoisomers produced larger hSERT-mediated inward currents than the METH stereoisomers. Although the S(+)MDMA-induced current was slightly larger than R(–)MDMA-induced current, the S(+)METH-induced hSERT current was substantially larger than the R(–)METH-induced current (about twice as large). Accordingly, the compounds inducing the largest inward currents (S(+)METH, S(+)MDMA, and R(–)MDMA) induced measurable persistent leak currents with strength corresponding to the order of the drug's induced hSERT-mediated peak amplitudes (S(+)MDMA > R(–)MDMA > S(+)METH). This effect holds true for all time exposures tested, and is discernable more clearly at the longer time exposure (150 s, Figure 38).

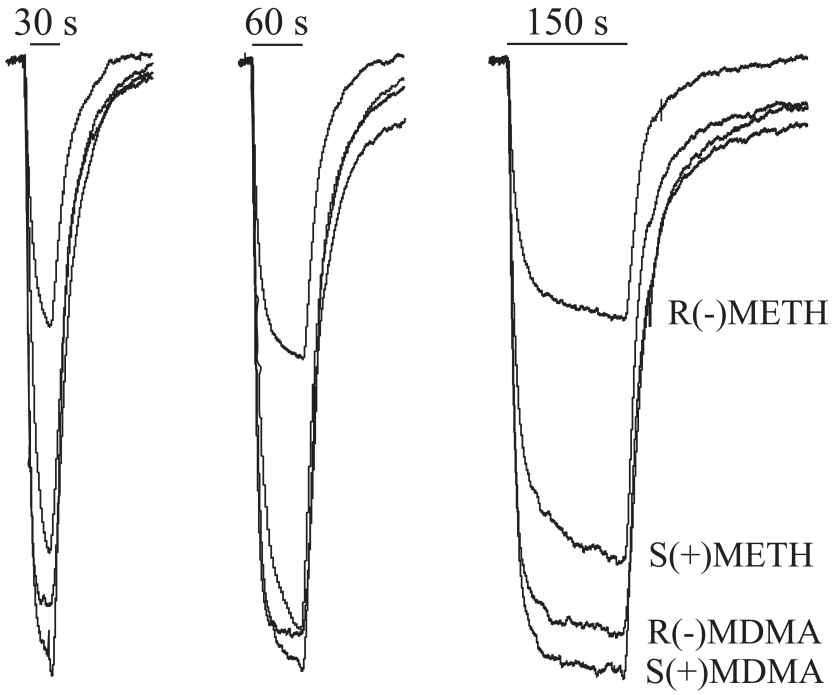

Figure 38. Effect of varying time of exposure of MDMA and METH stereoisomers on hSERT currents. Exposing voltage-clamped (V_{com} = –60 mV) hSERT-expressing oocytes to the stereoisomers of MDMA and METH yield distinct peak and persistent leak currents. S(+)MDMA, R(–)MDMA, and S(+)METH induce persistent leak currents more appreciable at longer exposure times (150 s treatment), whereas R(–) METH yields no discernable persistent peak current. Unpublished data from Solis, 2012.

The Persistent Leak Currents Induced by S(+)METH and S(+)MDMA on hDAT and hSERT are Time-dependent

Since the S(+) enantiomers for METH and MDMA (S(+)METH and S(+)MDMA, respectively) have been attributed to more potent behavioral effects, we narrowed our study to these two species. In hDAT-expressing cells, increasing the time of exposure to 10 μM S(+)METH in individual oocytes (from 30-200 s) produced more pronounced persistent leak currents (Figure 39A, Solis 2012, unpublished); however, 10 μM S(+)MDMA did not elicit persistent leak currents regardless of time exposure (Figure 39B, Solis 2012, unpublished). In contrast, both S(+)METH and S(+)MDMA induced persistent leak currents in hSERT-expressing oocytes that were enhanced with increased time exposure (from 30-200 s) to the drugs (effect of S(+)METH shown in Figure 40A, and effect of S(+)MDMA shown in Figure 40B, Solis 2012, unpublished).

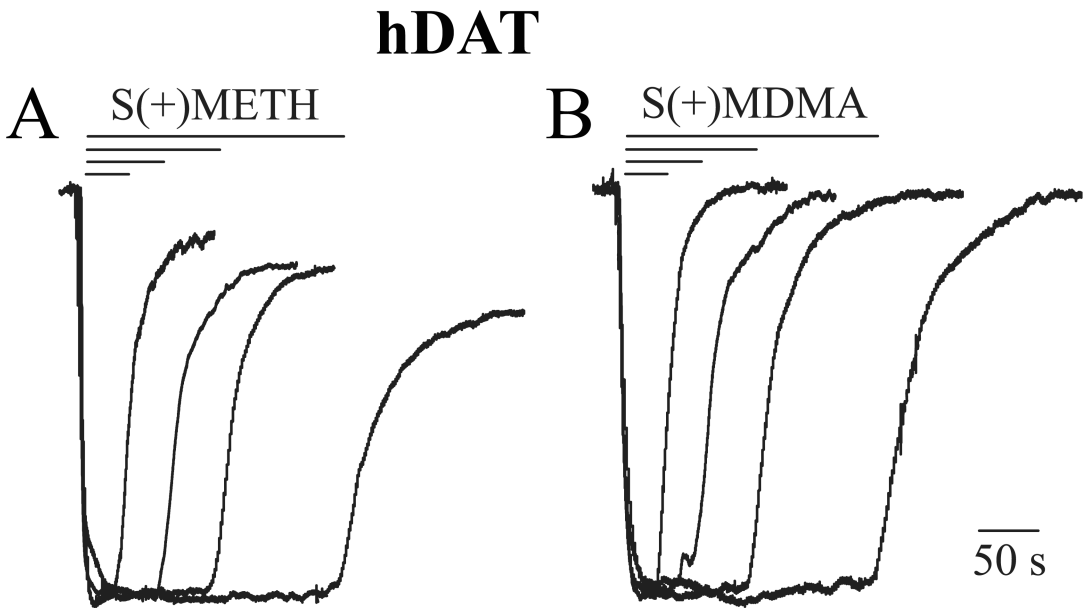

Figure 39. Time-dependence of S(+)METH- and S(+)MDMA-induced hDAT-mediated currents. Voltage-clamped (V_{com} = –60 mV) hDAT-expressing oocytes were exposed to different durations of 10 μM S(+)METH or 10 μM S(+)MDMA (30, 60, 100, or 200 s). (A) Exposure to S(+)METH induced larger persistent leak currents with increased time exposure. (B) S(+)MDMA did not produce persistent leak currents regardless of time exposure. Traces were obtained in individual oocytes, normalized to the largest drug-induced response, and aligned to the beginning of drug application. Unpublished data from Solis, 2012.

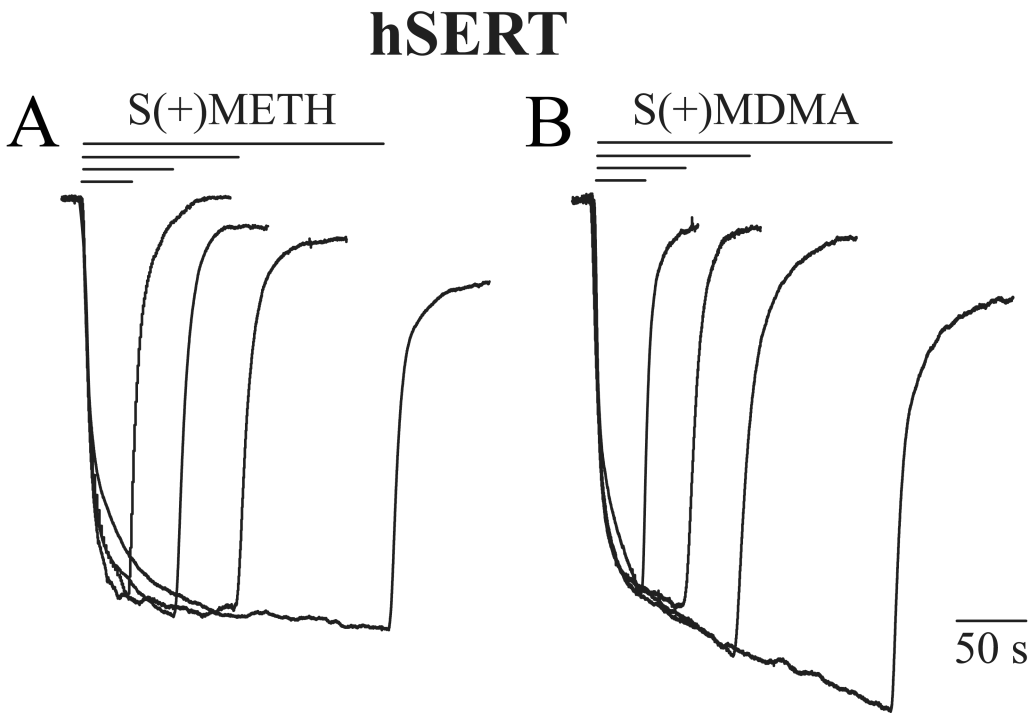

Figure 40. Time-dependence of S(+)METH- and S(+)MDMA-induced hSERT-mediated currents. Voltage-clamped (V_{com} = –60 mV) hSERT-expressing oocytes were exposed to different durations of 10 µM S(+)METH or 10 µM S(+)MDMA (30, 60, 100, or 200 s). Exposure to both (A) S(+)METH and (B) S(+)MDMA induced larger persistent leak currents with increased time exposure. Traces were obtained in individual oocytes, normalized to the largest drug-induced response, and aligned to the beginning of drug application. Unpublished data from Solis, 2012.

While S(+)METH and S(+)MDMA Induce Concentration-dependent hDAT-mediated Peak Currents, Only S(+)METH Induces hDAT-mediated Persistent Leak Currents

We further characterized the effect of S(+)MDMA and S(+)METH on hDAT by performing concentration response curves. We recorded currents in voltage-clamped (–60 mV) hDAT-expressing oocytes in response to 0.1-30 μM S(+)METH and S(+)MDMA application (100 s duration, data not shown). Increasing S(+)METH concentration produced increasingly larger hDAT-mediated inward currents, and beginning at 3 μM S(+)METH exposure, discernable persistent leak currents are observed, which are inhibited by the hDAT inhibitor cocaine (COC, 1 μM) (data not shown). The concentration-response values for S(+)METH-induced hDAT-mediated peak amplitude (selected points 30 s after drug exposure, 0.1-30 μM values used) were fit to the Hill 1 equation, which yielded a k_m value of 0.25 μM. In contrast, although hDAT-mediated inward currents became larger in response to increasing S(+)MDMA concentration, there was no persistent leak currents produced in response to any S(+)MDMA concentration tested (data not shown). The concentration-response values for S(+)MDMA-induced hDAT-mediated peak amplitude (selected points 30 s after drug exposure, 0.1-30 μM values used) were fit to the Hill 1 equation, which yielded a k_m value of 1.66 μM (see Table 3 for available affinity values for S(+)METH and S(+)MDMA to induce peak and persistent leak currents at hDAT). While S(+)METH produced an effect comparable to DA in regards to the hDAT-mediated amplitude, S(+)MDMA produced only about 70% of the effect of S(+)METH and was nearly seven-fold less potent.

Both Peak and Persistent Leak Currents Induced by S(+)METH and S(+)MDMA on hSERT are Concentration-dependent

To further characterize the effect of S(+)MDMA and S(+)METH on hSERT, we performed concentration response curves. We recorded currents in voltage-clamped (–60 mV) hSERT-expressing oocytes in response to 0.1-30 μM S(+)METH and S(+)MDMA application (100 s duration, Figure 41 and Figure 42, respectively, Solis 2012, unpublished). Increasing S(+)METH concentration produced increasingly larger hSERT-mediated inward currents (Figure 41A), and beginning at 3 μM S(+)METH exposure, discernable persistent leak currents are observed, which are inhibited by the SSRI fluoxetine (FLX, 1 μM) (data shown for 30 μM S(+)METH, Figure 41A). The concentration-response values for S(+)METH-induced hSERT-mediated peak amplitude (selected points 30 s after drug exposure, 0.1-30 μM values used) and persistent leak current (selected 60 s after drug washout, 1-30 μM used) were fit to the Hill 1 equation (Figure 41B and Figure 41C), which yielded k_m values of 4.55 ± 0.40 μM (n = 1.27 ± 0.09) and 8.76 μM (n = 2), respectively. Similarly, hSERT-mediated inward currents became larger in response to increasing S(+)MDMA concentration, and persistent leak currents were produced beginning at 1 μM S(+)MDMA exposure, which were inhibited by 1 μM FLX (data shown for 30 μM S(+)MDMA, Figure 42A). The concentration-response values for S(+)MDMA-induced hSERT-mediated peak amplitude (selected points 30 s after drug exposure, 0.1-30 μM values used) and persistent leak current (selected 60 s after drug washout, 1-30 μM values used) were fit to the Hill 1 equation (Figure 42B and Figure 42C), which yielded k_m values of 1.58 ± 0.15 μM (n = 1.39 ± 0.13) and 15.80 μM (n = 2), respectively.

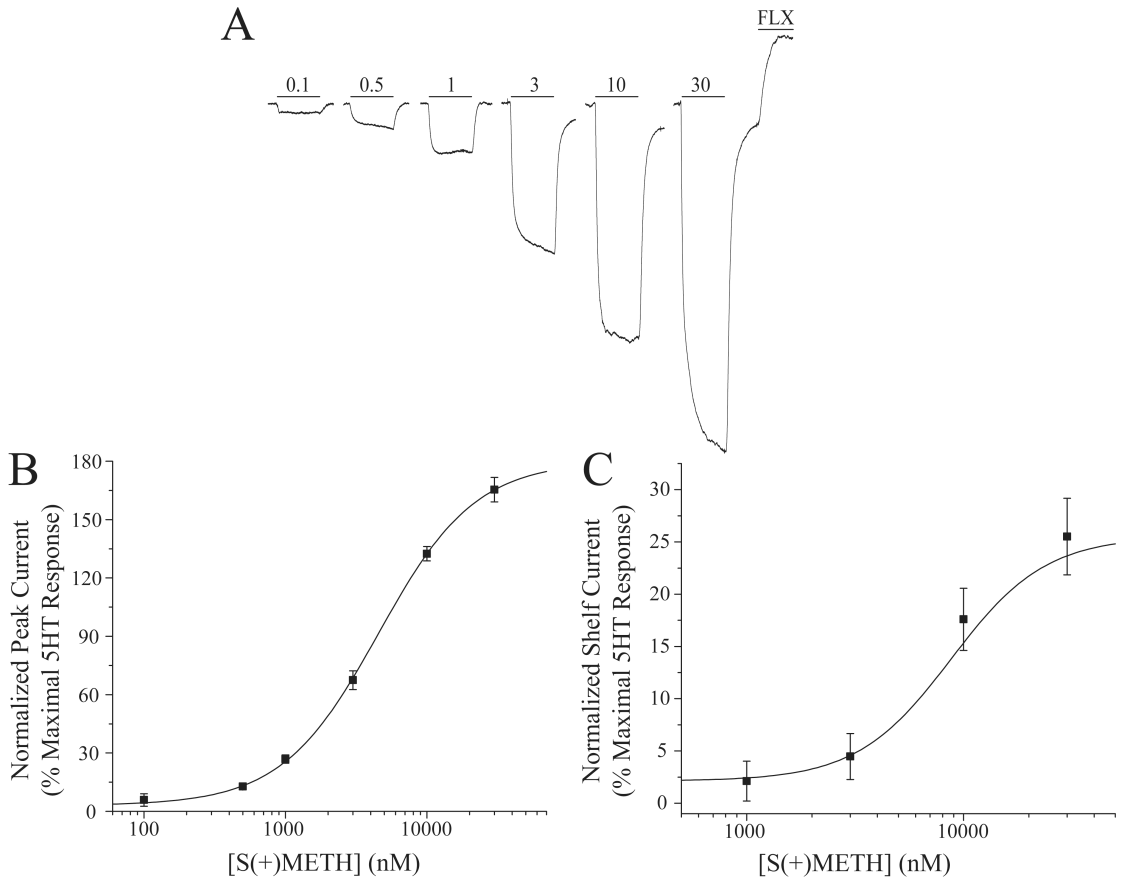

Fig. 41. Concentration-dependence of S(+)METH-induced hSERT-mediated currents. (A) Voltage-clamped (V_{com} = –60 mV) hSERT-expressing oocytes generate inward currents in response to increasing [S(+)METH] (from 0.1 – 30 μM, labeled 0.1, 0.5, 1, 3, 10, 30). Fluoxetine (1 μM, FLX) is applied during the persistent leak current induced after application of 30 μM S(+)METH, which inhibits the persistent leak current and elicits an outward current. (B) Fitting peak currents from several recordings as in A (amplitude point taken 30 second after drug application) to the Hill 1 equation, $y = V_{min} + (V_{max} - V_{min}) * x^n / (k^n + x^n)$, yields k_m = 4.55 ± 0.40 μM and n = 1.27 ± 0.09 for S(+)METH. (C) Fitting persistent leak currents from several recordings (amplitude point taken 60 second after drug application) to the Hill 1 equation yields k_m = 8.76 μM and n = 2 for S(+)METH. N = 5 and error bars represent SEM. Unpublished data from Solis, 2012.

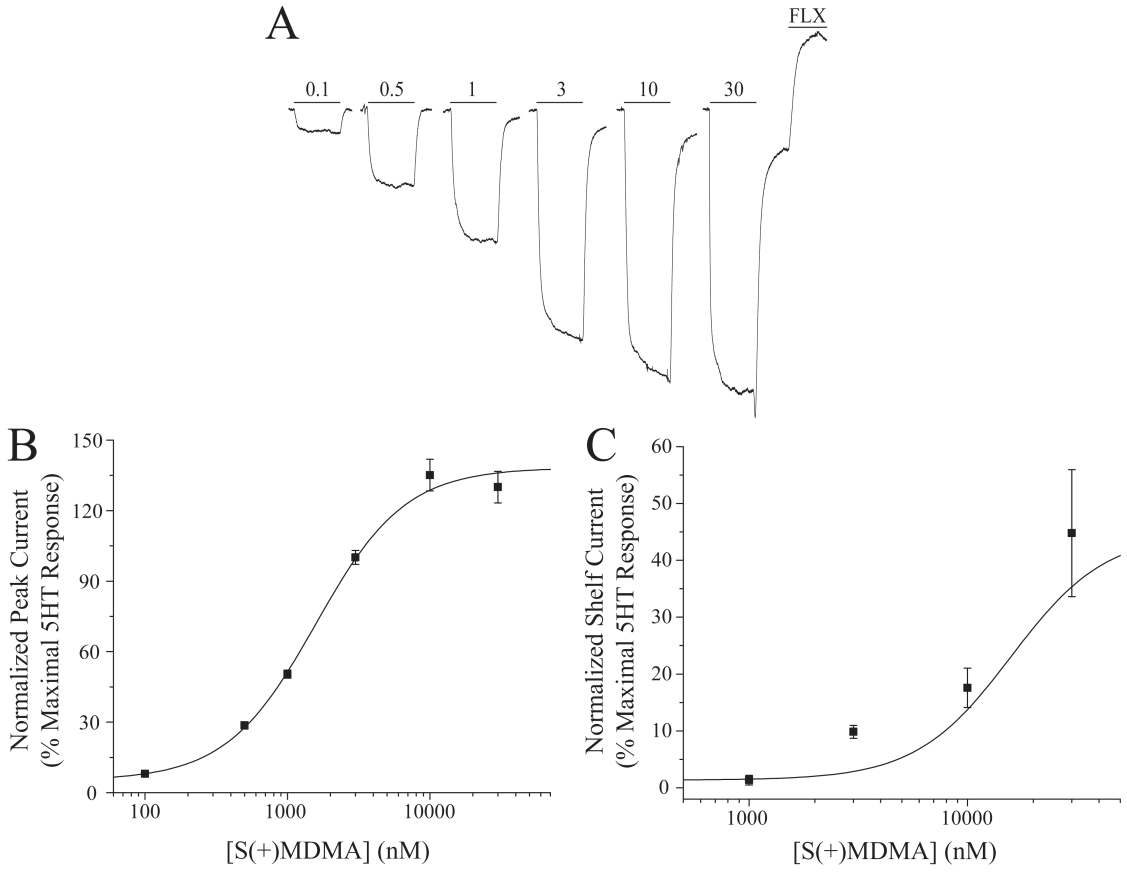

Fig. 42. Concentration-dependence of S(+)MDMA-induced hSERT-mediated currents. (A) Voltage-clamped (V_{com} = –60 mV) hSERT-expressing oocytes generate inward currents in response to increasing [S(+)MDMA] (from 0.1 – 30 μM, labeled 0.1, 0.5, 1, 3, 10, 30). Fluoxetine (1 μM, FLX) is applied during the persistent leak current induced after application of 30 μM S(+)MDMA, which inhibits the persistent leak current and elicits an outward current. (B) Fitting peak currents from several recordings as in A (amplitude point taken 30 seconds after drug application) to the Hill 1 equation, $y = V_{min} + (V_{max} - V_{min}) * x^n / (k^n + x^n)$, yields k_m = 1.58 ± 0.15 μM and n = 1.39 ± 0.13. (C) Fitting persistent leak currents from several recordings (amplitude point taken 60 seconds after drug application) to the Hill 1 equation yields k_m = 15.80 μM and n = 2. N = 5 and error bars represent SEM. Unpublished data from Solis, 2012.

	hDAT			hSERT		
	Peak (μM)	ILC (μM)	Efflux (nM)	Peak (μM)	ILC (μM)	Efflux (nM)
S(+)METH	0.87	13.25	24.1 ± 2.1	4.55 ± 0.40	8.76	736 ± 45
S(+)MDMA	2.68	DNE	142 ± 4	1.58 ± 0.15	15.8	74 ± 3

Table 3. Affinity values for S(+)METH and S(+)MDMA on hDAT and hSERT. Values for peak and persistent leak currents were obtained from voltage-clamped (V_{com} = –60 mV) *Xenopus laevis* oocytes expressing either hSERT or hDAT. Efflux values are from studies measuring reverse transport (efflux) of radiolabeled endogenous transmitters through DAT and SERT in synaptosome preparations (Rothman and Baumann 2006). Abbreviations: Peak (peak current), ILC (induced leak current or persistent leak current), DNE (does not exist).

A Large hSERT Persistent Leak Current is Elicited by Para-chloroamphetamine

Since the hSERT persistent leak currents induced by METH and MDMA were not as large as the ones observed in hDAT – induced by S(+)METH or S(+)AMPH (Rodriguez-Menchaca, Solis et al. 2012), we sough to identify a larger persistent leak current in hSERT. Certain compounds that are structurally related to AMPH are known to elicit a greater effect on SERT. Specifically, the AMPH derivative *para*-chloroamphetamine (pCA), has been shown to selectively kill serotonergic neurons (Berger, Grzanna et al. 1992; Zhou, Schreinert et al. 1996; Brown and Molliver 2000), is transported by hSERT, and induces substantial hSERT-mediated 5HT efflux (Hilber, Scholze et al. 2005). Also, hSERT-expressing mammalian cells (HEK293 cells transiently transfected with hSERT) under whole-cell patch-clamp (V_{hold} –70 mV) display depressed currents after exposure to pCA that resembles our METH- or MDMA- induced hSERT-mediated persistent leak currents (Hilber, Scholze et al. 2005). In this same study, hSERT-mediated currents elicited by other hSERT substrates, including tyramine, MPP^+, and MDMA, seem to return to baseline.

We deemed pCA to be a great candidate to induce a persistent leak current at hSERT, and therefore, exposed hSERT-expressing oocytes to 10 μM pCA, which produced an hSERT-mediated inward current that was larger than the 5HT-induced peak current, and also a potent persistent leak current at short (60 s, Figure 43A, Solis 2012, unpublished) and long time exposure (200 s, Figure 43B, Solis 2012, unpublished), which can be inhibited by fluoxetine application. The longer pCA time exposure (200 s) yields an enhanced persistent leak current. The persistent leak current evoked by pCA is larger than the one produced in response to either stereoisomer of METH or MDMA (Figure 37

and Figure 38) or the more potent S(+) isomers for METH (Figure 40A and Figure 41) and MDMA (Figure 40B and Figure 42).

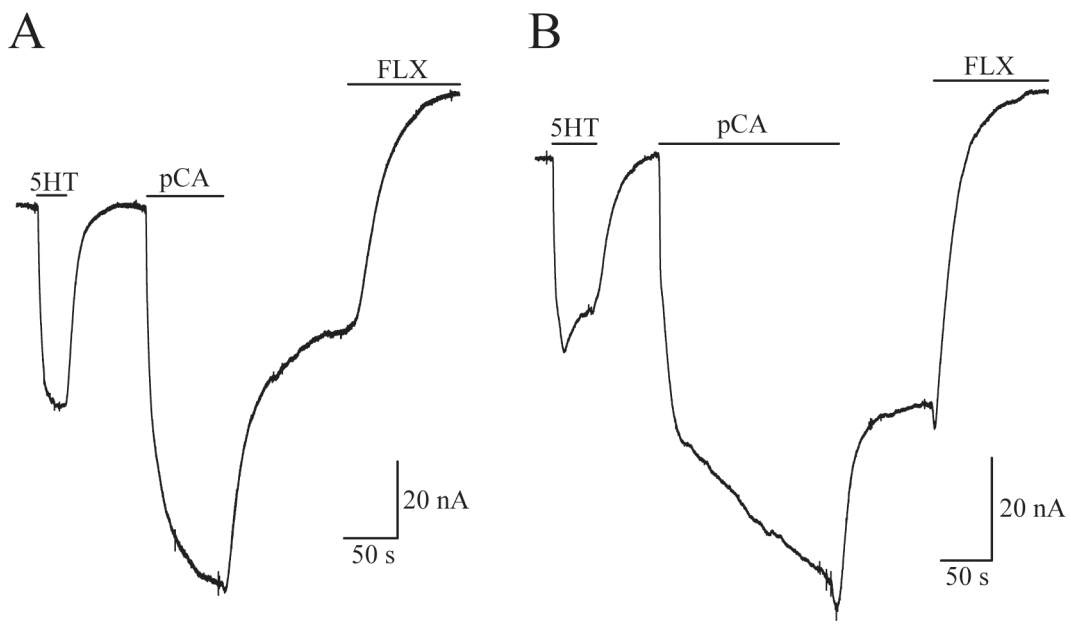

Figure 43. Exposure to *para*-chloroamphetamine (pCA) produces a strong hSERT-mediated persistent leak current. Application of 10 μM pCA to voltage-clamped (V_{com} = –60 mV) hSERT-expressing oocyte for (A) 60 s or (B) 200 s induces a potent hSERT-mediated persistent leak current that is blocked by the SSRI fluoxetine (FLX, Prozac). Unpublished data from Solis, 2012.

DISCUSSION

METH and MDMA Stereoisomers Produce Distinct Behavioral Actions

It is recognized that the behavioral actions of MDMA are more complex than those of AMPH and METH; nevertheless, given that AMPH, METH, and MDMA are locomotor stimulants, drugs of abuse, and optically-active phenylisopropylamines that are related structurally, they seemed like ideal examples to evaluate in the present investigation. Despite chemical and behavioral similarities, it is well-established that the stereoisomers of METH and MDMA produce distinguishable clinical effects (Green, Mechan et al. 2003). The distinct behavioral effects exerted by METH and MDMA are attributed to their differences in affinity at their molecular targets – hSERT and hDAT. While METH displays higher affinity than MDMA at hDAT, MDMA is more potent at hSERT.

Furthermore, the stereoisomers of METH and MDMA also confer distinct behavioral effects. Though both S(+)METH and R(–)METH are psychoactive, the R(–)METH isomer generally produces less pleasurable effects than doses containing S(+)METH in humans (Mendelson, Uemura et al. 2006). Similarly, in rhesus monkey, S(+)MDMA isomer displays stronger reinforcing effects than the R(–)MDMA isomer (Fantegrossi 2008). These differences in enantiomer-specific behavioral effects could be attributed to the selectivity of the compounds at the monoamine transporters. S(+)METH displays better affinity than R(–)METH at hDAT, and similarly, S(+)MDMA displays better affinity than R(–)MDMA at both hDAT and hSERT (Rothman and Baumann 2006; Fantegrossi 2008). Lastly, it cannot be discounted that the distinct behavioral actions

elicited by METH and MDMA are partly caused by these drugs having effects on other targets, such as receptors. In fact, METH and MDMA interact at central nicotinic receptors (Garcia-Rates, Camarasa et al. 2007), which have been targeted to prevent neurotoxicity induced by METH and MDMA (Escubedo, Camarasa et al. 2009).

In Search of Persistent Leak Currents

The question arises whether the persistent leak current is a phenomenon common to abused drugs that are structurally similar to AMPH, and whether other monoamine transporters exhibit the same phenomenon. Based on our previous work, we might expect the enhanced leak current to be of particular interest with regard to DA release at dopaminergic synapses; and furthermore, identifying a persistent leak current at SERT would have implications for neurotransmission at the serotonergic synapse. Since AMPH induces a persistent leak current through hDAT (Rodriguez-Menchaca, Solis et al. 2012), we expect that the AMPH analog METH, which displays high affinity at hDAT, would also produce a persistent leak current through hDAT. MDMA seemed like a prudent candidate to evoke a persistent leak current through hSERT because it has high affinity at hSERT and is closely related to AMPH and METH.

Since S(+)METH displays better affinity than R(–)METH at hDAT, and S(+)MDMA displays better affinity than R(–)MDMA at hSERT (Rothman and Baumann 2006), we posited the S(+) enantiomers of METH and MDMA would confer a stronger effect on hDAT and hSERT, respectively. In addition, the fact that METH and MDMA target hDAT and hSERT non-specifically opens the possibility that various substrates can evoke a persistent leak current through each monoamine transporter. Thus, we extended our original studies (Rodriguez-Menchaca, Solis et al. 2012) to test whether the structural attributes of the stereoisomers of MDMA or METH would enable them to generate the persistent leak current in either hDAT or hSERT.

Implications of Peak Currents on Synaptic Neurotransmission

The inward currents elicited by METH and MDMA through hDAT and hSERT (in oocytes clamped to –60 mV) are depolarizing currents. These inward currents, also called peak currents, can be significant for synaptic neurotransmission because they would depolarize the plasma membrane of neurons containing these transporters. Since transporters are located at the presynaptic terminal of monoaminergic neurons, the terminal would be depolarized and the release of the monoamine neurotransmitter would be precipitated either through vesicular fusion or by non-vesicular mechanisms including reverse transport (Kahlig, Binda et al. 2005; Sulzer, Sonders et al. 2005).

Implications of the Persistent Leak Current on Synaptic Neurotransmission

The persistent leak current, which is the monoamine transporter-mediated current that persists after application and removal of a stimulant, such as S(+)AMPH or S(+)METH for hDAT, results in prolonged depolarization of transporter-expressing oocytes. In excitable cells, such as neurons, the cell membrane would be depolarized to a potential more proximal to the threshold of the voltage-gated sodium channels responsible to initiate an action potential; therefore, depolarization induced by the persistent leak current favors neurotransmitter release. Thus, the existence of a persistent leak current at monoaminergic neurons implies a mechanism for long-lasting DA or 5HT release at a dopaminergic or serotonergic synapse, respectively.

Structural Determinants to Induce the Persistent Leak Current in hDAT

Only the S(+), but not the R(–), enantiomer of METH is capable of producing the persistent leak current through hDAT. This result is consistent with our previous work, in which only the S(+) enantiomer of AMPH evoked a persistent leak current through hDAT (Rodriguez-Menchaca, Solis et al. 2012). Hence, stereochemistry seems to play a role in producing the persistent leak current at least for hDAT. However, it is yet to be determined if this difference could be attributed to diminished uptake of the R(–) enantiomers due to their lower affinity at hDAT. Further experiments accounting for uptake of these substrates are warranted.

Unlike S(+)AMPH and S(+)METH, however, neither MDMA optical isomer produced a persistent shelf current through hDAT once they were washed out. Structurally, DA and AMPH are primary amines. Because S(+)METH behaves similar to S(+)AMPH, it is unlikely that the *N*-methyl group is responsible for the observed differences. DA lacks an α-methyl group, whereas both AMPH and METH possess this functionality. Thus, it might be thought that the presence of the α-methyl group is responsible for the shelf; however, although S(+)MDMA bears such a group, it does not produce the persistent leak current at hDAT. There is a possibility that the lower affinity of S(+)MDMA at hDAT precludes its transport into the cell, and thus, the internal S(+)MDMA concentration is not enough to bind and activate the internal hDAT binding site surmised to be responsible for producing the persistent leak current. Another possibility is that the pentameric ring in S(+)MDMA disallows for the compound to bind at the binding site. Perhaps, a smaller chemical structure than S(+)MDMA, without the

pentameric ring, is required in order to bind at the internal binding site of hDAT, such as S(+)METH or S(+)AMPH.

Lastly, perhaps the presence of the oxygenated ring group impedes induction of the hDAT–mediated persistent leak current. Fittingly, the one structural feature common to MDMA and DA (a substrate that does not inducing a persistent leak current), but lacking in AMPH and METH, is the presence of these oxygen substituents; therefore, they may account for some of the observed differences. Additional compounds will need to be examined to test these hypotheses and form a complete structure-activity relationship (SAR) analysis.

Structural Determinants to Induce the Persistent Leak Current in hSERT

Similarly to hDAT, only the S(+) enantiomer of METH is able to induce a persistent leak current through hSERT, which validates a role for stereochemistry in generating a persistent leak current across different monoamine transporters. Surprisingly, the MDMA stereoisomers are able to produce a persistent leak current at hSERT, which, if the drugs act directly on the transporter, implies that hSERT possesses a less selective internal binding site. Further studies to investigate whether a direct interaction of drugs to the transporter induce the persistent leak current are warranted. An adequate technique to perform these studies is the voltage-clamp, cut-open oocyte preparation (Adams and DeFelice 2003).

The peak and persistent leak currents induced by S(+)METH and S(+)MDMA on hSERT seem qualitatively similar. The affinity values for the inducing hSERT-mediated peak currents by S(+)METH and S(+)MDMA are 4.55 and 1.58 μM, respectively, which is approximately three times better for S(+)MDMA than S(+)METH. Since the affinity to induce the persistent leak current is comparable for S(+)METH and S(+)MDMA (8.76 and 15.8 μM, respectively), this might indicate a relationship between affinity and ability to produce a persistent leak current.

Relationship Between METH/MDMA Reinforcement and the Persistent Leak Current

It is thought that if a drug produces mostly a dopaminergic stimulus, it will produce stimulant behavior and will have more potential to be addictive (Rothman and Baumann 2006). Since S(+)MDMA activates a DA response (by releasing DA through hDAT), it would be expected to mediate addictive behaviors; moreover, since R(–)MDMA only activates a mild DA response (due to its weak affinity for hDAT) it is expected to confer diminished addictive properties than S(+)MDMA. This is exactly what happened in a study comparing the reinforcing strength of MDMA stereoisomers that showed both enantiomers possess reinforcing effects, but S(+)MDMA was clearly stronger than R(–)MDMA as a reinforcer and had better affinity at DAT (Fantegrossi 2008). However, the reinforcing effects of MDMA (racemic or of either enantiomer of MDMA) are weaker than the reinforcing effects of METH; furthermore, the reinforcing effects of racemic MDMA, which is the chemical form that would be used in the streets, is weaker than the reinforcing of S(+)MDMA (Wang and Woolverton 2007). This would be in agreement with the finding that MDMA and its analogs do not tend to exhibit behavioral effects congruent with those of AMPH-like drugs; in particular, it is known that MDMA is typically taken intermittently by people, usually in the context of raves or dance parties, rather than in the compulsive binge pattern characteristic of psychostimulants (Fantegrossi 2008). Since MDMA elicits more 5HT to DA release (as compared to METH), these findings support the hypothesis that greater 5HT to DA releasing potency (increasing 5HT releasing potency relative to DA) leads to weaker reinforcing effects (Wang and Woolverton 2007).

In the context of our study, the fact that S(+)METH induces a diminished persistent leak current through hSERT and produces a strong one through hDAT, indicates that the long-lasting effects this drug produces are primarily mediated by DA, and is consistent with the high abuse potential S(+)METH is known to have. Since inducing a persistent depolarizing leak current through hSERT would be proficient at prolonging serotonergic neurotransmission, perhaps having an hSERT-mediated persistent leak current induced by S(+)MDMA is partially responsible for reducing the reinforcing effects S(+)MDMA possesses relative to S(+)METH (again, S(+)METH induces a substantial persistent leak current through hDAT and a small one through hSERT). In the case of R(–)MDMA, qualitatively it does elicit a slightly smaller hSERT-mediated persistent leak current than S(+)MDMA, which could indicate its action as a weaker reinforcer (as compared to S(+)MDMA), but the electrophysiological actions of R(–)MDMA on hSERT need to explored further.

Increasing Serotonergic Involvement Decreases Abuse Potential

Studies supporting the hypothesis that as serotonergic involvement increases, addictive potential decreases include that treating rats with the 5HT precursor L-tryptophan, which increases 5HT levels, decreases self-administration of cocaine and AMPH, pre-treating rats and squirrel monkeys with SERT reuptake inhibitors reduces intravenous cocaine self-administration, and cocaine analogs that are more potent at SERT are weaker at maintaining self-administration behavior than cocaine analogs with weak affinity for SERT (Rothman, Blough et al. 2008).

Since these and other lines of evidence support the hypothesis that elevating synaptic 5HT concentrations counteract the stimulant and reinforcing effects mediated by elevations in synaptic DA levels, an emerging idea to decrease abuse liability in the development of therapeutic agents is to add 5HT-releasing properties to these drugs (Rothman, Blough et al. 2008). In addition to measurements of potency of drugs to release neurotransmitters by distinct monoamine transporters, perhaps inclusion of the ability for a candidate compound to elicit a persistent leak current, in particular by SERT, could help strengthen the contribution of serotonergic signaling and diminish the abuse potential of the candidate compound.

Contribution of Persistent Leak Currents to Predicting Behavioral Effects

It is already known that substrate-induced monoamine transporter-mediated peak currents increase neuronal excitability, which would result in enhanced neurotransmitter release (Ingram, Prasad et al. 2002; Branch and Beckstead 2012); in like manner, assuming persistent leak currents lead to long-lasting release of monoamine neurotransmitters, we would expect for drugs that induce persistent leak currents selectively through hDAT to confer higher abuse potential than drugs that elicit persistent leak currents through hSERT.

Moreover, we would expect any contribution of the serotonergic system to diminish the reinforcing effects of the drugs that are more selective at inducing hDAT currents. Therefore, a shift in drug selectivity from hDAT to hSERT to induce a persistent leak current would be predictive of abuse potential. In addition, it is probable that the existence of persistent leak currents could be a measure used to predict the behavioral effects, and abuse liability, of drugs that are substrates for monoamine transporters.

Relationship Between Monoamine Release and Transporter Currents

The main contributing factor underlying the different behavioral effects produced by related AMPH-like drugs of abuse is thought to be their distinct affinities to release monoamine neurotransmitters through the monoamine transporters. It is known that drugs such as AMPH and phentermine, which release [^{3}H]-DA more potently than [^{3}H]-5HT *in vitro*, increase endogenous extracellular DA more than extracellular 5HT *in vivo*; and likewise, drugs such as fenfluramine and chlorphentermine, which release [^{3}H]-5HT more potently than [^{3}H]-DA *in vitro*, increase endogenous extracellular 5HT more than extracellular DA. Furthermore, while METH is much more potent at releasing DA and NE (from DAT and NET, respectively) than at releasing 5HT through SERT, structurally related MDMA produces a rapid, acute release of both 5HT and DA from nerve terminals in experimental animals (Rothman and Baumann 2006). Making a correlation between releasing affinity of compounds tested in this study and their ability/affinity to produce (peak and shelf) currents would validate a relationship between these mechanisms.

Comparing METH- and MDMA-induced DAT-mediated Peak Currents and DAT-mediated Neurotransmitter Release

In terms of peak currents, first, we determined that when applied to hDAT, METH and MDMA stereoisomers produced hDAT-mediated inward currents that are comparable those in response to DA. Pertaining to the more active METH and MDMA enantiomers we studied, S(+)MDMA produced a visibly smaller peak current than S(+)METH and was nearly seven-fold less potent. The relative difference in affinities for S(+)METH and S(+)MDMA at inducing hDAT-mediated peak currents (k_m = 0.25 and 1.66 μM, respectively) are in agreement with the six-fold affinity difference reported for the ability of these isomers to release [^{3}H]-DA from DAT in synaptosomes (k_m = 24.1 and 142 nM, respectively) (Rothman and Baumann 2006). Obtaining the k_m for both R(–)METH- and R(–)MDMA-induced hDAT-mediated peak currents would enable to further compare this property to DAT-mediated neurotransmitter release.

Comparing METH- and MDMA-induced DAT-mediated Persistent Leak Currents and DAT-mediated Neurotransmitter Release

Regarding persistent leak currents, since S(+)METH (and not R(–)METH, S(+)MDMA, nor R(–)MDMA) induces an hDAT-mediated persistent leak current, S(+)METH is expected to induce the greatest DA release (at least as compared to the other agents tested here), which correlates with it having the highest affinity at hDAT. Since neither MDMA enantiomer induces an hDAT-mediated persistent leak current, we can deduce racemic MDMA has minimal effect on long-term DAT-mediated neurotransmitter release. Furthermore, although S(+)MDMA has substantially higher affinity than R(–)MDMA to release neurotransmitter at DAT (k_m = 142 and 3700 nM, respectively), perhaps the contribution of R(–)MDMA in racemic MDMA weakens the overall affinity of MDMA resulting in lessened DAT-mediated release. In regards to METH, it is known that S(+)METH has nearly 20 times better affinity than R(–)METH to release DA through DAT (k_m = 24.1 and 416 nM, respectively), which would be in agreement with the fact that only S(+)METH induces an hDAT-mediated persistent leak current.

Comparing METH- and MDMA-induced SERT-mediated Peak Currents and SERT-mediated Neurotransmitter Release

In terms of peak currents, akin to 5HT-induced currents, all four compounds tested induced hSERT-mediated inward currents. However, S(+)MDMA, R(–)MDMA, and S(+)METH induced hSERT-mediated currents that were substantially larger than the one induced by R(–)METH. Pertaining to the more active METH and MDMA enantiomers we studied, the relative difference in affinities for S(+)METH and S(+)MDMA at inducing hSERT-mediated peak currents (k_m = 4.55 and 1.58 μM, respectively) are in agreement with the ten-fold affinity difference reported for the ability of these isomers to release [^{3}H]-5HT from SERT in synaptosomes (k_m = 736 and 74 nM, respectively) . Obtaining the k_m for both R(–)METH- and R(–)MDMA-induced hSERT-mediated peak currents would enable to further compare this property to SERT-mediated neurotransmitter release.

Comparing METH- and MDMA-induced SERT-mediated Persistent Leak Currents and SERT-mediated Neurotransmitter Release

Regarding persistent leak currents, S(+)MDMA, R(–)MDMA, and S(+)METH, but not R(–)METH, induce substantial hSERT-mediated persistent leak currents, which might induce long-lasting hSERT-mediated 5HT release. In terms of the MDMA stereoisomers, the slightly smaller R(–)MDMA-induced persistent leak current (as compared to the one induced by S(+)MDMA) might correlate with the respective affinities to induce neurotransmitter release by SERT (S(+)MDMA k_m = 74 nM and R(–)MDMA k_m = 340 nM). S(+)METH and S(+)MDMA display comparable affinities at inducing hSERT-mediated persistent leak currents induced (k_m = 8.76 μM and k_m = 15.80 μM, respectively), which does not seem to correlate with the ability for these isomers to release [^{3}H]-5HT from SERT in synaptosomes (k_m = 736 and 74 nM, respectively). To further study if this discrepancy is consistent, we would have to compare affinities to induce the persistent leak current with the R(–) isomers of both METH and MDMA at both hSERT and hDAT. Regardless, as noted, S(+)METH is strongest acting on DAT, both for release and at inducing persistent leak current. The weak k_m for persistent leak current (and therefore neurotransmitter release) by SERT agrees with the fact that METH induces very little 5HT release in the brain. Lastly, the affinity for R(–)METH at inducing SERT-mediated release is relatively much weaker (k_m = 4640 nM) than its S(+)METH counterpart (k_m = 736 nM), which agrees with the ability of only S(+)METH to induce a persistent leak current. In conclusion, the effects S(+)METH and S(+)MDMA induce on current and efflux are in agreement at both hDAT and hSERT.

MONOAMINE TRANSPORTER SUBSTRATES AND INHIBITORS: CLOSING REMARKS

Although we have grouped compounds that act on the monoamine neurotransmitter transporters into two categories, substrates, which are taken up by transporters, and inhibitors, which bind to transporters and block their ability to take up substrates, through the work described here (and in other studies), we are now seeing that this categorization is not the entire story. For example, we now know that ASP^+ can act as a substrate for hNET, but has inhibitor-like actions at hSERT and can also be taken up by hSERT at a slower rate than other substrates. On the other hand, APP^+ is a superior fluorescent substrate for hSERT that, once inside the cell, binds to organelles and even intercalates DNA. Moreover, the AMPH-like transmitter-releasing compounds constitute a different class of substrates than the endogenous "classic" transmitters. These "releaser" compounds are even able to produce the persistent induced leak current, which illustrates further complexities in the classification of compounds acting on transporters. Thus, compounds can be more complex than simply being deemed substrates or inhibitors.

Yet, knowing whether a compound is a substrate or an inhibitor is useful to help understand how transporters operate. Accordingly, the advent of distinct experimental techniques in combination with substrates and inhibitors has allowed for our understanding of transporters to increase. Whether it is fluorescent compounds, such as APP^+ or ASP^+, which can be employed to study monoamine transporter activity in live-cells in real-time using fluorescence microscopy, or drugs of abuse, such as cocaine or AMPH-like compounds, which produce distinct responses that are measureable through

electrophysiological approaches, we have the instruments and are in the position to continue expanding our knowledge of transporter function. The persistent shelf current described in my work is an example of a transporter property at an inchoate level of understanding, and through use of relevant synthetic compounds (related to AMPH) and multiple experimental techniques we can elucidate the structural determinant underlying this interesting property. In like manner, researchers are performing structure-activity relationship (SAR) studies that require series of chemical compounds (substrates or inhibitors) and a functional assay to learn what the specific chemical moieties of compounds are that contribute to their action (as substrates or inhibitors) on transporters. Since new advances, such as the FlexStation, allow for high-throughput measurement of fluorescent compounds, perhaps introduction of fluorescent analogs of APP^+ would be appropriate for SAR studies. Moreover, homology models based on the crystallized leucine transporter belonging to the same neurotransmitter symporter family as the monoamine transporters, in combination with docking techniques, provide an additional resource to study the action of substrates and inhibitors on monoamine transporters (the models can even be employed for SAR studies).

We have come a long way from the time we were limited to the use of radiolabeled compounds to study uptake through monoamine transporters in nerves. My work is only a small step forward in the advancement of our understanding into the complex nature of monoamine transporters. Surely, much more knowledge will be uncovered in the upcoming years, which will hopefully benefit the efforts to alleviate medical conditions that implicate these transporters and will lead to improvements in the quality of life of people.

REFERENCES

Abramson, J., I. Smirnova, V. Kasho, G. Verner, S. Iwata and H. R. Kaback (2003). "The lactose permease of Escherichia coli: overall structure, the sugar-binding site and the alternating access model for transport." FEBS Lett **555**(1): 96-101.

Abramson, J., I. Smirnova, V. Kasho, G. Verner, H. R. Kaback and S. Iwata (2003). "Structure and mechanism of the lactose permease of Escherichia coli." Science **301**(5633): 610-615.

Adams, S. V. and L. J. DeFelice (2002). "Flux coupling in the human serotonin transporter." Biophys J **83**(6): 3268-3282.

Adams, S. V. and L. J. DeFelice (2003). "Ionic currents in the human serotonin transporter reveal inconsistencies in the alternating access hypothesis." Biophys J **85**(3): 1548-1559.

Amara, S. G. and M. S. Sonders (1998). "Neurotransmitter transporters as molecular targets for addictive drugs." Drug Alcohol Depend **51**(1-2): 87-96.

Andersen, J., O. Taboureau, K. B. Hansen, L. Olsen, J. Egebjerg, K. Stromgaard and A. S. Kristensen (2009). "Location of the antidepressant binding site in the serotonin transporter: importance of Ser-438 in recognition of citalopram and tricyclic antidepressants." J Biol Chem **284**(15): 10276-10284.

Arias, H. R. (2009). "Is the inhibition of nicotinic acetylcholine receptors by bupropion involved in its clinical actions?" Int J Biochem Cell Biol **41**(11): 2098-2108.

Bancaud, A., S. Huet, N. Daigle, J. Mozziconacci, J. Beaudouin and J. Ellenberg (2009). "Molecular crowding affects diffusion and binding of nuclear proteins in heterochromatin and reveals the fractal organization of chromatin." EMBO J **28**(24): 3785-3798.

Barbeau, A. (1970). "Dopamine and disease." Can Med Assoc J **103**(8): 824-832.

Barker, E. L. and R. D. Blakely (1996). "Identification of a single amino acid, phenylalanine 586, that is responsible for high affinity interactions of tricyclic antidepressants with the human serotonin transporter." Mol Pharmacol **50**(4): 957-965.

Barker, E. L., K. R. Moore, F. Rakhshan and R. D. Blakely (1999). "Transmembrane domain I contributes to the permeation pathway for serotonin and ions in the serotonin transporter." J Neurosci **19**(12): 4705-4717.

Barr, C. L., K. Wigg, M. Malone, R. Schachar, R. Tannock, W. Roberts and J. L. Kennedy (1999). "Linkage study of catechol-O-methyltransferase and attention-deficit hyperactivity disorder." Am.J.Med.Genet. **88**(6): 710-713.

Baumann, M. H., R. D. Clark and R. B. Rothman (2008). "Locomotor stimulation produced by 3,4-methylenedioxymethamphetamine (MDMA) is correlated with dialysate levels of serotonin and dopamine in rat brain." Pharmacol Biochem Behav **90**(2): 208-217.

Bedard, A. C., K. P. Schulz, E. H. Cook, Jr., J. Fan, S. M. Clerkin, I. Ivanov, J. M. Halperin and J. H. Newcorn (2010). "Dopamine transporter gene variation modulates activation of striatum in youth with ADHD." Neuroimage **53**(3): 935-942.

Berger, U. V., R. Grzanna and M. E. Molliver (1992). "The neurotoxic effects of p-chloroamphetamine in rat brain are blocked by prior depletion of serotonin." Brain Res **578**(1-2): 177-185.

Biel, J. H. and B. A. Bopp (1978). "Amphetamines: Structure-activity relationships." Handbook of Psychopharmacology, L. L. Iversen, S. D. Iversen, and S. H. Snyder, eds **11**: 1-39.

Bolan, E. A., B. Kivell, V. Jaligam, M. Oz, L. D. Jayanthi, Y. Han, N. Sen, E. Urizar, I. Gomes, L. A. Devi, S. Ramamoorthy, J. A. Javitch, A. Zapata and T. S. Shippenberg (2007). "D2 receptors regulate dopamine transporter function via an extracellular signal-regulated kinases 1 and 2-dependent and phosphoinositide 3 kinase-independent mechanism." Mol Pharmacol **71**(5): 1222-1232.

Branch, S. Y. and M. J. Beckstead (2012). "Methamphetamine produces bidirectional, concentration-dependent effects on dopamine neuron excitability and dopamine-mediated synaptic currents." J Neurophysiol **108**(3): 802-809.

Brown, P. and M. E. Molliver (2000). "Dual serotonin (5-HT) projections to the nucleus accumbens core and shell: relation of the 5-HT transporter to amphetamine-induced neurotoxicity." J Neurosci **20**(5): 1952-1963.

Bruns, D. (1998). "Serotonin transport in cultured leech neurons." Methods Enzymol. **296**: 593-607.

Bruns, D., F. Engert and H. D. Lux (1993). "A fast activating presynaptic reuptake current during serotonergic transmission in identified neurons of Hirudo." Neuron **10**(4): 559-572.

Bryan-Lluka, L. J., G. A. Siebert and S. M. Pond (1999). "Potencies of haloperidol metabolites as inhibitors of the human noradrenaline, dopamine and serotonin transporters in transfected COS-7 cells." Naunyn Schmiedebergs Arch Pharmacol **360**(2): 109-115.

Buck, K. J. and S. G. Amara (1994). "Chimeric dopamine-norepinephrine transporters delineate structural domains influencing selectivity for catecholamines and 1-methyl-4-phenylpyridinium." Proc Natl Acad Sci U S A **91**(26): 12584-12588.

Budygin, E. A., C. E. John, Y. Mateo and S. R. Jones (2002). "Lack of cocaine effect on dopamine clearance in the core and shell of the nucleus accumbens of dopamine transporter knock-out mice." J Neurosci **22**(10): RC222.

Burnette, W. B., M. D. Bailey, S. Kukoyi, R. D. Blakely, C. G. Trowbridge and J. B. Justice, Jr. (1996). "Human norepinephrine transporter kinetics using rotating disk electrode voltammetry." Anal Chem **68**(17): 2932-2938.

Busch, A. E., S. Quester, J. C. Ulzheimer, S. Waldegger, V. Gorboulev, P. Arndt, F. Lang and H. Koepsell (1996). "Electrogenic properties and substrate specificity of the polyspecific rat cation transporter rOCT1." J Biol Chem **271**(51): 32599-32604.

Carvelli, L., R. D. Blakely and L. J. DeFelice (2008). "Dopamine transporter/syntaxin 1A interactions regulate transporter channel activity and dopaminergic synaptic transmission." Proc Natl Acad Sci U S A **105**(37): 14192-14197.

Carvelli, L., P. W. McDonald, R. D. Blakely and L. J. Defelice (2004). "Dopamine transporters depolarize neurons by a channel mechanism." Proc Natl Acad Sci U S A **101**(45): 16046-16051.

Celik, L., S. Sinning, K. Severinsen, C. G. Hansen, M. S. Moller, M. Bols, O. Wiborg and B. Schiott (2008). "Binding of serotonin to the human serotonin transporter. Molecular modeling and experimental validation." J Am Chem Soc **130**(12): 3853-3865.

Chang, A. S., J. V. Frnka, D. N. Chen and D. M. Lam (1989). "Characterization of a genetically reconstituted high-affinity system for serotonin transport." Proc Natl Acad Sci U S A **86**(23): 9611-9615.

Chang, J. C., I. D. Tomlinson, M. R. Warnement, A. Ustione, A. M. Carneiro, D. W. Piston, R. D. Blakely and S. J. Rosenthal (2012). "Single molecule analysis of serotonin transporter regulation using antagonist-conjugated quantum dots reveals restricted, p38 MAPK-dependent mobilization underlying uptake activation." J Neurosci **32**(26): 8919-8929.

Chen, N. H., M. E. Reith and M. W. Quick (2004). "Synaptic uptake and beyond: the sodium- and chloride-dependent neurotransmitter transporter family SLC6." Pflugers Arch **447**(5): 519-531.

Chen, R., M. R. Tilley, H. Wei, F. Zhou, F. M. Zhou, S. Ching, N. Quan, R. L. Stephens, E. R. Hill, T. Nottoli, D. D. Han and H. H. Gu (2006). "Abolished cocaine reward in mice with a cocaine-insensitive dopamine transporter." Proc Natl Acad Sci U S A **103**(24): 9333-9338.

Cody, J. T., S. Valtier and S. L. Nelson (2003). "Amphetamine enantiomer excretion profile following administration of Adderall." J Anal Toxicol **27**(7): 485-492.

Colado, M. I., J. Camarero, A. O. Mechan, V. Sanchez, B. Esteban, J. M. Elliott and A. R. Green (2001). "A study of the mechanisms involved in the neurotoxic action of 3,4-methylenedioxymethamphetamine (MDMA, 'ecstasy') on dopamine neurones in mouse brain." Br J Pharmacol **134**(8): 1711-1723.

Combs, S., K. Kaufmann, J. R. Field, R. D. Blakely and J. Meiler (2011). "Y95 and e444 interaction required for high-affinity s-citalopram binding in the human serotonin transporter." ACS Chem Neurosci **2**(2): 75-81.

Coppen, A., D. M. Shaw, B. Herzberg and R. Maggs (1967). "Tryptophan in the treatment of depression." Lancet **2**(7527): 1178-1180.

Daws, L. C. (2009). "Unfaithful neurotransmitter transporters: focus on serotonin uptake and implications for antidepressant efficacy." Pharmacol Ther **121**(1): 89-99.

DeFelice, L. J. (2004). "Going against the flow." Nature **432**(7015): 279.

DeFelice, L. J. and R. D. Blakely (1996). "Pore models for transporters?" Biophys J **70**(2): 579-580.

DeFelice, L. J. and A. Galli (1998). "Electrophysiological analysis of transporter function." Adv Pharmacol **42**: 186-190.

DeFelice, L. J. and A. Galli (1998). "Fluctuation analysis of norepinephrine and serotonin transporter currents." Methods Enzymol **296**: 578-593.

DeFelice, L. J. and T. Goswami (2007). "Transporters as channels." Annu Rev Physiol **69**: 87-112.

Desai, V. G., R. J. Feuers, R. W. Hart and S. F. Ali (1996). "MPP(+)-induced neurotoxicity in mouse is age-dependent: evidenced by the selective inhibition of complexes of electron transport." Brain Res **715**(1-2): 1-8.

Erreger, K., C. Grewer, J. A. Javitch and A. Galli (2008). "Currents in response to rapid concentration jumps of amphetamine uncover novel aspects of human dopamine transporter function." J Neurosci **28**(4): 976-989.

Escubedo, E., J. Camarasa, C. Chipana, S. Garcia-Rates and D. Pubill (2009). "Involvement of nicotinic receptors in methamphetamine- and MDMA-induced neurotoxicity: pharmacological implications." Int Rev Neurobiol **88**: 121-166.

Falkenburger, B. H., K. L. Barstow and I. M. Mintz (2001). "Dendrodendritic inhibition through reversal of dopamine transport." Science **293**(5539): 2465-2470.

Fantegrossi, W. E. (2008). "In vivo pharmacology of MDMA and its enantiomers in rhesus monkeys." Exp Clin Psychopharmacol **16**(1): 1-12.

Fantegrossi, W. E., R. M. Bauzo, D. M. Manvich, J. C. Morales, J. R. Votaw, M. M. Goodman and L. L. Howell (2009). "Role of dopamine transporters in the behavioral effects of 3,4-methylenedioxymethamphetamine (MDMA) in nonhuman primates." Psychopharmacology (Berl) **205**(2): 337-347.

Fantegrossi, W. E., T. Godlewski, R. L. Karabenick, J. M. Stephens, T. Ullrich, K. C. Rice and J. H. Woods (2003). "Pharmacological characterization of the effects of 3,4-methylenedioxymethamphetamine ("ecstasy") and its enantiomers on lethality, core temperature, and locomotor activity in singly housed and crowded mice." Psychopharmacology (Berl) **166**(3): 202-211.

Fantegrossi, W. E., N. Murai, B. O. Mathuna, N. Pizarro and R. de la Torre (2009). "Discriminative stimulus effects of 3,4-methylenedioxymethamphetamine and its enantiomers in mice: pharmacokinetic considerations." J Pharmacol Exp Ther **329**(3): 1006-1015.

Fantegrossi, W. E., T. Ullrich, K. C. Rice, J. H. Woods and G. Winger (2002). "3,4-Methylenedioxymethamphetamine (MDMA, "ecstasy") and its stereoisomers as reinforcers in rhesus monkeys: serotonergic involvement." Psychopharmacology (Berl) **161**(4): 356-364.

Fantegrossi, W. E., W. L. Woolverton, M. Kilbourn, P. Sherman, J. Yuan, G. Hatzidimitriou, G. A. Ricaurte, J. H. Woods and G. Winger (2004). "Behavioral and neurochemical consequences of long-term intravenous self-administration of MDMA and its enantiomers by rhesus monkeys." Neuropsychopharmacology **29**(7): 1270-1281.

Feighner, J. P. (1994). "[Clinical effects of serotonin reuptake inhibitors--a review]." Fortschr Neurol Psychiatr **62 Suppl 1**: 9-15.

Field, J. R., L. K. Henry and R. D. Blakely (2010). "Transmembrane domain 6 of the human serotonin transporter contributes to an aqueously accessible binding pocket for serotonin and the psychostimulant 3,4-methylene dioxymethamphetamine." J Biol Chem **285**(15): 11270-11280.

Fischer, J. F. and A. K. Cho (1979). "Chemical release of dopamine from striatal homogenates: evidence for an exchange diffusion model." J Pharmacol Exp Ther **208**(2): 203-209.

Fleckenstein, A. E., T. J. Volz, E. L. Riddle, J. W. Gibb and G. R. Hanson (2007). "New insights into the mechanism of action of amphetamines." Annu Rev Pharmacol Toxicol **47**: 681-698.

Fog, J. U., H. Khoshbouei, M. Holy, W. A. Owens, C. B. Vaegter, N. Sen, Y. Nikandrova, E. Bowton, D. G. McMahon, R. J. Colbran, L. C. Daws, H. H. Sitte, J. A. Javitch, A. Galli and U. Gether (2006). "Calmodulin kinase II interacts with the dopamine transporter C terminus to regulate amphetamine-induced reverse transport." Neuron **51**(4): 417-429.

Fowler, A., N. Seifert, V. Acker, T. Woehrle, C. Kilpert and A. de Saizieu (2006). "A nonradioactive high-throughput/high-content assay for measurement of the human serotonin reuptake transporter function in vitro." J Biomol Screen **11**(8): 1027-1034.

Fredriksson, R., K. J. Nordstrom, O. Stephansson, M. G. Hagglund and H. B. Schioth (2008). "The solute carrier (SLC) complement of the human genome: phylogenetic classification reveals four major families." FEBS Lett **582**(27): 3811-3816.

Friesner, R. A., R. B. Murphy, M. P. Repasky, L. L. Frye, J. R. Greenwood, T. A. Halgren, P. C. Sanschagrin and D. T. Mainz (2006). "Extra precision glide: docking and scoring incorporating a model of hydrophobic enclosure for protein-ligand complexes." J Med Chem **49**(21): 6177-6196.

Froehlich, T. E., J. N. Epstein, T. G. Nick, M. S. Melguizo Castro, M. A. Stein, W. B. Brinkman, A. J. Graham, J. M. Langberg and R. S. Kahn (2011). "Pharmacogenetic predictors of methylphenidate dose-response in attention-deficit/hyperactivity disorder." J Am Acad Child Adolesc Psychiatry **50**(11): 1129-1139 e1122.

Furman, C. A., R. Chen, B. Guptaroy, M. Zhang, R. W. Holz and M. Gnegy (2009). "Dopamine and amphetamine rapidly increase dopamine transporter trafficking to the surface: live-cell imaging using total internal reflection fluorescence microscopy." The Journal of neuroscience : the official journal of the Society for Neuroscience **29**(10): 3328-3336.

Gabrielsen, M., R. Kurczab, A. W. Ravna, I. Kufareva, R. Abagyan, Z. Chilmonczyk, A. J. Bojarski and I. Sylte (2012). "Molecular mechanism of serotonin transporter inhibition elucidated by a new flexible docking protocol." Eur J Med Chem **47**(1): 24-37.

Gainetdinov, R. R. (2008). "Dopamine transporter mutant mice in experimental neuropharmacology." Naunyn Schmiedebergs Arch Pharmacol **377**(4-6): 301-313.

Gainetdinov, R. R. and M. G. Caron (2003). "Monoamine transporters: from genes to behavior." Annu Rev Pharmacol Toxicol **43**: 261-284.

Galici, R., A. Galli, D. J. Jones, T. A. Sanchez, C. Saunders, A. Frazer, G. G. Gould, R. Z. Lin and C. P. France (2003). "Selective decreases in amphetamine self-administration and regulation of dopamine transporter function in diabetic rats." Neuroendocrinology **77**(2): 132-140.

Galli, A., R. D. Blakely and L. J. DeFelice (1996). "Norepinephrine transporters have channel modes of conduction." Proc Natl Acad Sci U S A **93**(16): 8671-8676.

Galli, A., R. D. Blakely and L. J. DeFelice (1998). "Patch-clamp and amperometric recordings from norepinephrine transporters: channel activity and voltage-dependent uptake." Proc Natl Acad Sci U S A **95**(22): 13260-13265.

Galli, A., L. J. DeFelice, B. J. Duke, K. R. Moore and R. D. Blakely (1995). "Sodium-dependent norepinephrine-induced currents in norepinephrine-transporter-transfected HEK-293 cells blocked by cocaine and antidepressants." J Exp Biol **198**(Pt 10): 2197-2212.

Galli, A., C. I. Petersen, M. deBlaquiere, R. D. Blakely and L. J. DeFelice (1997). "Drosophila serotonin transporters have voltage-dependent uptake coupled to a serotonin-gated ion channel." J Neurosci **17**(10): 3401-3411.

Garcia-Rates, S., J. Camarasa, E. Escubedo and D. Pubill (2007). "Methamphetamine and 3,4-methylenedioxymethamphetamine interact with central nicotinic receptors and induce their up-regulation." Toxicol Appl Pharmacol **223**(3): 195-205.

Gether, U., P. H. Andersen, O. M. Larsson and A. Schousboe (2006). "Neurotransmitter transporters: molecular function of important drug targets." Trends Pharmacol Sci **27**(7): 375-383.

Giros, B., M. Jaber, S. R. Jones, R. M. Wightman and M. G. Caron (1996). "Hyperlocomotion and indifference to cocaine and amphetamine in mice lacking the dopamine transporter." Nature **379**(6566): 606-612.

Glennon, R. A. (1999). "Arylalkylamine drugs of abuse: An overview of drug discrimination studies." Pharmacol. Biochem. Behav. **64**: 251-256.

Glennon, R. A., M. Yousif and G. Patrick (1988). "Stimulus properties of 1-(3,4-methylenedioxyphenyl)-2-aminopropane (MDA) analogs." Pharmacology, biochemistry, and behavior **29**(3): 443-449.

Gluck, M. R., S. K. Youngster, R. R. Ramsay, T. P. Singer and W. J. Nicklas (1994). "Studies on the characterization of the inhibitory mechanism of 4'-alkylated 1-methyl-4-phenylpyridinium and phenylpyridine analogues in mitochondria and electron transport particles." J Neurochem **63**(2): 655-661.

Gold, L. A., C. B. Hubner and G. F. Koob (1989). "A role of the mesolimbic dopamine system in the psychstimulant actions of MDMA. ." Psychopharmacology (Berl) **99**: 40-47.

Gold, L. H., G. F. Koob and M. A. Geyer (1988). "Stimulant and hallucinogenic behavioral profiles of 3,4-methylenedioxymethamphetamine and N-ethyl-3,4-methylenedioxyamphetamine in rats." The Journal of pharmacology and experimental therapeutics **247**(2): 547-555.

Gorboulev, V., J. C. Ulzheimer, A. Akhoundova, I. Ulzheimer-Teuber, U. Karbach, S. Quester, C. Baumann, F. Lang, A. E. Busch and H. Koepsell (1997). "Cloning and characterization of two human polyspecific organic cation transporters." DNA Cell Biol **16**(7): 871-881.

Green, A. R., A. O. Mechan, J. M. Elliott, E. O'Shea and M. I. Colado (2003). "The pharmacology and clinical pharmacology of 3,4-methylenedioxymethamphetamine (MDMA, "ecstasy")." Pharmacol Rev **55**(3): 463-508.

Greenwood, T. A., N. J. Schork, E. Eskin and J. R. Kelsoe (2006). "Identification of additional variants within the human dopamine transporter gene provides further evidence for an association with bipolar disorder in two independent samples." Mol Psychiatry **11**(2): 125-133, 115.

Gu, H., M. J. Caplan and G. Rudnick (1998). "Cloned catecholamine transporters expressed in polarized epithelial cells: sorting, drug sensitivity, and ion-coupling stoichiometry." Adv.Pharmacol. **42**: 175-179.

Gu, H., S. C. Wall and G. Rudnick (1994). "Stable expression of biogenic amine transporters reveals differences in inhibitor sensitivity, kinetics, and ion dependence." J Biol Chem **269**(10): 7124-7130.

Gudelsky, G. A. and B. K. Yamamoto (2008). "Actions of 3,4-methylenedioxymethamphetamine (MDMA) on cerebral dopaminergic, serotonergic and cholinergic neurons." Pharmacol Biochem Behav **90**(2): 198-207.

Guvench, O. and A. D. MacKerell, Jr. (2008). "Automated conformational energy fitting for force-field development." J Mol Model **14**(8): 667-679.

Hahn, M. K. and R. D. Blakely (2002). "Monoamine transporter gene structure and polymorphisms in relation to psychiatric and other complex disorders." Pharmacogenomics J **2**(4): 217-235.

Hahn, M. K. and R. D. Blakely (2007). "The functional impact of SLC6 transporter genetic variation." Annu Rev Pharmacol Toxicol **47**: 401-441.

Haunso, A. and D. Buchanan (2007). "Pharmacological characterization of a fluorescent uptake assay for the noradrenaline transporter." J Biomol Screen **12**(3): 378-384.

He, L., K. Vasiliou and D. W. Nebert (2009). "Analysis and update of the human solute carrier (SLC) gene superfamily." Hum Genomics **3**(2): 195-206.

Heal, D. J., S. C. Cheetham and S. L. Smith (2009). "The neuropharmacology of ADHD drugs in vivo: insights on efficacy and safety." Neuropharmacology **57**(7-8): 608-618.

Hediger, M. A., M. F. Romero, J. B. Peng, A. Rolfs, H. Takanaga and E. A. Bruford (2004). "The ABCs of solute carriers: physiological, pathological and therapeutic implications of human membrane transport proteinsIntroduction." Pflugers Arch **447**(5): 465-468.

Henry, L. K., E. M. Adkins, Q. Han and R. D. Blakely (2003). "Serotonin and cocaine-sensitive inactivation of human serotonin transporters by methanethiosulfonates targeted to transmembrane domain I." J Biol Chem **278**(39): 37052-37063.

Henry, L. K. and R. D. Blakely (2008). "Distinctions between dopamine transporter antagonists could be just around the bend." Mol Pharmacol **73**(3): 616-618.

Henry, L. K., J. R. Field, E. M. Adkins, M. L. Parnas, R. A. Vaughan, M. F. Zou, A. H. Newman and R. D. Blakely (2006). "Tyr-95 and Ile-172 in transmembrane segments 1 and 3 of human serotonin transporters interact to establish high affinity recognition of antidepressants." J Biol Chem **281**(4): 2012-2023.

Hilber, B., P. Scholze, M. M. Dorostkar, W. Sandtner, M. Holy, S. Boehm, E. A. Singer and H. H. Sitte (2005). "Serotonin-transporter mediated efflux: a pharmacological analysis of amphetamines and non-amphetamines." Neuropharmacology **49**(6): 811-819.

Hoffman, B. J., S. R. Hansson, E. Mezey and M. Palkovits (1998). "Localization and dynamic regulation of biogenic amine transporters in the mammalian central nervous system." Front Neuroendocrinol **19**(3): 187-231.

Hoglund, P. J., K. J. Nordstrom, H. B. Schioth and R. Fredriksson (2011). "The solute carrier families have a remarkably long evolutionary history with the majority of the human families present before divergence of Bilaterian species." Mol Biol Evol **28**(4): 1531-1541.

Hohage, H., A. Stachon, C. Feidt, J. R. Hirsch and E. Schlatter (1998). "Regulation of organic cation transport in IHKE-1 and LLC-PK1 cells. Fluorometric studies with 4-(4-dimethylaminostyryl)-N-methylpyridinium." J Pharmacol Exp Ther **286**(1): 305-310.

Holmes, J. C. and C. O. Rutledge (1976). "Effects of the d- and l-isomers of amphetamine on uptake, release and catabolism of norepinephrine, dopamine and 5-hydroxytryptamine in several regions of rat brain." Biochem Pharmacol **25**(4): 447-451.

Howell, L. L., F. I. Carroll, J. R. Votaw, M. M. Goodman and H. L. Kimmel (2007). "Effects of combined dopamine and serotonin transporter inhibitors on cocaine self-administration in rhesus monkeys." The Journal of pharmacology and experimental therapeutics **320**(2): 757-765.

Howell, L. L. and H. L. Kimmel (2007). ".Psychostimulants." Handbook of Contemporary Neuropharmacology: D. R. Sibley, I. Hanin, M. Kuhar, and P. Skolnick, eds. **2**: 567-611.

Indarte, M., J. D. Madura and C. K. Surratt (2008). "Dopamine transporter comparative molecular modeling and binding site prediction using the LeuT(Aa) leucine transporter as a template." Proteins **70**(3): 1033-1046.

Ingram, S. L. and S. G. Amara (2000). "Arachidonic acid stimulates a novel cocaine-sensitive cation conductance associated with the human dopamine transporter." J Neurosci **20**(2): 550-557.

Ingram, S. L., B. M. Prasad and S. G. Amara (2002). "Dopamine transporter-mediated conductances increase excitability of midbrain dopamine neurons." Nat Neurosci **5**(10): 971-978.

Iversen, L. (2006). "Neurotransmitter transporters and their impact on the development of psychopharmacology." Br J Pharmacol **147 Suppl 1**: S82-88.

Iwamoto, H., R. D. Blakely and L. J. DeFelice (2006). "Na+, Cl–, and pH Dependence of the Human Choline Transporter (hCHT) in Xenopus Oocytes: The Proton Inactivation Hypothesis of hCHT in Synaptic Vesicles." J Neuroscience **26**: 9851 - 9859.

Javitch, J. A. and S. H. Snyder (1984). "Uptake of MPP(+) by dopamine neurons explains selectivity of parkinsonism-inducing neurotoxin, MPTP." Eur J Pharmacol **106**(2): 455-456.

Jellinger, K. A. (1991). "Pathology of Parkinson's disease. Changes other than the nigrostriatal pathway." Mol Chem Neuropathol **14**(3): 153-197.

Johansen, P. O. and T. S. Krebs (2009). "How could MDMA (ecstasy) help anxiety disorders? A neurobiological rationale." J Psychopharmacol **23**(4): 389-391.

Johnson, L. V., M. L. Walsh, B. J. Bockus and L. B. Chen (1981). "Monitoring of relative mitochondrial membrane potential in living cells by fluorescence microscopy." J Cell Biol **88**(3): 526-535.

Johnson, L. V., M. L. Walsh and L. B. Chen (1980). "Localization of mitochondria in living cells with rhodamine 123." Proc Natl Acad Sci U S A **77**(2): 990-994.

Jones, S. R., R. R. Gainetdinov, R. M. Wightman and M. G. Caron (1998). "Mechanisms of amphetamine action revealed in mice lacking the dopamine transporter." J Neurosci **18**(6): 1979-1986.

Jorgensen, S., E. O. Nielsen, D. Peters and T. Dyhring (2008). "Validation of a fluorescence-based high-throughput assay for the measurement of

neurotransmitter transporter uptake activity." J Neurosci Methods **169**(1): 168-176.

Kahlig, K. M., F. Binda, H. Khoshbouei, R. D. Blakely, D. G. McMahon, J. A. Javitch and A. Galli (2005). "Amphetamine induces dopamine efflux through a dopamine transporter channel." Proc Natl Acad Sci U S A **102**(9): 3495-3500.

Kaufmann, K. W., E. S. Dawson, L. K. Henry, J. R. Field, R. D. Blakely and J. Meiler (2009). "Structural determinants of species-selective substrate recognition in human and Drosophila serotonin transporters revealed through computational docking studies." Proteins **74**(3): 630-642.

Kawarai, T., H. Kawakami, Y. Yamamura and S. Nakamura (1997). "Structure and organization of the gene encoding human dopamine transporter." Gene **195**(1): 11-18.

Keyes, S. R. and G. Rudnick (1982). "Coupling of transmembrane proton gradients to platelet serotonin transport." J Biol Chem **257**(3): 1172-1176.

Khoshbouei, H., N. Sen, B. Guptaroy, L. Johnson, D. Lund, M. E. Gnegy, A. Galli and J. A. Javitch (2004). "N-terminal phosphorylation of the dopamine transporter is required for amphetamine-induced efflux." PLoS Biol **2**(3): E78.

Khoshbouei, H., H. Wang, J. D. Lechleiter, J. A. Javitch and A. Galli (2003). "Amphetamine-induced dopamine efflux. A voltage-sensitive and intracellular Na+-dependent mechanism." J Biol Chem **278**(14): 12070-12077.

Kilic, F., D. Murphy and G. Rudnick (2003). "A human serotonin transporter mutation causes constitutive activation of transport activity." Mol Pharmacol **64**: 440-446.

Kilic, F. and G. Rudnick (2000). "Oligomerization of serotonin transporter and its functional consequences." Proc Natl Acad Sci U S A **97**(7): 3106-3111.

Krause, K. H., S. H. Dresel, J. Krause, H. F. Kung and K. Tatsch (2000). "Increased striatal dopamine transporter in adult patients with attention deficit hyperactivity disorder: effects of methylphenidate as measured by single photon emission computed tomography." Neurosci Lett **285**(2): 107-110.

Krueger, M. J., S. O. Sablin, R. Ramsay and T. P. Singer (1993). "Reactivation of NADH dehydrogenase (complex I) inhibited by 1-methyl-4-(4'-alkylphenyl)pyridinium analogues: a clue to the nature of the inhibition site." J Neurochem **61**(4): 1546-1548.

Kuczenski, R., D. S. Segal, A. K. Cho and W. Melega (1995). "Hippocampus norepinephrine, caudate dopamine and serotonin, and behavioral responses to the stereoisomers of amphetamine and methamphetamine." J Neurosci **15**(2): 1308-1317.

Kurian, M. A., J. Zhen, S. Y. Cheng, Y. Li, S. R. Mordekar, P. Jardine, N. V. Morgan, E. Meyer, L. Tee, S. Pasha, E. Wassmer, S. J. Heales, P. Gissen, M. E. Reith and E. R. Maher (2009). "Homozygous loss-of-function mutations in the gene encoding the dopamine transporter are associated with infantile parkinsonism-dystonia." J Clin Invest **119**(6): 1595-1603.

Larsson, H. P., S. A. Picaud, F. S. Werblin and H. Lecar (1996). "Noise analysis of the glutamate-activated current in photoreceptors." Biophys J **70**(2): 733-742.

Leary, G. P., E. F. Stone, D. C. Holley and M. P. Kavanaugh (2007). "The glutamate and chloride permeation pathways are colocalized in individual neuronal glutamate transporter subunits." J Neurosci **27**(11): 2938-2942.

Lesch, K. P., D. Bengel, A. Heils, S. Z. Sabol, B. D. Greenberg, S. Petri, J. Benjamin, C. R. Muller, D. H. Hamer and D. L. Murphy (1996). "Association of anxiety-related traits with a polymorphism in the serotonin transporter gene regulatory region." Science **274**(5292): 1527-1531.

Li, C., H. Zhong, Y. Wang, H. Wang, Z. Yang, Y. Zheng, K. Liu and Y. Liu (2006). "Voltage and ionic regulation of human serotonin transporter in Xenopus oocytes." Clin Exp Pharmacol Physiol **33**(11): 1088-1092.

Lin, F., H. A. Lester and S. Mager (1996). "Single-channel currents produced by the serotonin transporter and analysis of a mutation affecting ion permeation." Biophys J **71**(6): 3126-3135.

Lyles, J. and J. L. Cadet (2003). "Methylenedioxymethamphetamine (MDMA, Ecstasy) neurotoxicity: cellular and molecular mechanisms." Brain Res Brain Res Rev **42**(2): 155-168.

Machaca, K. and H. Hartzell (1998). "Assymetric Distribution of Ca-Activated Cl Channels in Xenopus Oocytes." Biophysical J **74**: 1286-1295.

Mager, S., C. Min, D. J. Henry, C. Chavkin, B. J. Hoffman, N. Davidson and H. A. Lester (1994). "Conducting states of a mammalian serotonin transporter." Neuron **12**(4): 845-859.

Mason, J. N., H. Farmer, I. D. Tomlinson, J. W. Schwartz, V. Savchenko, L. J. DeFelice, S. J. Rosenthal and R. D. Blakely (2005). "Novel fluorescence-based approaches for the study of biogenic amine transporter localization, activity, and regulation." J Neurosci Methods **143**(1): 3-25.

Mazei-Robinson, M. S. and R. D. Blakely (2006). "ADHD and the dopamine transporter: are there reasons to pay attention?" Handb Exp Pharmacol(175): 373-415.

Mazei-Robison, M. S., E. Bowton, M. Holy, M. Schmudermaier, M. Freissmuth, H. H. Sitte, A. Galli and R. D. Blakely (2008). "Anomalous dopamine release associated with a human dopamine transporter coding variant." J Neurosci **28**(28): 7040-7046.

Mazei-Robison, M. S., R. S. Couch, R. C. Shelton, M. A. Stein and R. D. Blakely (2005). "Sequence variation in the human dopamine transporter gene in children with attention deficit hyperactivity disorder." Neuropharmacology **49**(6): 724-736.

McElvain, J. S. and J. O. Schenk (1992). "A multisubstrate mechanism of striatal dopamine uptake and its inhibition by cocaine." Biochem Pharmacol **43**(10): 2189-2199.

Mehrens, T., S. Lelleck, I. Cetinkaya, M. Knollmann, H. Hohage, V. Gorboulev, P. Boknik, H. Koepsell and E. Schlatter (2000). "The affinity of the organic cation transporter rOCT1 is increased by protein kinase C-dependent phosphorylation." J Am Soc Nephrol **11**(7): 1216-1224.

Mendelson, J., N. Uemura, D. Harris, R. P. Nath, E. Fernandez, P. Jacob, 3rd, E. T. Everhart and R. T. Jones (2006). "Human pharmacology of the methamphetamine stereoisomers." Clin Pharmacol Ther **80**(4): 403-420.

Mithoefer, M. C., M. T. Wagner, A. T. Mithoefer, L. Jerome and R. Doblin (2011). "The safety and efficacy of {+/-}3,4-methylenedioxymethamphetamine-assisted psychotherapy in subjects with chronic, treatment-resistant posttraumatic stress disorder: the first randomized controlled pilot study." J Psychopharmacol **25**(4): 439-452.

Mofenson, H. C. and J. Greensher (1975). "Letter: Physostigmine as an antidote: use with caution." J Pediatr **87**(6 Pt 1): 1011-1012.

Murali, S. and W. Rettig (2006). "TICT formation in para- and meta-derivatives of N-phenylpyrrole." J Phys Chem A **110**(1): 28-37.

Murnane, K. S., N. Murai, L. L. Howell and W. E. Fantegrossi (2009). "Discriminative stimulus effects of psychostimulants and hallucinogens in S(+)-3,4-methylenedioxymethamphetamine (MDMA) and R(-)-MDMA trained mice." J Pharmacol Exp Ther **331**(2): 717-723.

Murphy, D. L., A. Lerner, G. Rudnick and K. P. Lesch (2004). "Serotonin transporter: gene, genetic disorders, and pharmacogenetics." Mol Interv **4**(2): 109-123.

Naftalin, R. (1984). "The thermostatics and thermodynamics of cotransport." Biochim Biophys Acta **778**: 155-175.

Naftalin, R. (2005). "My top 10 papers on biological salt, water and sugar transport." Physiology News **61**: 10-13.

Najib, J. (2009). "The efficacy and safety profile of lisdexamfetamine dimesylate, a prodrug of d-amphetamine, for the treatment of attention-deficit/hyperactivity disorder in children and adults." Clin Ther **31**(1): 142-176.

Nelson, N. (1998). "The family of Na+/Cl- neurotransmitter transporters." J Neurochem **71**(5): 1785-1803.

Nyola, A., N. K. Karpowich, J. Zhen, J. Marden, M. E. Reith and D. N. Wang (2010). "Substrate and drug binding sites in LeuT." Curr Opin Struct Biol **20**(4): 415-422.

O'Shea, E., B. Esteban, J. Camarero, A. R. Green and M. I. Colado (2001). "Effect of GBR 12909 and fluoxetine on the acute and long term changes induced by MDMA ('ecstasy') on the 5-HT and dopamine concentrations in mouse brain." Neuropharmacology **40**(1): 65-74.

Ozaki, N., D. Goldman, W. H. Kaye, K. Plotnicov, B. D. Greenberg, J. Lappalainen, G. Rudnick and D. L. Murphy (2003). "Serotonin transporter missense mutation associated with a complex neuropsychiatric phenotype." Mol Psychiatry **8**(11): 895, 933-896.

Petersen, C. I. and L. J. DeFelice (1999). "Ionic interactions in the Drosophila serotonin transporter identify it as a serotonin channel." Nat Neurosci **2**(7): 605-610.

Phillips, A. G., S. M. Brooke and H. C. Fibiger (1975). "Effects of amphetamine isomers and neuroleptics on self-stimulation from the nucleus accumbens and dorsal noradrenergic bundle." Brain Res **85**(1): 13-22.

Piscitelli, C. L., H. Krishnamurthy and E. Gouaux (2010). "Neurotransmitter/sodium symporter orthologue LeuT has a single high-affinity substrate site." Nature **468**(7327): 1129-1132.

Polanczyk, G., M. S. de Lima, B. L. Horta, J. Biederman and L. A. Rohde (2007). "The worldwide prevalence of ADHD: a systematic review and metaregression analysis." Am J Psychiatry **164**(6): 942-948.

Potkin, S. G., F. Karoum, L. W. Chuang, H. E. Cannon-Spoor, I. Phillips and R. J. Wyatt (1979). "Phenylethylamine in paranoid chronic schizophrenia." Science **206**(4417): 470-471.

Prasad, H. C., J. A. Steiner, J. S. Sutcliffe and R. D. Blakely (2009). "Enhanced activity of human serotonin transporter variants associated with autism." Philos Trans R Soc Lond B Biol Sci **364**(1514): 163-173.

Prasad, H. C., C. B. Zhu, J. L. McCauley, D. J. Samuvel, S. Ramamoorthy, R. C. Shelton, W. A. Hewlett, J. S. Sutcliffe and R. D. Blakely (2005). "Human serotonin transporter variants display altered sensitivity to protein kinase G and p38 mitogen-activated protein kinase." Proc Natl Acad Sci U S A **102**(32): 11545-11550.

Purves, D. (2008). Neuroscience. Sunderland, Mass., Sinauer.

Quick, M. W. (2002). "Role of syntaxin 1A on serotonin transporter expression in developing thalamocortical neurons." Int J Dev Neurosci **20**(3-5): 219-224.

Quick, M. W. (2003). "Regulating the conducting states of a mammalian serotonin transporter." Neuron **40**(3): 537-549.

Ramamoorthy, S., A. L. Bauman, K. R. Moore, H. Han, T. Yang-Feng, A. S. Chang, V. Ganapathy and R. D. Blakely (1993). "Antidepressant- and cocaine-sensitive human serotonin transporter: molecular cloning, expression, and chromosomal localization." Proc Natl Acad Sci U S A **90**(6): 2542-2546.

Ramsey, I. S. and L. J. DeFelice (2002). "Serotonin transporter function and pharmacology are sensitive to expression level: evidence for an endogenous regulatory factor." J Biol Chem **277**(17): 14475-14482.

Richelson, E. (1996). "Synaptic effects of antidepressants." J Clin Psychopharmacol **16**(3 Suppl 2): 1S-7S; discussion 7S-9S.

Rodriguez-Menchaca, A. A., E. Solis, Jr., K. Cameron and L. J. De Felice (2012). "S(+)amphetamine induces a persistent leak in the human dopamine transporter: molecular stent hypothesis." Br J Pharmacol **165**(8): 2749-2757.

Romanelli, F. and K. M. Smith (2006). "Clinical effects and management of methamphetamine abuse." Pharmacotherapy **26**(8): 1148-1156.

Rothman, R. B. and M. H. Baumann (2006). "Therapeutic potential of monoamine transporter substrates." Curr Top Med Chem **6**(17): 1845-1859.

Rothman, R. B., B. E. Blough and M. H. Baumann (2008). "Dual dopamine/serotonin releasers: potential treatment agents for stimulant addiction." Exp Clin Psychopharmacol **16**(6): 458-474.

Rudnick, G. (1998). "Bioenergetics of neurotransmitter transport." J Bioenerg Biomembr **30**(2): 173-185.

Rudnick, G. (1998). "Ion-coupled neurotransmitter transport: thermodynamic vs. kinetic determinations of stoichiometry." Methods Enzymol **296**: 233-247.

Rudnick, G. and S. C. Wall (1993). "Non-neurotoxic amphetamine derivatives release serotonin through serotonin transporters." Mol Pharmacol **43**(2): 271-276.

Ryan, R. M. and J. A. Mindell (2007). "The uncoupled chloride conductance of a bacterial glutamate transporter homolog." Nat Struct Mol Biol **14**(5): 365-371.

Samuvel, D. J., L. D. Jayanthi, S. Manohar, K. Kaliyaperumal, R. E. See and S. Ramamoorthy (2008). "Dysregulation of dopamine transporter trafficking and function after abstinence from cocaine self-administration in rats: evidence for differential regulation in caudate putamen and nucleus accumbens." J Pharmacol Exp Ther **325**(1): 293-301.

Sanchez, V., J. Camarero, B. Esteban, M. J. Peter, A. R. Green and M. I. Colado (2001). "The mechanisms involved in the long-lasting neuroprotective effect of fluoxetine against MDMA ('ecstasy')-induced degeneration of 5-HT nerve endings in rat brain." Br J Pharmacol **134**(1): 46-57.

Sarker, S., R. Weissensteiner, I. Steiner, H. H. Sitte, G. F. Ecker, M. Freissmuth and S. Sucic (2010). "The high-affinity binding site for tricyclic antidepressants resides in the outer vestibule of the serotonin transporter." Mol Pharmacol **78**(6): 1026-1035.

Saunders, C., J. V. Ferrer, L. Shi, J. Chen, G. Merrill, M. E. Lamb, L. M. Leeb-Lundberg, L. Carvelli, J. A. Javitch and A. Galli (2000). "Amphetamine-induced loss of human dopamine transporter activity: an internalization-dependent and cocaine-sensitive mechanism." Proc.Natl.Acad.Sci.U.S.A **97**(12): 6850-6855.

Schloss, P. and D. C. Williams (1998). "The serotonin transporter: a primary target for antidepressant drugs." J Psychopharmacol **12**(2): 115-121.

Schmid, J. A., H. Just and H. H. Sitte (2001). "Impact of oligomerization on the function of the human serotonin transporter." Biochem Soc Trans **29**(Pt 6): 732-736.

Schmid, J. A., P. Scholze, O. Kudlacek, M. Freissmuth, E. A. Singer and H. H. Sitte (2001). "Oligomerization of the human serotonin transporter and of the rat GABA transporter 1 visualized by fluorescence resonance energy transfer microscopy in living cells." J Biol Chem **276**(6): 3805-3810.

Schmitz, Y., C. J. Lee, C. Schmauss, F. Gonon and D. Sulzer (2001). "Amphetamine distorts stimulation-dependent dopamine overflow: effects on D2 autoreceptors, transporters, and synaptic vesicle stores." J Neurosci **21**(16): 5916-5924.

Schwartz, J. W., R. D. Blakely and L. J. DeFelice (2003). "Binding and transport in norepinephrine transporters. Real-time, spatially resolved analysis in single cells using a fluorescent substrate." J Biol Chem **278**(11): 9768-9777.

Schwartz, J. W., G. Novarino, D. W. Piston and L. J. DeFelice (2005). "Substrate binding stoichiometry and kinetics of the norepinephrine transporter." J Biol Chem **280**(19): 19177-19184.

Schwartz, J. W., D. Piston and L. J. DeFelice (2006). "Molecular microfluorometry: converting arbitrary fluorescence units into absolute molecular concentrations to study binding kinetics and stoichiometry in transporters." Handb Exp Pharmacol(175): 23-57.

Seidel, S., E. A. Singer, H. Just, H. Farhan, P. Scholze, O. Kudlacek, M. Holy, K. Koppatz, P. Krivanek, M. Freissmuth and H. H. Sitte (2005). "Amphetamines take two to tango: an oligomer-based counter-transport model of neurotransmitter transport explores the amphetamine action." Mol Pharmacol **67**(1): 140-151.

Seiden, L. S., K. E. Sabol and G. A. Ricaurte (1993). "Amphetamine: effects on catecholamine systems and behavior." Annual review of pharmacology and toxicology **33**: 639-677.

Sellings, L. H. and P. B. Clarke (2003). "Segregation of amphetamine reward and locomotor stimulation between nucleus accumbens medial shell and core." The Journal of neuroscience : the official journal of the Society for Neuroscience **23**(15): 6295-6303.

Setola, V., S. J. Hufeisen, K. J. Grande-Allen, I. Vesely, R. A. Glennon, B. Blough, R. B. Rothman and B. L. Roth (2003). "3,4-Methylenedioxymethamphetamine (MDMA, "Ecstasy") induces fenfluramine-like proliferative actions on human cardiac valvular interstitial cells in vitro." Mol. Pharmacol **63**: 1223-1229.

Sghendo, L. and J. Mifsud (2012). "Understanding the molecular pharmacology of the serotonergic system: using fluoxetine as a model." J Pharm Pharmacol **64**(3): 317-325.

Shan, J., J. A. Javitch, L. Shi and H. Weinstein (2011). "The substrate-driven transition to an inward-facing conformation in the functional mechanism of the dopamine transporter." PLoS One **6**(1): e16350.

Shi, L., M. Quick, Y. Zhao, H. Weinstein and J. A. Javitch (2008). "The mechanism of a neurotransmitter:sodium symporter--inward release of Na+ and substrate is triggered by substrate in a second binding site." Mol Cell **30**(6): 667-677.

Singh, S. K. (2008). "LeuT: A prokaryotic stepping stone on the way to a eukaryotic neurotransmitter transporter structure." Channels (Austin) **2**(5).

Singh, S. K., A. Yamashita and E. Gouaux (2007). "Antidepressant binding site in a bacterial homologue of neurotransmitter transporters." Nature **448**(7156): 952-956.

Solis, E., Jr., I. Zdravkovic, I. D. Tomlinson, S. Y. Noskov, S. J. Rosenthal and L. J. De Felice (2012). "4-(4-(dimethylamino)phenyl)-1-methylpyridinium (APP+) is a fluorescent substrate for the human serotonin transporter." J Biol Chem **287**(12): 8852-8863.

Sonders, M. S. and S. G. Amara (1996). "Channels in transporters." Curr Opin Neurobiol **6**(3): 294-302.

Sonders, M. S., S. J. Zhu, N. R. Zahniser, M. P. Kavanaugh and S. G. Amara (1997). "Multiple ionic conductances of the human dopamine transporter: the actions of dopamine and psychostimulants." J Neurosci **17**(3): 960-974.

Spielewoy, C., F. Gonon, C. Roubert, V. Fauchey, M. Jaber, M. G. Caron, B. P. Roques, M. Hamon, C. Betancur, R. Maldonado and B. Giros (2000). "Increased

rewarding properties of morphine in dopamine-transporter knockout mice." Eur.J.Neurosci. **12**(5): 1827-1837.

Stahl, S. M. (1998). "Basic psychopharmacology of antidepressants, part 1: Antidepressants have seven distinct mechanisms of action." J Clin Psychiatry **59 Suppl 4**: 5-14.

Stahl, S. M. (1998). "Mechanism of action of serotonin selective reuptake inhibitors. Serotonin receptors and pathways mediate therapeutic effects and side effects." J Affect Disord **51**(3): 215-235.

Stein, W. D. (1986). Transport and Diffusion Across Cell Membranes Academic Press.

Storustovu, S., C. Sanchez, P. Porzgen, L. T. Brennum, A. K. Larsen, M. Pulis and B. Ebert (2004). "R-citalopram functionally antagonises escitalopram in vivo and in vitro: evidence for kinetic interaction at the serotonin transporter." Br J Pharmacol **142**(1): 172-180.

Sulzer, D., T. K. Chen, Y. Y. Lau, H. Kristensen, S. Rayport and A. Ewing (1995). "Amphetamine redistributes dopamine from synaptic vesicles to the cytosol and promotes reverse transport." J Neurosci **15**(5 Pt 2): 4102-4108.

Sulzer, D. and A. Galli (2003). "Dopamine transport currents are promoted from curiosity to physiology." Trends Neurosci **26**(4): 173-176.

Sulzer, D., N. T. Maidment and S. Rayport (1993). "Amphetamine and other weak bases act to promote reverse transport of dopamine in ventral midbrain neurons." J Neurochem **60**(2): 527-535.

Sulzer, D., M. S. Sonders, N. W. Poulsen and A. Galli (2005). "Mechanisms of neurotransmitter release by amphetamines: a review." Progress in neurobiology **75**(6): 406-433.

Sutcliffe, J. S., R. J. Delahanty, H. C. Prasad, J. L. McCauley, Q. Han, L. Jiang, C. Li, S. E. Folstein and R. D. Blakely (2005). "Allelic heterogeneity at the serotonin transporter locus (SLC6A4) confers susceptibility to autism and rigid-compulsive behaviors." Am J Hum Genet **77**(2): 265-279.

Talvenheimo, J., P. J. Nelson and G. Rudnick (1979). "Mechanism of imipramine inhibition of platelet 5-hydroxytryptamine transport." J Biol Chem **254**(11): 4631-4635.

Tao-Cheng, J. H. and F. C. Zhou (1999). "Differential polarization of serotonin transporters in axons versus soma-dendrites: an immunogold electron microscopy study." Neuroscience **94**(3): 821-830.

Torres-Altoro, M. I., K. J. White, G. J. Rodriguez, D. E. Nichols and E. L. Barker (2008). "Helix XI contributes to the entrance of the serotonin transporter permeation pathway." Protein Sci **17**(10): 1761-1770.

Tsuruda, P. R., J. Yung, W. J. Martin, R. Chang, N. Mai and J. A. Smith (2010). "Influence of ligand binding kinetics on functional inhibition of human recombinant serotonin and norepinephrine transporters." J Pharmacol Toxicol Methods **61**(2): 192-204.

Van der Schoot, J. B., E. J. Ariens, J. M. Van Rossum and J. A. Hurkmans (1961). "Phenylisopropylamine derivatives, structure and action." Arzneimittelforschung **9**: 902-907.

Vaswani, M. and H. Kalra (2004). "Selective serotonin re-uptake inhibitors in anorexia nervosa." Expert Opin Investig Drugs **13**(4): 349-357.

Vaswani, M., F. K. Linda and S. Ramesh (2003). "Role of selective serotonin reuptake inhibitors in psychiatric disorders: a comprehensive review." Prog Neuropsychopharmacol Biol Psychiatry **27**(1): 85-102.

Verrico, C. D., G. M. Miller and B. K. Madras (2007). "MDMA (Ecstasy) and human dopamine, norepinephrine, and serotonin transporters: implications for MDMA-induced neurotoxicity and treatment." Psychopharmacology (Berl) **189**(4): 489-503.

Verstraete, A. G. (2005). "Oral fluid testing for driving under the influence of drugs: history, recent progress and remaining challenges." Forensic science international **150**(2-3): 143-150.

Verstraete, A. G. and F. V. Heyden (2005). "Comparison of the sensitivity and specificity of six immunoassays for the detection of amphetamines in urine." Journal of analytical toxicology **29**(5): 359-364.

Volz, T. J., G. R. Hanson and A. E. Fleckenstein (2007). "The role of the plasmalemmal dopamine and vesicular monoamine transporters in methamphetamine-induced dopaminergic deficits." J Neurochem **101**(4): 883-888.

Wall, S. C., H. Gu and G. Rudnick (1995). "Biogenic amine flux mediated by cloned transporters stably expressed in cultured cell lines: amphetamine specificity for inhibition and efflux." Mol.Pharmacol. **47**(3): 544-550.

Wang, H. W., C. Z. Li, Z. F. Yang, Y. Q. Zheng, Y. Zhang and Y. M. Liu (2006). "Electrophysiological effect of fluoxetine on Xenopus oocytes heterologously expressing human serotonin transporter." Acta Pharmacol Sin **27**(3): 289-293.

Wang, Z. and W. L. Woolverton (2007). "Estimating the relative reinforcing strength of (+/-)-3,4-methylenedioxymethamphetamine (MDMA) and its isomers in rhesus monkeys: comparison to (+)-methamphetamine." Psychopharmacology (Berl) **189**(4): 483-488.

Weinshenker, D. and J. P. Schroeder (2007). "There and back again: a tale of norepinephrine and drug addiction." Neuropsychopharmacology **32**(7): 1433-1451.

White, K. J., C. C. Walline and E. L. Barker (2005). "Serotonin transporters: implications for antidepressant drug development." AAPS J **7**(2): E421-433.

Williams, J. M. and A. Galli (2006). "The dopamine transporter: a vigilant border control for psychostimulant action." Handbook of experimental pharmacology(175): 215-232.

Wimalasena, K. (2011). "Vesicular monoamine transporters: structure-function, pharmacology, and medicinal chemistry." Med Res Rev **31**(4): 483-519.

Winslow, B. T., K. I. Voorhees and K. A. Pehl (2007). "Methamphetamine abuse." Am Fam Physician **76**(8): 1169-1174.

Wise, R. A. (1996). "Addictive drugs and brain stimulation reward." Annu Rev Neurosci **19**: 319-340.

Wright, A. M., J. Bempong, M. L. Kirby, R. L. Barlow and J. R. Bloomquist (1998). "Effects of haloperidol metabolites on neurotransmitter uptake and release: possible role in neurotoxicity and tardive dyskinesia." Brain Res **788**(1-2): 215-222.

Wu, X. and H. H. Gu (1999). "Molecular cloning of the mouse dopamine transporter and pharmacological comparison with the human homologue." Gene **233**(1-2): 163-170.

Yamashita, A., S. K. Singh, T. Kawate, Y. Jin and E. Gouaux (2005). "Crystal structure of a bacterial homologue of Na+/Cl--dependent neurotransmitter transporters." Nature **437**(7056): 215-223.

Yernool, D., O. Boudker, Y. Jin and E. Gouaux (2004). "Structure of a glutamate transporter homologue from Pyrococcus horikoshii." Nature **431**(7010): 811-818.

Young, R. and R. A. Glennon (2008). "MDMA (N-methyl-3,4-methylenedioxyamphetamine) and its stereoisomers: Similarities and differences in behavioral effects in an automated activity apparatus in mice." Pharmacol Biochem Behav **88**(3): 318-331.

Zapata, A., B. Kivell, Y. Han, J. A. Javitch, E. A. Bolan, D. Kuraguntla, V. Jaligam, M. Oz, L. D. Jayanthi, D. J. Samuvel, S. Ramamoorthy and T. S. Shippenberg (2007). "Regulation of dopamine transporter function and cell surface expression by D3 dopamine receptors." J Biol Chem **282**(49): 35842-35854.

Zhao, Y., D. S. Terry, L. Shi, M. Quick, H. Weinstein, S. C. Blanchard and J. A. Javitch (2011). "Substrate-modulated gating dynamics in a Na+-coupled neurotransmitter transporter homologue." Nature **474**(7349): 109-113.

Zheng, C., Y. Shen and Q. Xu (2012). "Association of intron 1 variants of the dopamine transporter gene with schizophrenia." Neurosci Lett **513**(2): 137-140.

Zhou, D., M. Schreinert, J. Pilz and G. Huether (1996). "Rat strain differences in the vulnerability of serotonergic nerve endings to neurotoxic damage by p-chloroamphetamine." J Neural Transm **103**(12): 1381-1395.

Zhou, Z., J. Zhen, N. K. Karpowich, R. M. Goetz, C. J. Law, M. E. Reith and D. N. Wang (2007). "LeuT-desipramine structure reveals how antidepressants block neurotransmitter reuptake." Science **317**(5843): 1390-1393.

Zhou, Z., J. Zhen, N. K. Karpowich, C. J. Law, M. E. Reith and D. N. Wang (2009). "Antidepressant specificity of serotonin transporter suggested by three LeuT-SSRI structures." Nat Struct Mol Biol.